Anonymous Referee #1

General comments:

- ***This manuscript provided an interesting study investigating the factors that affect the WRF-Chem performance of diurnal cycle of surface $PM_{2.5}$ concentrations in East China. This study suggested that PBL mixing coefficient is the key factor controlling the WRFChem model performance instead of PBL height and the diurnal cycle and injection height of emissions. This manuscript points out the importance of improving the PBL mixing process in WRF-Chem to achieve better results of diurnal $PM_{2.5}$ cycle. The topic is applicable for Atmospheric Chemistry and Physics. The text is concisely written and well documented. This study has comprehensive analysis and detailed explanation/discussion.***

We thank the reviewer for the detailed and constructive comments. They are very helpful for improving the quality of the manuscript.

In the revised manuscript, we added a few new figures in the supporting material to support some statements in the text and to address the review comments. Specifically, the evaluation of model performance in spatial distribution of surface $PM_{2.5}$ concentration is added. The PBL height is evaluated with the climatological estimate derived from the air sounding observations. More information about how to calculate the contribution from each process to surface $PM_{2.5}$ concentration is added in the methodology section. Other text and figures have also been revised as the reviewer suggested.

Major comments:

- ***This manuscript only discussed the normalized diurnal amplitude (i.e, DI) from observations and WRF-Chem simulations, but lacked the evaluation of model performance of actual $PM_{2.5}$ concentrations in East China.***

First of all, this paper focuses on the modeling of diurnal variation of surface $PM_{2.5}$. The evaluation of WRF-Chem simulated daily or monthly mean surface $PM_{2.5}$ has been conducted by previous studies (e.g., Gong et al., 2007; Ding et al., 2013; Gao et al., 2014; Chen et al., 2014; Zhao et al., 2014; Zhang B et al., 2015; Huang et al., 2016). The modeling biases of daily or monthly mean surface $PM_{2.5}$ can be affected by many other factors besides the boundary mixing, therefore beyond the scope of this study. In addition, besides focusing on the modeling of diurnal variation, we also investigated the impact of diurnal variation on daily mean concentration in the manuscript, and provided evaluation of actual monthly mean surface $PM_{2.5}$ at all stations over East China in Fig. 12. Fig. 12 shows the control simulation CTL1 significantly overestimates the observed surface $PM_{2.5}$ concentration with the normalized mean biases (NMB) of 22% (winter) - 109% (summer) on regional average. In the sensitivity experiment EXP1 with increased nighttime boundary mixing, the NMB is reduced to 7% (winter) - 38% (summer) on regional average. Therefore, we do have some discussion about the evaluation of actual surface $PM_{2.5}$ concentration over East China, although it is not the focus of this study. Now we also show the spatial distribution of modeling biases of surface $PM_{2.5}$ concentration in the four months from the experiments CTL1, CTL2, CTL3, EXP1 and EXP2 compared to the observations in Fig S9. We add more discussion in the text as

"The model overestimates largely the monthly mean surface $PM_{2.5}$ at the stations of East China in the seasons other than winter from the control experiments. These modeling biases are significantly reduced at most stations of East China (Fig. S15 in the supporting material) in the sensitivity experiments."

- ***The comparison of monthly mean $PM_{2.5}$ concentrations between CTL1 and EXP1 (Figure 12) suggested that WRF-Chem had moderate model performance in winter (Jan) and poor performance in other 3 seasons (Apr, Jul, and Oct) even after increasing the PBL mixing coefficient. Note in winter the PBL is usually shallow and if we assume the MEIC emissions are accurate, my hypothesis is that the accuracy of PBL height simulations dominated the model performance of surface $PM_{2.5}$ in these 3 seasons. We cannot rule out that the PBL height was significantly underestimated in WRF-Chem, while increasing the PBL mixing could slightly improve the surface $PM_{2.5}$ simulations. The current manuscript claimed that the mixing coefficient is more important than the PBL height, but it did not show any comparison of PBL height from observations and simulations. I suggested the authors added 1) evaluate $PM_{2.5}$ simulations especially the spatial distribution with observations; 2) evaluate the WRF-Chem simulated PBL height with sonde or LIDAR observations to rule out the possibility that PBL height is more important.***

Fig. 12 shows that the control simulation CTL1 significantly overestimates the surface $PM_{2.5}$ concentration with the normalized mean biases (NMB) of 22% (winter) - 109% (summer) on regional average compared to the observations. In the sensitivity experiment EXP1 with increased nighttime boundary mixing, the NMB is reduced to 7% (winter) – 38% (summer) on regional average. Therefore, we would not agree that the performance in seasons other than winter with increasing nighttime boundary mixing is judged as poor. Emery et al. (2017) summarized many modeling applications in air quality studies and established a criterion for model evaluation. They concluded that the NMB<±15% for surface $PM_{2.5}$ on regional average can be set as the best goal that a model can be expected to achieve. Currently, only one-third of modeling applications reached. The NMB<±30% for surface $PM_{2.5}$ can be viewed as the acceptable performance of a model. Therefore, in our study, in terms of monthly mean surface $PM_{2.5}$ concentration averaged over East China, the sensitivity modeling performance with the increasing nighttime boundary mixing is acceptable in all seasons (it is a little worse than the criteria in summer), compared to the control modeling performance that is only acceptable in winter. As the reviewer suggested, now we also show the spatial distribution of modeling biases of surface $PM_{2.5}$ concentration in the four months from the experiments CTL1, CTL2, CTL3, EXP1 and EXP2 compared to the observations in Fig S15. We add more discussion in the revised manuscript as

"The model overestimates largely the monthly mean surface $PM_{2.5}$ at the stations of East China in the seasons other than winter from the control experiments. These modeling biases are significantly reduced at most stations of East China (Fig. S15 in the supporting material) in the sensitivity experiments."

We agree with the reviewer that the PBL height is very important in determining the PBL mixing. We are sorry to make the conclusion misleading. We did not intend to rule out the

importance of modeling PBL height reasonably. Now, we revise the statement in the text, such as

in the key points "Besides the PBL height, PBL mixing coefficient is also the key factor controlling the simulated diurnal cycle of surface $PM_{2.5}$ concentration in WRF-Chem"

in the abstract "Besides the PBL height, the PBL mixing coefficient is found as the critical factor determining the PBL mixing of pollutants in WRF-Chem. With reasonable PBL height, the increase of lower limit of PBL mixing coefficient during the night can significantly reduce the modeling biases in diurnal $PM_{2.5}$ and also the mean concentrations, particularly at the major cities of East China."

in the summary "The analysis indicates that although PBL height is an important factor to reflect the PBL mixing strength, the PBL mixing process is more explicitly controlled by the PBL mixing coefficient instead of the PBL height in WRF-Chem, particularly during the night."

in the discussion "However, this study reveals that the PBL mixing flux is also critical in addition to the PBL height in terms of understanding the mixing of pollutants within PBL, particularly during the night, which can not only significantly affect the diurnal variation but also the daily mean of surface pollutant concentration."

In order to evaluate the simulated PBL heights, the long-term averaged PBL heights derived from the air sounding observations at four cities (Hangzhou, Nanjing, Shanghai, Anqing) provided in Guo et al. (2016) are used for comparison. Now Fig. S11 is added to show the comparison of simulation and observation-based estimation of PBL heights at 8 am and 8 pm (local time) at four stations. In general, throughout the four seasons, the CTL3 with the YSU scheme simulates reasonable PBL heights in the early morning and night, while the CTL1 and CTL2 with the MYNN scheme overestimate the PBL heights compared to the derived values. Therefore, the positive modeling biases of surface $PM_{2.5}$ concentration during the night is not due to the model underestimation of the PBL heights, instead that it is likely due to the underestimation of PBL mixing coefficient even with reasonable PBL height. Now, more discussion is added into the revised manuscript as

"The simulated PBL heights are evaluated with the long-term averaged PBL heights, primarily for 8 am and 8 pm local time, derived based on the air sounding observations available at four stations of East China as reported by Guo et al. (2016) (Fig. S11 in the supporting material). In general, throughout the four seasons, the CTL3 with the YSU scheme simulates reasonable PBL heights in the early morning and night, while the CTL1 and CTL2 with the MYNN scheme overestimate the PBL heights compared to the derived values. The comparison between simulations and observations (Fig. 2 and 3) suggests the positive modeling biases of DI during the night may be partly due to the underestimation of the PBL mixing during the night, which cannot be explained by the modeling biases of PBL heights during the night."

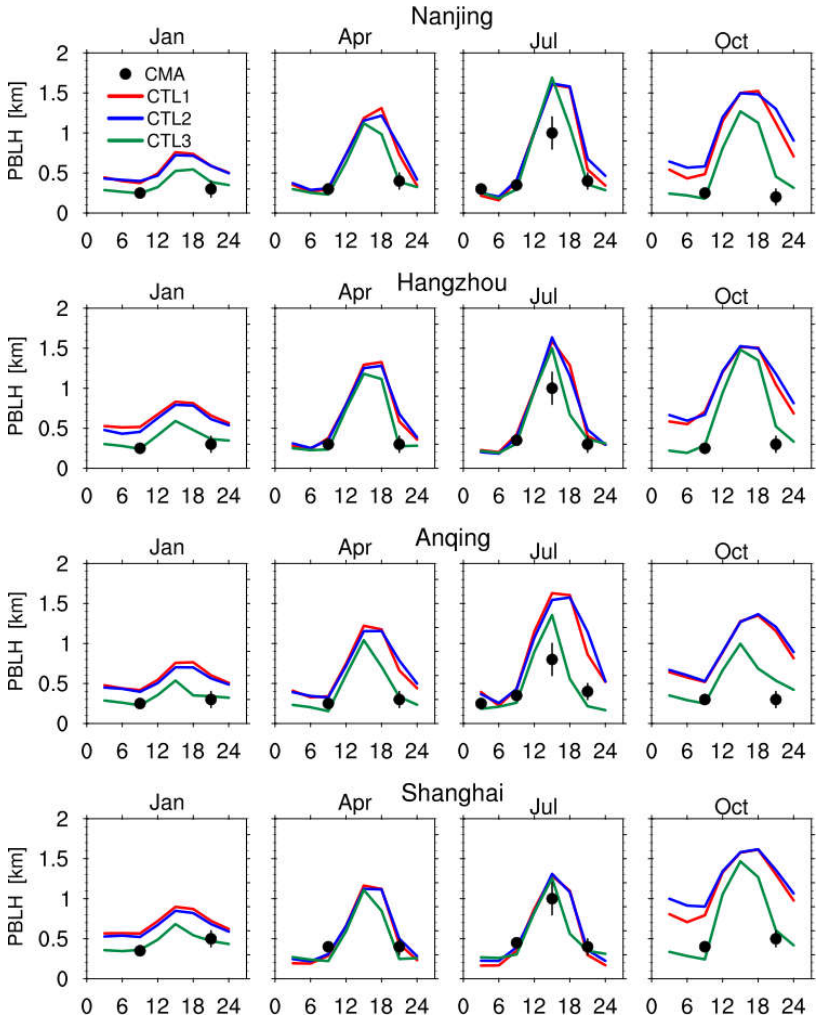

Figure S11. Diurnal variation of PBL height within 24-hour averaged at four stations in the cities of Nanjing, Hangzhou, Anqing, and Shanghai, respectively, for January, April, July, and October of 2018 from the experiments CTL1, CTL2, and CTL3. The long-term PBL heights at specific time derived from the air sounding observations at the corresponding stations are also shown as the black solid circle.

Specific comments:

- ***line 48: 'significantly overestimated' the $PM_{2.5}$ concentrations compared with observations?***

Sorry for the confusion. Now the sentence is revised as "…, and is significantly overestimated against the observation during the night".

- ***lines 72: The format of reference such as 'Davidson C I et al.' should be 'Davidson et al.'. Please correct all the references based on ACP bibliography requirement.***

Thanks for your suggestion. Now most references cited are corrected, except for those published in the same year and with first authors having the same surname. For those references, in order to distinguish them, abbreviations of first name are retained, for example, "Liu M et al., 2018" and "Liu T et al., 2018".

- ***line 94: Should 'Hu et al. (2017)' be 'Hu et al. (2016)'?***

Corrected as suggested.

- ***line 96: 'CAMQ' should be 'CMAQ'***

Corrected as suggested.

- ***line 294: In spring (Figure 2), I don't see two peaks of DI from observations. There is only one peak around 8 am in the morning. Similarly, the 'two peaks' in Oct is also not very clear. If the black dots are centered on 8 am, only one peak exists.***

Thanks for correction. Now it is revised as "In spring and autumn, the observed diurnal variation of DI is similar, showing the peak during the night, and reaching the minimum in the afternoon".

- ***line 305: I think the Figure S1 should be moved to the main article. It provided the spatial evaluation of DI from observations and simulations.***

As we discussed in the manuscript, the result shown in Fig. S1 is consistent with that in Fig. 2. There is no much additional information provided by Fig. S1. In order to keep the manuscript more concise, we decide to still keep Fig. S1 in the supporting material for the readers who are interested.

- ***line 328-329: I don't quite understand how the contribution was calculated. Looks like it is a unique function in the USTC version of WRF-Chem. Please add further explanation here.***

Yes, it is an added function in the USTC version of WRF-Chem in this study. We have mentioned briefly in the Methodology as "Particularly, in order to understand the modeling mechanisms driving the diurnal variations of surface $PM_{2.5}$ concentration over East China, this study updates the USTC version of WRF-Chem to include the diagnosis of contribution to surface $PM_{2.5}$ concentration from individual process including transport, emission, dry and wet deposition, PBL mixing, and chemical production/loss through estimating the difference of surface $PM_{2.5}$ concentration before and after individual process during the simulation.".

Now, we add more detailed description of the process contribution estimation in the Methodology as "More specifically, the contribution of each process is estimated in the following formula:

$$CT_{P,S,T} = C_{P,S,T} - C_{P,S,T0}$$

where $C_{P,S,T0}$ and $C_{P,S,T}$ represent the concentration of species *S* before (model time *T0*) and after (model time *T*), respectively, the process P. Therefore, $CT_{P,S,T}$ represents the contribution of the process *P* to the change of concentration of species *S* during the time period (*T*-*T0*). For example, if *C0* and *C* represent the surface concentrations of $PM_{2.5}$ before (*T0*) and after (*T*), respectively, the PBL mixing, the contribution (*CT*) of PBL mixing to the change of surface concentrations of $PM_{2.5}$ during the time period (*T*-*T0*) can be estimated as (*C*-*C0*). The overall contribution during a specific time period (e.g., one day) can be obtained through integrating $CT_{P,S,T}$ for that time period."

- ***line 332: Similar as above, please explain how the tendency was calculated.***

We add clarification in the revised manuscript as "The 3-hourly tendency (the difference between the current time and 3-hour ago) of surface $PM_{2.5}$ concentration is also shown."

- ***Line 355: Figure 5 shows the chemical composition of $PM_{2.5}$ simulated by WRF-Chem. Are there observations available to verify the accuracy of WRF-Chem?***

Very few observations of chemical composition of $PM_{2.5}$ at multiple stations over East China are publicly available, particularly for the simulation period of this study. Therefore, we acknowledged this need in the manuscript and suggested that the long-term measurements of $PM_{2.5}$ components at multiple stations are needed to further investigate the characteristics of diurnal variation of $PM_{2.5}$.

In addition, in the conclusion of this study, we discussed that the PBL mixing of the primary $PM_{2.5}$ determines the modelled diurnal variation of surface $PM_{2.5}$ concentration and may contribute to the modeling biases over East China. Although the observation of $PM_{2.5}$ components is not available to evaluate the diurnal variation of primary $PM_{2.5}$, the simulated diurnal variation of surface mixing ratio of CO that is normally used to represent the primary pollutant is compared with the observations (Fig. S19 in the supporting material). The results from experiments with enhanced nighttime PBL mixing are more consistent with the observations compared to the control experiments, which supports the findings about $PM_{2.5}$.

We searched the literatures, and found some observations about surface OC concentrations at Nanjing in April of 2015 (Wang, et al., 2016). We compared our simulated results with their observations at Nanjing and also found the control simulations overestimate nighttime surface OC concentrations, and the sensitivity experiments produce more consistent results (Fig. R1).

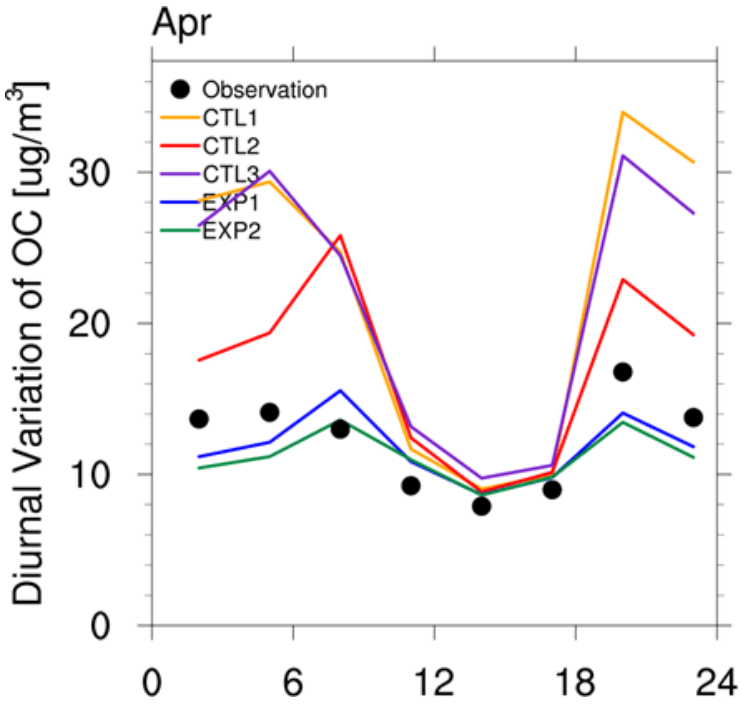

Figure R1. Diurnal variation of surface OC concentrations within 24-hour at Nanjing averaged in April. The modeling results are from the experiments in this study for 2018, and the observations are for 2015 obtained from Wang et al. (2016).

- ***Line 358: What are 'OM' and 'OIN'? I guess OM is equal to OC in Figure 5, while OIN is the total of NH4, NO3, and SO4?***

Sorry for the confusion. OC is represented as OM in WRF-Chem. OIN represents the unidentified aerosol species other than OC, BC, SO4, NH4, and NO3 in emissions, which are composed mostly of minerals in emissions. OC in Figure 5 and Figure 9 have been corrected as OM and the explanation of OIN is added in the revised manuscript "OIN represents the unidentified aerosol species other than OM, BC, sulfate, ammonium, and nitrate in emissions if any, which are composed mostly of minerals in emissions in this study.".

- ***Line 378-379: More vertical layers in the lower atmosphere could also better simulate the PBL height, which influence the surface $PM_{2.5}$ concentrations. The authors should evaluate the PBL height with observations (if available) or at least make sure the PBL heights simulated in all WRF-Chem runs are comparable.***

Yes, the configuration of vertical layers could affect the simulation of PBL height. In fact, we have shown the comparison of PBL heights from the simulations with different vertical configuration in Fig. 6 in the manuscript. As we can see that the difference in PBLH between CTL1 and CTL2 is very small. In addition, now, we add the evaluation of PBLH from different experiments with the long-term averaged PBL heights derived from the air sounding observations at four cities (Hangzhou, Nanjing, Shanghai, Anqing) provided in Guo et al. (2016) in the revised manuscript (Fig. S11). Now, in the revised manuscript, Fig. S11 shows that the PBLH from the experiments with different vertical configurations is comparable. The details can be found in our response to your comment above.

- ***Line 412-413: As above, this statement is only valid if the PBL heights simulated in CTL1-3 runs are comparable.***

First of all, the PBL height and PBL mixing are related instead of discrepant. This statement only means that the PBL mixing between CTL3 and CTL2 is different. It is not necessary to conclude that the PBL heights between them are comparable or different. More detailed analysis about the reason of different PBL mixing is discussed in section 3.2.2. The comparison between the PBL heights from CTL1-3 is shown in Fig. 6 and Fig. S11 in the revised manuscript. More discussion is added as in the response to your comments above.

- ***Line 434: Hard to tell from the figure, but I think the PBL height from CTL 1-3 are substantially different. For instance, at 8 am in Apr with the maximum surface $PM_{2.5}$ simulated, CTL 3 has much lower PBL height as compared with CTL1 and 2. Again, if observations such as LIDAR are available, it will be great to see which run has the better PBL height. Same as in Figure 7, I suggest plotting all the PBL height from WRF-Chem runs in one figure to see the difference.***

See our response to your comments above. Now Fig. S11 is added in the revised manuscript

for direct comparison of PBLH among all the experiments and observation derived dataset. The PBLH is comparable between CTL1 and CTL2, while it is true that the PBLH is different between CTL2 and CLT3. In fact, we discussed about their different PBLH in the manuscript as "This leads to the large difference of DI between CTL1 and CTL2 with different thicknesses of first model layer during the night although they simulate similar PBL heights. Another example in autumn, the PBL heights during the night are lower in CTL3 than in CTL1, while the DI during the night are higher in CTL1 than in CTL3 (Fig. 3) due to the weak PBL mixing coefficients during the night that cannot mix the pollutants up to the PBL height. This further demonstrates that the WRF-Chem simulated diurnal variation of surface PM2.5 concentration is not explicitly controlled by the PBL height instead by the PBL mixing coefficient.".

We add more discussion about the PBLH among the experiments in the revised manuscript as "The CTL3 simulates similar PBL height during the daytime but lower values during the night, particularly in October. The simulated PBL heights are evaluated with the long-term averaged PBL heights, primarily for 8 am and 8 pm local time, derived from the air sounding observations available at the four stations of East China as reported by Guo et al. (2016) (Fig. S11 in the supporting material). In general, throughout the four seasons, the CTL3 with the YSU scheme simulates reasonable PBL heights in the early morning and night, while the CTL1 and CTL2 with the MYNN scheme overestimate the PBL heights compared to the derived values."

- ***Line 474: Any reference or data to support the 5 m2/s rate is reasonable?***

The one of the key points of this study is that the PBL mixing during the night over East China may be underestimated by WRF-Chem. Increasing of PBL mixing during the night can significantly reduce the modeling biases of surface $PM_{2.5}$ concentration and also the modeling sensitivity to the PBL configuration. The exact value of PBL mixing coefficient cannot be obtained by this study. The lower limit rate of 5 m^2/s was selected to show the sensitivity. We acknowledged in the manuscript as "It is noteworthy that the lower limit parameter of 5 m^2/s is entirely empirical. It is selected to represent the moderate mixing strength between the full PBL mixing and no PBL mixing. A few other values such as 1 m^2/s and 10 m^2/s are also tested. The results do not change the conclusion found in this study and therefore are not shown."

- ***Line 575-576: Does MEIC inventory treat power plants as point sources? For instance, US EPA has lat/lon information and hourly emission rate to process power plants as point sources in SMOKE. If not, how to support this argument?***

Yes, the power plant emissions in the MEIC inventory are treated as point sources. As shown in Figure R2, the power plant emissions of SO_2 and $PM_{2.5}$, for example, in the MEIC inventory are distributed discretely.

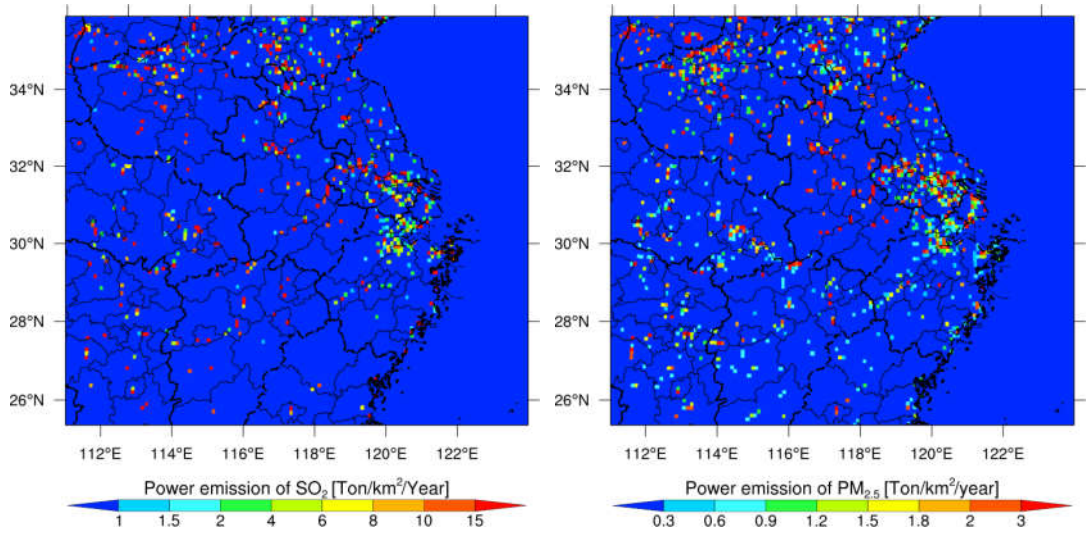

Figure R2. Spatial distribution of power plant emissions of SO_2 and $PM_{2.5}$ from the MEIC inventory.

- ***Line 588: The current version of Section 4 is too long. A concise summary of the paper is needed. I suggest the authors to revise this session.***

Thanks for your suggestion. The Section 4 is now split into two sections, Section 4 (Summary) and Section 5 (Discussion) in the revised manuscript. The summary section is more concise in the revised manuscript.

- ***Line 1183: The unit is %?***

Yes, it is. Now it is clarified.

- ***Line 1187: Plots in Figure 1a are small and hard to see the details. Please remove the black box and symbols for cities in NOx and SO2 plots.***

Figure 1a is revised following your suggestion.

- ***Line 1245: Surprised to see the chemistry contributed so little in the surface $PM_{2.5}$ concentrations. Does 'chemistry' stand for chemical evolution such as formation of SOA?***

Based on Fig. 4, we can only say the relative contribution from chemistry to the change of $PM_{2.5}$ concentration is small compared to the processes of emission, transport, and PBL mixing. As we respond to your comment above, if *C0* and *C* represent the surface concentrations of $PM_{2.5}$ before (*T0*) and after (*T*), respectively, the chemical production/loss of aerosols, the contribution (*CT*) of chemistry to the change of surface concentrations of $PM_{2.5}$ during the time period (*T-T0*) is estimated as (*C-C0*). Therefore, the chemistry contribution includes all the chemical evolution such as the secondary production. However, as we mentioned in the manuscript, the WRF-Chem simulations conducted in this study do not consider the SOA production that still has large uncertainties in mechanisms.

The relatively small contribution from chemical production may be due to that the stations are mostly urban and suburban areas, where the surface $PM_{2.5}$ concentrations are dominated by the primary emissions. We checked that the chemical contribution to the surface $PM_{2.5}$

concentration over the rural areas can be comparable to transport, and larger than emission.

- ***Line 1373: A map of data in Figure 12 is needed, maybe in the SI to show the spatial performance of WRF-Chem.***

In fact, we have shown the observational sites in Fig. 1a. Now we clarify it in the caption of Fig. 12. For the spatial performance of model, now we add Fig. S15 in the supporting material to show the spatial distribution of modeling biases of surface $PM_{2.5}$ concentration in the four months from the experiments CTL1, CTL2, CTL3, EXP1 and EXP2 compared to the observations. Please see our response to your comments above for details.

Anonymous Referee #2

General comments:

- ***This study investigates the simulation of diurnal variation of surface $PM_{2.5}$ concentration over East China in WRF-Chem. The authors test sensitive of model simulations to PBL configuration, PBL mixing coefficient, emission diurnal variation and injection height, etc. It is found that diurnal variation of surface $PM_{2.5}$ is mostly sensitive to PBL mixing coefficient, while diurnal cycle and injection height of anthropogenic emission has smaller impacts than PBL mixing coefficient. It is a nice model sensitivity study. However, the evaluation of the model performance is simply based on surface $PM_{2.5}$ observations. As discussed in the manuscript, the diurnal variation of surface $PM_{2.5}$ is impacted by emission, PBL mixing and transport. It will make the results more convincing by including more model evaluation on the simulation of aerosol and meteorological variables, such as temperature, moisture, wind, stability, PBL height, aerosol speciation, vertical distribution of aerosols, etc.***

We thank the reviewer for the detailed and constructive comments. They are very helpful for improving the quality of the manuscript.

In the revised manuscript, we added a few new figures in the supporting material to support some statements in the text and to address the review comments. Specifically, the evaluation of model performance in some associated meteorological fields, such as temperature, wind, and PBL height, is added. The observed vertical profiles of aerosol are not available for evaluation, and are discussed in the revised manuscript. The publicly available aerosol speciation observations are few over East China. We evaluated the diurnal variation of CO as the representative primary pollutant. In this response, we found some data about OC during other period and added here as the reference. The information about how to calculate the PBL mixing coefficient is briefly described in the methodology section. Other text and figures have also been revised as the reviewer suggested.

Specific comments:

- ***L78: and precipitation.***

Revised as suggested.

- ***L136: What about Liu M et al. (2018)? What are they findings?***

Liu, M et al. (2018) used the nested GEOS-Chem CTM version 9-02 and WRF/CMAQ v5.0.1 to simulate NO2, $PM_{2.5}$, and other pollutants over China in October–December 2013. They found that the air quality model (WRF-CMAQ v5.0.1) also overestimated the surface concentration of $PM_{2.5}$ during the nighttime in October-December, 2013. They speculated that the overestimation is due to the weak PBL mixing in the nighttime, and claimed that the newer version of CMAQ v5.1 driven by WRF v3.7 revised the PBL mixing scheme (ACM2) and might reduce the nighttime biases. According to the technical documentation of CMAQ v5.1, the PBL mixing scheme (ACM2) in the previous versions produce too weak mixing under stable atmospheric conditions due to the assumption of the same value for the eddy diffusivity of momentum (K_m) and heat (K_h) and the unity Prandtl number (Pr = Km/Kh). In CMAQ v5.1 driven by WRF v3.7, the ACM2 estimates and applies different eddy

diffusivities for momentum (K_m) and heat (K_h) and develop new stability functions for both momentum and heat for stable conditions, so the deficiency in boundary mixing under stable atmospheric condition may be improved.

To verify the effect of this modification, we conduct two experiments use ACM2 PBL schemes in WRF-Chem v3.5 (ACM2.v3.5) and WRF-Chem v4.0 (ACM2.v4.0), respectively, over East China for October of 2018. As shown in Figure R3, the PBL mixing coefficients in ACM2.v4.0 are enhanced compare to that in ACM2.v3.5, especially during night. In addition, the simulated surface $PM_{2.5}$ concentrations from ACM2.v4.0 are reduced during night compared to ACM2.v3.5 (Fig. R4). However, the model still significantly overestimates the surface $PM_{2.5}$ concentration comparing to the observations (Fig. R4). We add the discussion in the revised manuscript as "Liu M et al. (2018) found that the air quality model (WRF-CMAQ v5.0.1) also overestimated the surface concentration of $PM_{2.5}$ during the nighttime in October-December, 2013. They speculated that the overestimation is due to the weak PBL mixing in the nighttime, and claimed that the newer version of CMAQ v5.1 driven by WRF v3.7 revised the PBL mixing scheme (ACM2) and might reduce the nighttime biases. To verify this, two experiments are conducted using the ACM2 PBL scheme with WRF-Chem v3.5 and WRF-Chem v4.0, respectively, over East China for October of 2018. The results showed that the PBL mixing of ACM2 scheme is enhanced in v4.0 compared to v3.5 especially during the night, and the simulated nighttime surface $PM_{2.5}$ concentrations are reduced to some extent in v4.0 compared to v3.5 (not shown). However, the simulation still significantly overestimates the surface $PM_{2.5}$ concentration during the night. Therefore, the changes of PBL schemes and vertical configurations within the PBL can affect the simulated DI but cannot improve the simulations to reproduce the observations."

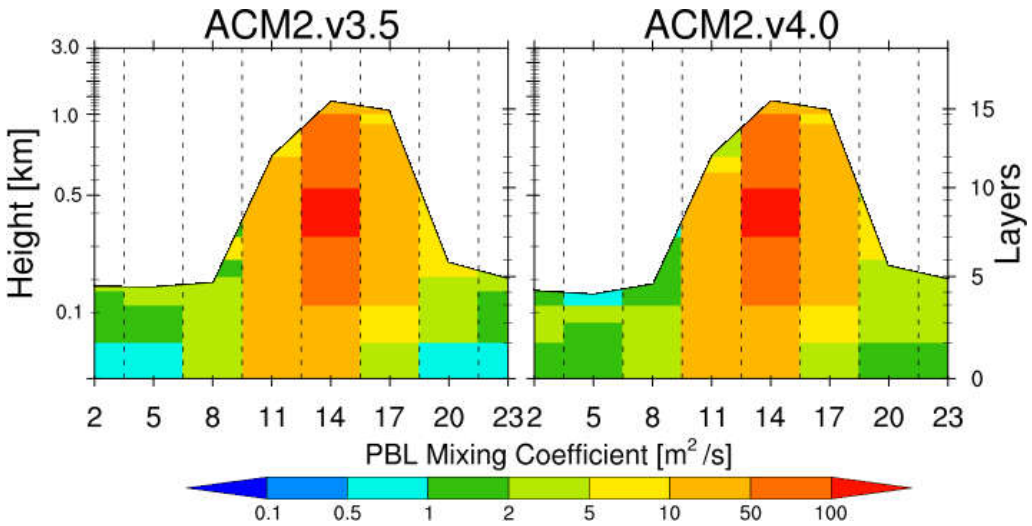

Figure R3. Diurnal variation of PBLH and PBL mixing coefficient below PBLH averaged over Hefei for October of 2018 from the experiments ACM2.v3.5, ACM2.v4.0.

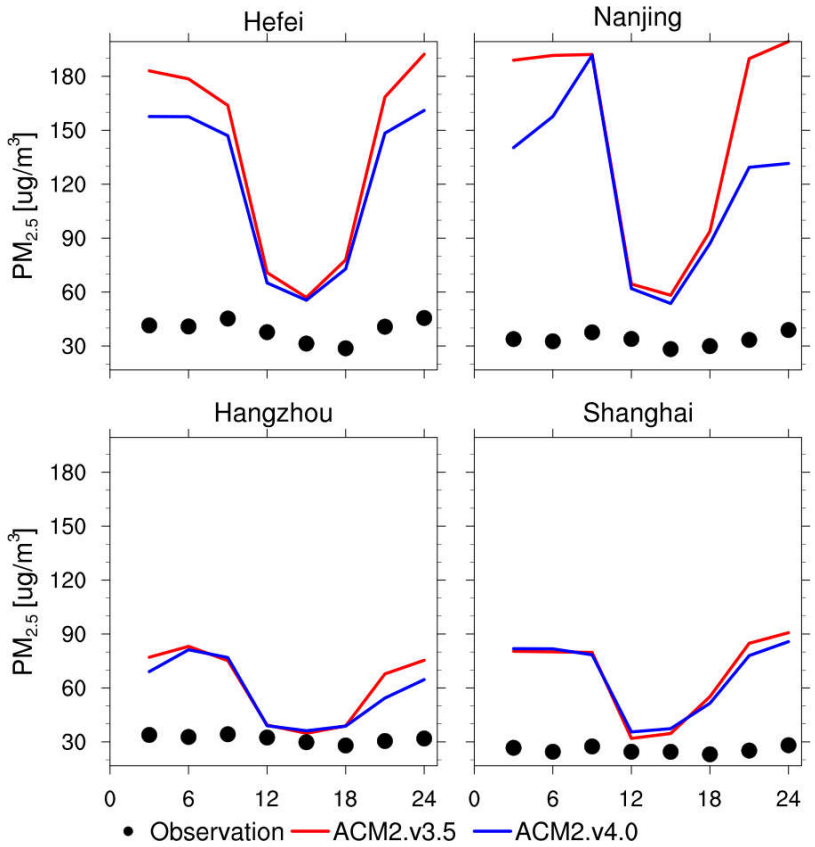

Figure R4. Diurnal variation of surface $PM_{2.5}$ concentrations within 24-hour averaged over four cities (Hefei, Nanjing, Hangzhou, Shanghai) for October of 2018 from the experiments ACM2.v3.5, ACM2.v4.0 and observations.

- ***L233: Which emission (anthropogenic emission, biomass burning, dust or others) is the primary contributor(s) to the surface $PM_{2.5}$ over East China in different season?***

As shown in Fig. 5, over East China, the dominant emission for surface $PM_{2.5}$ concentration in all seasons are from anthropogenic emission.

- ***L325-327: How does the model simulate the diurnal cycle of temperature, moisture, wind, stability and PBL height? Could the biases in model simulated meteorological variables contribute to the bias in diurnal cycle of surface $PM_{2.5}$?***

Yes, the basic meteorological fields are important for simulating air pollutants. We didn't evaluate them because our simulations are nudged to the reanalysis and WRF simulations has been widely evaluated over China in previous studies. Following your suggestion, now we add Fig. S6-S11 in the revised manuscript about evaluating the simulated wind, temperature, and PBL height. We also add the discussion in the revised manuscript as "In order to understand the possible reasons for this modeling biases, some basic meteorological fields are evaluated with available observations. Since the modeled winds at the layers above the PBL are nudged towards the reanalysis data, the large-scale circulation can be well simulated. The winds at 850 hPa for each season are compared with the NCEP Final reanalysis dataset (FNL) and ERA5 reanalysis dataset (https://rda.ucar.edu/datasets/ds630.0/, last access: 28 December 2019) (Fig. S6 in the supporting material). The simulated wind circulation is highly correlated with the two reanalysis datasets with the spatial correlation coefficients of 0.9-0.97

over East China. The simulated temperature at 2m is also evaluated with the available observations by the China Meteorological Administration (CMA) at the stations of East China (Fig. S7 and Fig. S8 in the supporting material). The model captures the diurnal variation of near-surface temperature very well over East China. For near surface winds, although the model generally overestimates the observed values by less than 10%, the simulated diurnal variation is generally consistent with the observations over East China (Fig. S9 and Fig. S10 in the supporting material). As the evaluation shows, the basic meteorological fields are generally simulated reasonably. The characteristics associated with the PBL mixing are further investigated below."

And "The simulated PBL heights are evaluated with the long-term averaged PBL heights, primarily for 8 am and 8 pm local time, derived from the air sounding observations available at the four stations of East China as reported in Guo et al. (2016) (Fig. S11 in the supporting material). In general, throughout the four seasons, the CTL3 with the YSU scheme simulates reasonable PBL heights in the early morning and night, while the CTL1 and CTL2 with the MYNN scheme overestimate the PBL heights compared to the derived values. The comparison between simulations and observations (Fig. 2 and 3) suggests the positive modeling biases of DI during the night may be partly due to the underestimation of the PBL mixing during the night, which cannot be explained by the positive modeling biases of PBL heights during the night."

- ***L356-357: Is there any aerosol speciation data available to evaluate the model performance?***

Very few observations of chemical composition of $PM_{2.5}$ at multiple stations over East China are publicly available, particularly for the simulation period of this study. Therefore, we acknowledged this need in the manuscript and suggested that the long-term measurements of $PM_{2.5}$ components at multiple stations are needed to further investigate the characteristics of diurnal variation of $PM_{2.5}$.

In addition, in the conclusion of this study, we discussed that the PBL mixing of the primary $PM_{2.5}$ determines the modelled diurnal variation of surface $PM_{2.5}$ concentration and may contribute to the modeling biases over East China. Although the observation of $PM_{2.5}$ components is not available to evaluate the diurnal variation of primary $PM_{2.5}$, the simulated diurnal variation of surface mixing ratio of CO that is normally used to represent the primary pollutant is compared with the observations (Fig. S19 in the supporting material). The results from experiments with enhanced nighttime PBL mixing are more consistent with the observations compared to the control experiments, which supports the findings about $PM_{2.5}$.

We searched the literatures, and found some observations about surface OC concentrations at Nanjing in April of 2015 (Wang, et al., 2016). We compared our simulated results with their observations at Nanjing and also found the control simulations overestimate nighttime surface OC concentrations, and the sensitivity experiments produce more consistent results (Fig. R1).

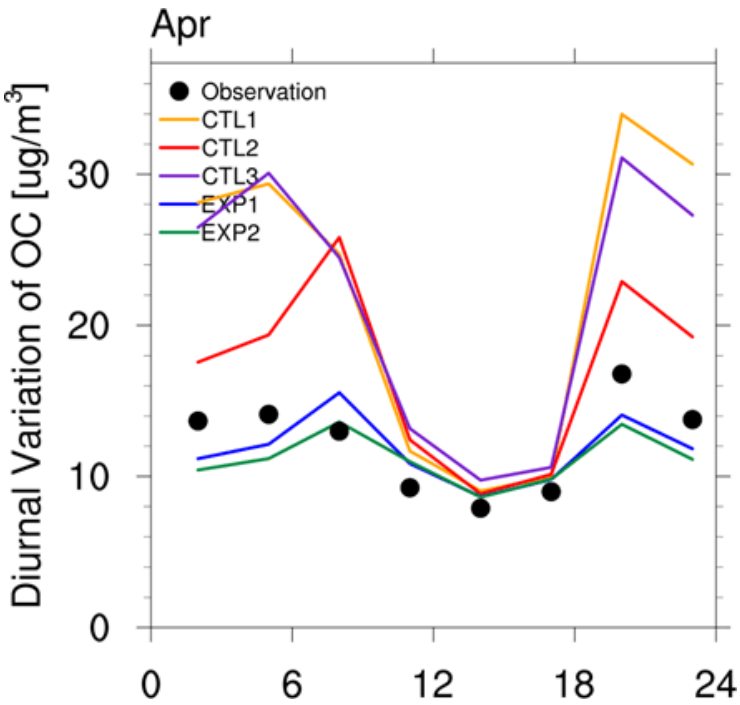

Figure R1. Diurnal variation of surface OC concentrations within 24-hour at Nanjing averaged in April. The modeling results are from the experiments in this study for 2018, and the observations are for 2015 obtained from Wang et al. (2016).

- ***L430: How is PBL mixing coefficient calculated?***

The calculations of PBL mixing coefficient are different in different turbulence closure type of PBL schemes. Now we add more description in the revised manuscript as "Since this study focuses on understanding the PBL mixing impact, the calculation of PBL mixing coefficient within the MYNN2 and YSU PBL schemes is briefly described here. In the local closure PBL scheme MYNN, the PBL mixing coefficient is calculated following Mellor et al. (1982):

$$K_{h,m} = lqS_{h,m}$$

where l is the mixing-length scale, S_h and S_m are stability functions, q is related to the turbulent kinetic energy (TKE) in the following formula:

$$q = (2 * TKE)^{1/2}$$

In the non-local closure PBL scheme YSU, the momentum mixing coefficient K_m is formulated following Hong et al. (2006):

$$K_m = kw_s z(1 - \frac{z}{h})^p$$

where p is the profile shape exponent taken to be 2, k is the von-karman constant, z is the height from the surface and h is PBL height. For the eddy mixing coefficient for temperature and moisture K_h can be estimated from K_m with the relationship of the *Prandtl* number as in Noh et al. (2003):

$$\mathrm{Pr} = K_m / K_h$$

$$\mathrm{Pr} = 1 + (\mathrm{Pr}_0 - 1)\exp[\frac{-3(z-sh)^2}{h^2}]$$

Two additional sensitivity experiments (EXP1 and EXP2, Table 1) are also conducted corresponding to the experiments CTL1 and CTL2, respectively, except that the PBL mixing

coefficient is modified (see details in Section 3.2.2)."

- ***L364: Is there any in-situ observation of the vertical distribution of aerosols in the boundary layer? The CALIPSO data may be useful to validate the simulated aerosol profiles.***

It would be great if there are in-situ observed vertical profiles of pollutants over cities to evaluate the simulations, particularly for below 200 m and during the night. However, as we are aware, there is no dataset publicly available for evaluation of our simulations over East China. It is encouraged in the discussion section as "Therefore, this study suggests that the long-term measurements of $PM_{2.5}$ components at more stations and the in-situ measurements of vertical profiles of $PM_{2.5}$ concentration within PBL during the night are needed to further investigate the characteristics of diurnal variation of $PM_{2.5}$".

CALIPSO retrievals are useful, particularly during the night. However, over the urban area such as East China with a lot of tall buildings, the retrievals near the surface (< 100 m) are mostly contaminated by the surface reflection signals. We did check the CALIPSO retrievals. Few of the vertical profiles near the surface is valid.

- ***Figure 4: What is the unit of each variable? And what is the black line?***

In Fig. 4, the contribution and tendency are normalized values by monthly mean surface $PM_{2.5}$ concentration for each month. The original units of contribution and tendency are ug/m^3. After normalization, they are relative values as the ratios. The black line is the 3-hourly relative tendency of surface $PM_{2.5}$ concentrations. It is now clarified in the caption of Fig. 4 as "Relative contribution (normalized by monthly mean surface $PM_{2.5}$ concentration for each month) to surface $PM_{2.5}$ concentration every 3-hour from individual process (transport, emission, dry and wet deposition, PBL mixing, chemical production/loss) averaged over Hefei for January, April, July, and October of 2018 from the experiments CTL1, CTL2, and CTL3. The 3-hourly relative tendency of surface $PM_{2.5}$ concentration is also shown as the black line."

Anonymous Referee #3

General comments:

- ***This study is focused on one of the key uncertainties in modeling and forecasting of air pollution, the parameterization of turbulent mixing of chemical species and its impact on hourly variability of the modeled concentrations of fine particulate matter ($PM_{2.5}$). The sensitivity of the $PM_{2.5}$ simulations to the diurnal cycle and vertical distribution of the anthropogenic emissions is analyzed here as well. The modeling study deploys one of the widely used atmospheric chemistry models - WRF-CHEM. A number of WRFCHEM model simulations are conducted over East China for all the seasons, year of accurate simulation of diurnal variability of the ground level $PM_{2.5}$ is crucial for air quality forecasting applications. It is great to see that this topic is addressed by such rigorous modeling study. This study deserves a publication, but I have reservations on the interpretation of some of the results and conclusions presented here. I suggest addressing the following comments before a final publication in ACP.***

We thank the reviewer for the detailed and constructive comments. They are very helpful for improving the quality of the manuscript. In the revised manuscript, we add the discussion about using the simple modification to enhance the nighttime PBL mixing and its difference from the existing scheme in WRF-Chem. We add more clarification about the model and emission configurations. Other text and figures have also been revised as the reviewer suggested.

Major comments:

- ***The authors show that setting a minimum exchange coefficient for chemicals in WRFCHEM improves the simulation results, especially in winter. Actually the WRF-CHEM model has already included this feature for many years. In the community version of the model the exchange coefficients (ECs) that are used for mixing of the chemical species are modified based on the anthropogenic CO and primary $PM_{2.5}$ emissions. This simple parameterization isn't perfect, but it was designed to help with the strong accumulation of air pollutants near surface, when the modeled boundary layers are too shallow. Why didn't the authors use the existing parameterization in WRF-CHEM? Instead they set the lower limit of the ECs everywhere in the model grid.***

Yes, we noticed that this parameterization is in the community version of WRF-Chem and also in our USTC version of WRF-Chem. Although it is included in WRF-Chem for a few years, we didn't notice any publications about its application, particularly over China. We didn't find the reference for this parameterization in the code as well. If the reviewer can provide the reference, we'd like to cite it.

In addition, it is only for gases if the MOSAIC or MADE/SORGAM aerosol schemes are used because it does not couple with the aerosol activation scheme even in the latest version of WRF-Chem (v4.1), although it can be modified to be compatible with the MOSAIC scheme. This parameterization treats the enhancement of exchange coefficient up to half number of model vertical layers, which is beyond the PBL in most cases during the night and may not be suitable. We prefer adjusting the coefficient only within PBLH. This parameterization also assumes the PBL mixing is only enhanced in the region with intense emission due to urban island effect. For example, Fig. R5a and 5b show the spatial

distributions of anthropogenic emissions of $PM_{2.5}$ and CO exceeding the threshold defined inside of the parameterization. They occur mostly over the big cities of East China. We acknowledged this urban effect in our discussion section, and in fact are working on this issue. However, we noticed that the issue of PBL mixing during the night may not only occur over these urban areas. Therefore, in this study, we omitted this modification and simply adjusted the minimum value of coefficient within PBL height everywhere. It is noteworthy that our study intended to conduct the sensitivity experiments to raise this issue in using WRF-Chem to simulate surface $PM_{2.5}$ over East China and provide the suggestion about potential influential factors, instead of to provide a simple empirical parameterization.

Now, we add this discussion in the revised manuscript as "In fact, in WRF-Chem, there is an existing empirical parameterization to enhance the PBL mixing of pollutants in urban area based on the strength of anthropogenic emissions. However, it is only applied to gas pollutants if the MOSAIC aerosol scheme is selected as this study. It also tends to enhance the mixing up to half number of model vertical layers, which is beyond the PBL in most cases during the night. In this study, in order to examine the sensitivity of simulated DI to the PBL mixing coefficient, the sensitivity experiments, EXP1 and EXP2, are conducted corresponding to CTL1 and CTL2, respectively, through setting the lower limit of PBL mixing coefficient from 0.1 m2/s (default in the publically released version of WRF-Chem) to 5 m2/s within the PBL, which is applied to both gas and aerosol pollutants."

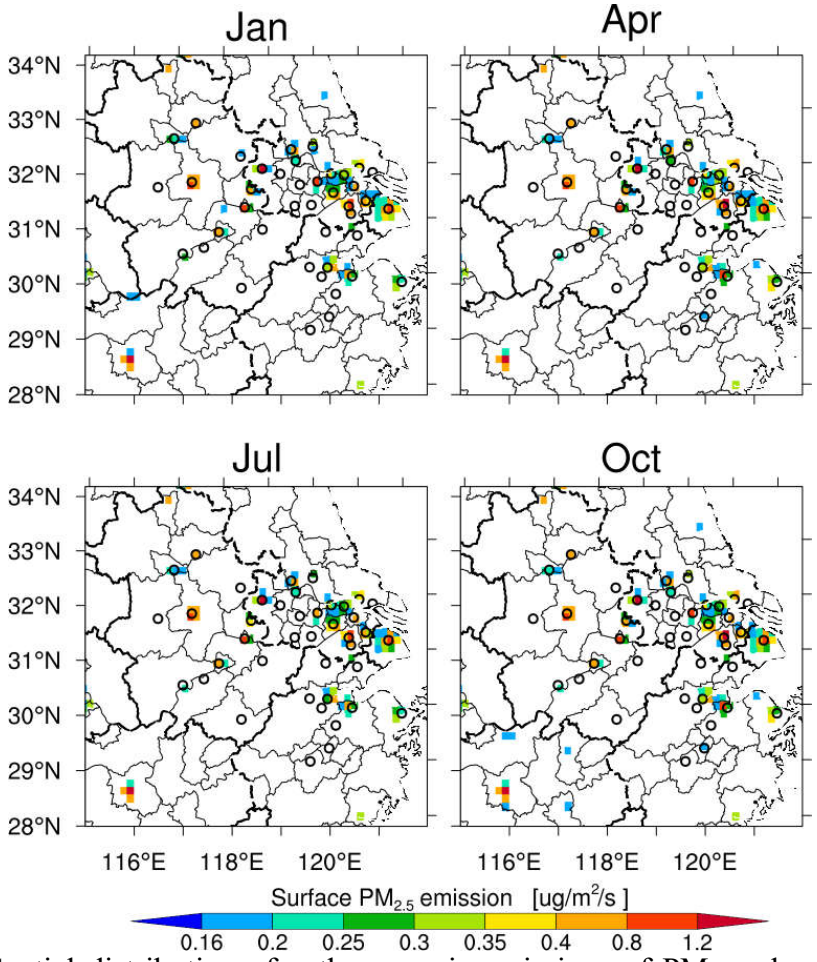

Figure R5a. Spatial distribution of anthropogenic emissions of $PM_{2.5}$ where the exchange coefficient will be modified if using the current parameterization in WRF-CHEM.

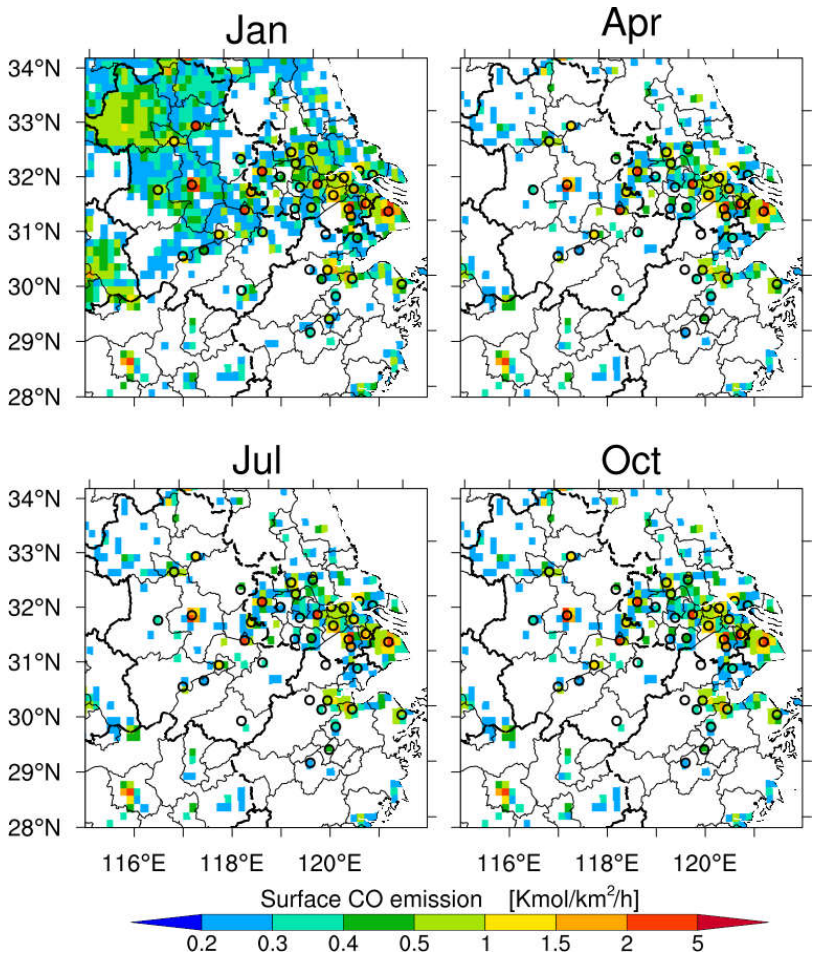

Figure R5b. Same as Fig. R5a, but for anthropogenic emissions of CO.

- ***There are discussions of the mismatch between the diagnosed planetary boundary layer (PBL) heights and ECs in WRF-CHEM. I want to remind that both the YSU and MYNN PBL schemes are non-local schemes. The non-local mixing is omitted in vertical mixing of chemicals as ECs from the PBL schemes are only used in the chemical mixing part of WRF-CHEM. Therefore, the vertical mixing of the chemicals isn't always consistent with the parameterization of PBLs in the WRF part of the model.***

According to Hong et al. (2006) and Nakanishi and Niino (2006), YSU and MYNN PBL schemes are non-local and local schemes, respectively. Therefore, both types of PBL schemes are examined in our study. The results show that two schemes lead to difference in surface $PM_{2.5}$ concentration, but are consistent in overestimating nighttime concentrations. For PBL mixing of chemical species, the scheme only needs the input of PBL mixing coefficient diagnosed from the PBL schemes. The non-local and local PBL schemes will diagnose different mixing coefficients that will affect the mixing of chemical species. Therefore, in this sense, the mixing in chemistry part is consistent with the meteorological part in terms of the difference in local and non-local treatments. Now we add more details about the two PBL schemes and their estimation of PBL mixing coefficients in the revised manuscript as response to other reviewers.

- ***Another uncertainty in the PBL parameterization is that the PBL height is diagnosed differently in the individual PBL schemes of WRF. For consistency I suggest using the same diagnostics (e.g. based on bulk Richardson number) to determine the PBL height from the model cases with the YSU and MYNN schemes.***

The PBL height diagnosis is normally treated as the part of PBL scheme when use WRF or WRF-Chem, unless studies are investigating the difference between PBL parameterizations, which is beyond the scope of this study. This study focuses on the PBL mixing of pollutants, and the PBL mixing coefficient is the only input parameter into the chemical mixing scheme in WRF-Chem.

- ***The sensitivity of the diurnal variation of the simulated $PM_{2.5}$ to the model vertical resolution is presented here. The horizontal resolution of the nested model grid is 15km. This is quite coarse resolution, which makes harder to capture the effects of the urban island effect, inversions in the valleys, cold pool events and so forth. The authors are trying to improve the simulation of the PBL structure by refining the vertical resolution, while the horizontal grid remains the same. This shortcoming of the horizontal model grid needs to be discussed. I suggest moving the sensitivity case with the modified vertical resolution into SI.***

We agree that the modeling results of pollutant surface concentrations may vary with model horizontal resolution. However, many studies conducted the WRF-Chem simulations at horizontal resolutions of 10 km and coarser to investigate air pollution issue over China (e.g., Jiang et al., 2012; Tao et al., 2015; Gao et al., 2016; Zhang et al., 2016; Zhong et al., 2016; Zhao et al., 2017; Liu et al., 2018; Miao et al., 2018; Du et al., 2019; Wang et al., 2019). Specifically, Tao et al. (2015) examined the impacts of urbanization on meteorology and air quality during the month of July from 2008 to 2012 over East China at the comparable horizontal resolution (10 km) with this study, and found that urbanization tends to decrease surface concentration of $PM_{2.5}$ and increase it at higher altitudes. We believe the sensitivity experiments with varied vertical resolution at 15 km horizontal resolution are informative to readers and can provide useful reference for other researchers. Therefore, we decide to keep this part in the main text of manuscript.

In addition, although modeling studies at higher horizontal resolution may provide different values of pollutant surface concentration, we did one sensitivity experiment at 4 km and found it did not change the conclusion of this study. We add the discussion in the revised manuscript as "The model horizontal resolution may also affect the modeling results of PBL mixing and urbanization. However, one sensitivity experiment at 4 km horizontal resolution shows that the PBL mixing at the stations does not change significantly (not shown). The modeling at higher resolution particularly down to large-eddy scale deserves further investigation."

- ***The authors consider the injection height of the anthropogenic emissions from the point sources in the model domain. This is advantageous as in many models (especially most of the global atmospheric chemistry models) all the anthropogenic emissions are released in the first model layer. However, it isn't clear how the injection heights for the emissions in East China are estimated in the study. Do the injection heights vary by***

weather and/or season? This will have a significant impact on the sulfate simulations, for example.

This study uses the vertical variation profiles of power plant emissions following Wang et al., (2010). They derived the vertical profiles for East Asia based on the dataset of the U.S. and found that the profiles are comparable to those estimated in China and Japan (Woo et al., 2003; Wang et al., 2010). The injection heights are prescribed without temporal variations. Now we add the clarification in the revised manuscript as "Since diurnal variation of emissions and injection height of power plant emissions may have impacts on diurnal variation of surface pollutants, the experiments discussed above apply the diurnal profiles of anthropogenic emissions from five individual sector (i.e., agriculture, industry, transport, energy, and residential) following Olivier et al. (2003) and Wang et al. (2005) as shown in Fig. 1c and vertical distributions of anthropogenic power plant emissions following Wang et al. (2010) as shown in Table 2. Wang et al. (2010) derived the vertical profiles for East Asia based on the dataset of the U.S. and found that the profiles are comparable to those estimated in China and Japan (Woo et al., 2003; Wang et al., 2010)." and "Both diurnal and vertical variation profiles of anthropogenic emissions are prescribed without temporal variability."

- ***3.1. Why the model results are sampled on 3 hourly intervals, when the observations are available every hour?***

The outputs of pollutant concentrations in our experiments are every 3-hour to reduce the disk storage and increase the computational speed. This should not affect our investigation of diurnal variation. When comparing modeling results and observations, hourly observations are sampled at the model output frequency, i.e., 3-hourly.

- ***The uncertainties related to simulation of the biogenic VOC emissions aren't discussed in the paper. The modeled fluxes of the BVOC species will vary depending on the PBL scheme and model grid.***

The most significant impact of BVOC on surface $PM_{2.5}$ concentration may be through its impact on SOA. As we discussed, the SOA production is not considered in this study and its impact is mainly in summer. Therefore, we did not discuss the impact of BVOC in this study.

- ***How are the biomass burning emissions vertically distributed in the model? What diurnal cycle is applied to them?***

The biomass burning emissions in this study are from the global FINNv1.5 emission dataset, which was derived based on the MODIS Collection 6 (C6) fire detections. The FINN biomass burning dataset provides diurnal variations of emission fluxes following the Western Regional Air Partnership profile-WRAP (Freitas et al., 2009; Wiedinmyer et al., 2011; WRAP 2005). In this study, biomass burning emissions are vertically distributed following the injection heights suggested by Dentener et al. (2006) from the Aerosol Comparison between Observations and Models (AeroCom) project. Now, we add the clarification in the revised manuscript as "The biomass burning emissions follow the diurnal variation provided by WRAP (2005) and the injection heights suggested by Dentener et al. (2006) from the Aerosol Comparison between Observations and Models (AeroCom) project."

- ***The importance of accurate SOA simulations during summertime is discussed in the Summary. The simulation of the SOA contribution to the total $PM_{2.5}$ concentrations can help to capture the daytime maxima of the $PM_{2.5}$ concentrations in summer. This point has to be made clear in the main text, not in Summary. Why the authors didn't include the simulations with the SOA scheme in the main text?***

As we mentioned in the discussion section, we didn't consider the SOA production mechanism in this study because the current SOA mechanism in WRF-Chem is still highly uncertain. There is scarce observation for SOA evaluation over East China. We tend to avoid introducing another highly uncertain factor when focusing on studying the PBL mixing. As we discussed, it only affects significantly the diurnal variation of surface $PM_{2.5}$ concentration in summer. Therefore, we decide to just mention it in the discussion section and suggest future investigation.

Minor comments:

- ***Line 140: For WRF and WRF-Chem you can also cite this paper: Powers, J. G., et al. (2017), THE WEATHER RESEARCH AND FORECASTING MODEL Overview, System Efforts, and Future Directions, Bull. Amer. Meteorol. Soc., 98(8), 1717-1737, doi:10.1175/bams-d-15-00308.1.***

Thanks for your suggestion. Now this paper is cited.

- ***Throughout the text "s" is omitted in plural words: e.g. lines 386, 399, 419. There are other spelling errors as well.***

Thanks for checking. Now all of them are corrected.

- ***Line 199: I believe this reference is wrong: Lacono et al.. . .***

Now the reference is revised as "Iacono et al., 2000".

Reference

Chen, S., Zhao, C., Qian, Y., Leung, L. R., Huang, J., Huang, Z., Bi, J., Zhang, W., Shi, J., Yang, L., Li, D., and Li, J.: Regional modeling of dust mass balance and radiative forcing over East Asia using WRF-Chem, Aeolian Research, 15, 15–30, doi:10.1016/j.aeolia.2014.02.001, 2014.

Dentener, F., Kinne, S., Bond, T., Boucher, O., Cofala, J., Generoso, S., Ginoux, P., Gong, S., Hoelzemann, J. J., Ito, A., Marelli, L., Penner, J. E., Putaud, J.-P., Textor, C., Schulz, M., van der Werf, G. R., and Wilson, J.: Emissions of primary aerosol and precursor gases in the years 2000 and 1750, prescribed data-sets for AeroCom, Atmos. Chem. Phys., 6, 4321-4344, 2006.

Ding, A. J., Fu, C. B., Yang, X. Q., Sun, J. N., Petäjä, T., Kerminen, V. M., Wang, T., Xie, Y., Herrmann, E., Zheng, L. F., Nie, W., Liu, Q., Wei, X. L., Kulmala, M.: Intense atmospheric pollution modifies weather: a case of mixed biomass burning with fossil fuel combustion pollution in eastern China, Atmospheric Chemistry and Physics, 13, 10545–10554, 2013.

Du J, Zhang X, Huang T, et al.: Removal of PM2. 5 and secondary inorganic aerosols in the

North China Plain by dry deposition, Science of The Total Environment, 651: 2312-2322, 2019.
Emery C, Liu Z, Russell A G, et al.: Recommendations on statistics and benchmarks to assess photochemical model performance, Journal of the Air & Waste Management Association, 67(5): 582-598, 2017.
Freitas, S. R., Longo, K. M., Silva Dias, M. A. F., Chatfield, R., Silva Dias, P., Artaxo, P., Andreae, M. O., Grell, G., Rodrigues, L. F., Fazenda, A., and Panetta, J.: The Coupled Aerosol and Tracer Transport model to the Brazilian developments on the Regional Atmospheric Modeling System (CATT-BRAMS) – Part 1: Model description and evaluation, Atmos. Chem. Phys., 9, 2843- 2861, doi:10.5194/acp-9-2843-2009, 2009.
Gao M, Carmichael G R, Saide P E, et al.: Response of winter fine particulate matter concentrations to emission and meteorology changes in North China, Atmospheric Chemistry and Physics, 16(18): 11837, 2016.
Gao, Y., Zhao, C., Liu, X., Zhang, M., and Leung, L. R.: WRF-Chem simulations of aerosols and anthropogenic aerosol radiative forcing in East Asia, Atmospheric Environment, 92, 250–266, doi:10.1016/j.atmosenv.2014.04.038, 2014.
Gong, D.Y., Ho, C.-H., Chen, D., Qian, Y., Choi, Y.-S., and Kim, J.: Weekly cycle of aerosol-meteorology interaction over China, J. Geophys. Res., 112, L03819, doi:10.1029/2007JD008888, 2007.
Guo J, Miao Y, Zhang Y, et al.: The climatology of planetary boundary layer height in China derived from radiosonde and reanalysis data, Atmospheric Chemistry and Physics, 16(20): 13309, 2016.
Hong S Y, Noh Y, Dudhia J.: A new vertical diffusion package with an explicit treatment of entrainment processes, Monthly weather review, 134(9): 2318-2341, 2006.
Huang, X., Ding, A., Liu, L., Liu, Q., Ding, K., Nie, W., Xu, Z., Chi, X., Wang, M., Sun, J., Guo, W., and Fu, C.: Effects of aerosol-radiation interaction on precipitation during biomass-burning season in East China, Atmos. Chem. Phys., 16, 2016.
Jiang F, Liu Q, Huang X, et al.: Regional modeling of secondary organic aerosol over China using WRF/Chem, Journal of aerosol science, 43(1): 57-73, 2012.
Liu S, Hua S, Wang K, et al.: Spatial-temporal variation characteristics of air pollution in Henan of China: Localized emission inventory, WRF/Chem simulations and potential source contribution analysis, Science of the total environment, 624: 396-406, 2018.
Mellor G L, Yamada T.: Development of a turbulence closure model for geophysical fluid problems, Reviews of Geophysics, 20(4): 851-875, 1982.
Miao Y, Guo J, Liu S, et al.: Impacts of synoptic condition and planetary boundary layer structure on the trans-boundary aerosol transport from Beijing-Tianjin-Hebei region to northeast China, Atmospheric environment, 181: 1-11, 2018.
Nakanishi, M. and Niino, H.: An Improved Mellor–Yamada Level-3 Model: Its Numerical Stability and Application to a Regional Prediction of Advection Fog, Boundary-Layer Meteorol, 119, 397–407, doi:10.1007/s10546-005-9030-8, 2006.
Noh, Y., W.-G. Cheon, S.-Y. Hong, and S. Raasch.: Improvement of the K-profile model for the planetary boundary layer based on large eddy simulation data, Bound.-Layer Meteor., 107, 401–427, doi:10.1023/A:1022146015946, 2003.
Olivier, J., Peters, J., Granier, C., Petron, G., Muller, J. F., and Wallens, S.: Present and Future surface emissions of anthropogenic compounds, POET report #2, EU project EVK2-1999-00011, 2003
Tao W, Liu J, Ban-Weiss G A, et al.: Effects of urban land expansion on the regional meteorology and air quality of eastern China, Atmos. Chem. Phys, 15(15): 8597-8614, 2015.
Wang J, Ge X, Chen Y, et al.: Highly time-resolved urban aerosol characteristics during

springtime in Yangtze River Delta, China: insights from soot particle aerosol mass spectrometry, Atmospheric Chemistry and Physics, 16(14): 9109-9127, 2016.
Wang Q, Liu S, Li N, et al.: Impacts of short-term mitigation measures on PM 2.5 and radiative effects: a case study at a regional background site near Beijing, China, Atmospheric Chemistry and Physics, 19(3): 1881-1899, 2019.
Wang X, Liang X Z, Jiang W, et al.: WRF-Chem simulation of East Asian air quality: Sensitivity to temporal and vertical emissions distributions, Atmospheric Environment, 44(5): 660-669, 2010.
Wiedinmyer C, Akagi S K, Yokelson R J, et al.: The Fire INventory from NCAR (FINN): A high resolution global model to estimate the emissions from open burning, Geoscientific Model Development, 4(3): 625, 2011.
Woo J H, Baek J M, Kim J W, et al.: Development of a multi-resolution emission inventory and its impact on sulfur distribution for Northeast Asia, Water, air, and soil pollution, 148(1-4): 259-278, 2003.
WRAP (Western Regional Air Partnership): 2002 Fire Emission Inventory for the WRAP Region- Phase II, Project No. 178-6, available at: http://www.wrapair.org/forums/fejf/tasks/FEJFtask7PhaseII.html (last access: 02 January 2020), 22 July 2005.
Zhang Y, Zhang X, Wang L, et al.: Application of WRF/Chem over East Asia: Part I. Model evaluation and intercomparison with MM5/CMAQ, Atmospheric environment, 124: 285-300, 2016.
Zhang, B., Wang, Y., and Hao, J.: Simulating aerosol–radiation–cloud feedbacks on meteorology and air quality over eastern China under severe haze conditionsin winter, Atmos. Chem. Phys., 15, 2387–2404, doi:10.5194/acp-15-2387-2015, 2015.
Zhao B, Liou K N, Gu Y, et al.: Enhanced PM 2.5 pollution in China due to aerosol-cloud interactions, Scientific reports, 7(1): 4453, 2017.
Zhao, C., Hu, Z., Qian, Y., Leung, L. R., Huang, J., Huang, M., Jin, J., Flanner, M., Zhang, R., Wang, H., Yan, H., Lu, Z., and Streets, D. G.: Simulating black carbon and dust and their radiative forcing in seasonal snow: a case study over North China with field campaign measurements, Atmospheric Chemistry and Physics, 14, 11475-11491, 2014.

Modeling diurnal variation of surface $PM_{2.5}$ concentration over East China with WRF-Chem: Impacts from boundary layer mixing and anthropogenic emission

[1]Qiuyan Du, [1]Chun Zhao*, [1]Mingshuai Zhang, [1,2]Xue Dong, [1]Yu Chen, [3]Zhen Liu, [4]Zhiyuan Hu, [5]Qiang Zhang, [6]Yubin Li, [1]Renmin Yuan, [7]Shiguang Miao

[1]School of Earth and Space Sciences, University of Science and Technology of China, Hefei, China, 230026

[2]PowerChina Huadong Engineering Corporation Limited, Hangzhou, China

[3]School of Geosciences, University of Edinburgh, U.K.

[4]Key Laboratory for Semi-Arid Climate Change of the Ministry of Education, College of Atmospheric Sciences, Lanzhou University, Lanzhou, China

[5]Department of Earth System Science, Tsinghua University, Beijing, China

[6]School of Atmospheric Physics, Nanjing University of Information and Technology, Nanjing, China

[7]Institute of Urban Meteorology, Chinese Meteorology Administration, Beijing, China

Manuscript for submission to *Atmos. Chem. Phys.*

*Corresponding authors: Chun Zhao (chunzhao@ustc.edu.cn)

Key points:

1. Planetary boundary layer (PBL) mixing is the determinant factor in modeling the diurnal cycle of surface $PM_{2.5}$ ~~concentration~~concentrations over East China
2. Besides the PBL height, PBL mixing coefficient ~~instead of PBL height is~~is also the key factor controlling the simulated diurnal cycle of surface $PM_{2.5}$ ~~concentration~~concentrations in WRF-Chem
3. The PBL mixing during the night over East China may be underestimated by WRF-Chem; Increase of PBL mixing during the night can significantly reduce the modeling biases of surface $PM_{2.5}$ ~~concentration~~concentrations and also the modeling sensitivity to the PBL configuration
4. The diurnal cycle and injection height of anthropogenic emission have impacts on simulating diurnal cycle of surface $PM_{2.5}$ ~~concentration~~concentrations but smaller than that from PBL mixing

Abstract

Diurnal variation of surface $PM_{2.5}$ concentration (diurnal $PM_{2.5}$) could dramatically affect aerosol radiative and healthy impact, and can also well reflect the physical and chemical mechanisms of air pollution formation and evolution. So far, diurnal $PM_{2.5}$ and its modeling capability over East China ~~have~~has not been investigated, and therefore, ~~are~~is examined in this study. Based on the observations, the normalized diurnal amplitude of surface $PM_{2.5}$ concentrations averaged over East China is the weakest (~1.2) in winter, and reaches ~1.5 in other seasons. The diurnal $PM_{2.5}$ shows the peak concentration during the night in spring and fall and during the daytime in summer. The simulated diurnal $PM_{2.5}$ with WRF-Chem and its contributions from multiple physical and chemical processes are examined in the four seasons. The simulated diurnal $PM_{2.5}$ with WRF-Chem is primarily controlled by planetary boundary layer (PBL) mixing and emission variations, and is significantly ~~overestimates~~overestimated against the ~~observations~~observation during the night. This modeling bias is likely primarily due to the inefficient PBL mixing of primary $PM_{2.5}$ during the night. The simulated diurnal $PM_{2.5}$ is sensitive to the PBL schemes and vertical layer configurations with WRF-Chem. ~~The~~Besides the PBL height, the PBL mixing coefficient ~~instead of PBL height is~~is also found as the critical factor determining the PBL mixing of pollutants in WRF-Chem. ~~The~~With reasonable PBL height, the increase of lower limit of PBL mixing coefficient during the night can significantly reduce the modeling biases in diurnal $PM_{2.5}$ and also the mean concentrations, particularly at the major cities of East China. It can also reduce the modeling sensitivity to the PBL vertical layer configurations. The diurnal variation and injection height of anthropogenic emissions also play roles on simulating diurnal $PM_{2.5}$, but the impact is relatively smaller than that from the PBL mixing. This study underscores that more efforts are needed to improve the boundary mixing process of pollutants in models with observations of PBL structure and mixing fluxes in addition to PBL height, in order to simulate reasonably the diurnal $PM_{2.5}$ over East China. The diurnal variation and injection height of anthropogenic emissions are also necessary to be included to simulate the diurnal $PM_{2.5}$ over East China.

1. Introduction

The Yangtze River Delta (YRD) region of East China hosts the economic engine and a major portion of the Chinese population. During the past two decades, the rapid economic growth has resulted in significant elevated surface air pollutants over East China, especially particulate matter (PM), also called aerosols. Previous studies have indicated that exposure to the high concentrations of $PM_{2.5}$ (fine particulate matter with aerodynamic diameter less than 2.5 μm) can cause many health issues such as lung cancer (LC), ischemic heart disease(IHD), asthma, and nervous system breakdown (e.g., Seaton ~~A~~ et al., 1995; Davidson ~~C I~~ et al., 2005; Pope III ~~C A~~ et al., 2006; Ho et al., 2018; Li ~~T~~ et al., 2018; Liu T et al., 2018). It has become the fourth risk factor of deaths in China and 11.1% of all deaths are attributable to the ambient elevated ~~concentration~~concentrations of particulate matter (Gakidou et al., 2017). Besides the health impacts, atmospheric ~~aerosol~~aerosols can also influence the radiative energy budget of the Earth's system through interacting with radiation, and serving as cloud condensation nuclei (CCN) and ice nuclei (IN) and hence modifying cloud microphysics and precipitation (e.g., Ackerman ~~T P.,~~ 1977; Dickerson ~~R R~~ et al., 1997; Jacobson ~~M. Z.,~~ 1998).

Many studies have investigated spatial and temporal variations of atmospheric aerosol over China in last decades. The $PM_{2.5}$ concentrations are higher in North China than in South China. The highest surface $PM_{2.5}$ concentrations appear in winter and the lowest in summer, and the highest and lowest surface $PM_{2.5}$ ~~concentration~~concentrations of a day often ~~occurs~~occur in the evening and afternoon, respectively (e.g., Gong et al., 2007; Fu et al., 2008; Hu et al., 2014; Wang ZF et al., 2014; Wang YG et al., 2014; Wang YJ et al., 2014; Geng et al., 2015; Xie et al., 2015; Zhang and Cao, 2015; Zhang H et al., 2015). Moreover, modeling analysis can help understand the chemical and physical processes affecting aerosol formation and evolution (e.g., Ying et al., 2009; Zhang et al., 2010; Liao et al., 2014; Wang YX et al., 2014; Wang YJ et al., 2014; Hu Z et al., 2016; Li et al., 2016; Yang et al., 2016; Hu J et al., ~~2017~~2016; Zhao ~~B~~ et al., 2017). Yang et al. (2016) reproduced an increasing trend of winter $PM_{2.5}$ concentrations averaged over East China for 1985-2005 with the GEOS-Chem model, and found that the variations in anthropogenic emissions dominated the increase of winter surface $PM_{2.5}$ concentrations over East China and the variations in meteorological fields also played an important role in influencing the decadal increase in winter $PM_{2.5}$ concentrations over East China. Hu J. et al., (~~2017~~2016) investigated the spatial and temporal distribution of secondary organic aerosol (SOA) in China in 2013 with the WRF-~~CAMQ~~CMAQ model and

found that the formation of SOA from biogenic emissions was significantly enhanced due to anthropogenic emissions.

Most of previous modeling studies focused on understanding the mechanisms driving PM variation on daily or seasonal scales or/and evaluating the simulation of daily and monthly mean PM concentrations over East China. Few studies evaluated the model performance in simulating diurnal cycle of surface PM ~~concentration~~concentrations and investigated the mechanisms underneath. However, the model capability of capturing diurnal cycle of surface PM ~~concentration~~concentrations is critical for revealing mechanisms of PM formation and evolution and may also affect simulating mean ~~concentration.~~concentrations. Some studies also found that diurnal variation of surface PM ~~concentration~~concentrations can affect the daily average radiative forcing (e.g., Arola A et al., 2013; Kassianov ~~E~~ et al., 2013; Kuang ~~Y~~ et al., 2015; Wang Z et al., 2015; Song et al., 2018). Based on the ground-based data collected in Hefei from 2007 to 2013, Wang Z et al. (2015) demonstrated that using daily averaged aerosol properties to retrieve the 24-h average direct aerosol radiative forcing can have positive biases of up to 7.5 W m^{-2} for the cases. Arola et al. (2013) found that the aerosol optical depth (AOD) diurnal cycles have significant impacts on the daily mean aerosol radiative forcing.

Previous studies have observed evident diurnal variations of surface PM over East China (e.g., Gong et al., 2007; Gu et al., 2010; Pathak ~~R K~~ et al., 2011; Feng et al., 2014; Hu et al., 2014; Huang et al., 2014; Ma et al., 2014; Zhang and Cao, 2015; Chen et al., 2016; Tao et al., 2016; Zhao et al., 2016; Chen et al., 2017; Jia et al., 2017; Guo H et al., 2017; Guo J et al., 2017;). Zhang and Cao (2015) used a long-term dataset of surface $PM_{2.5}$ ~~concentration~~concentrations measured at 190 cities of China, and found that the diurnal variation of the $PM_{2.5}$-to-CO ratio consistently displayed a pronounced peak during the afternoon, reflecting a significant contribution of secondary PM formation. Guo H et al. (2017) investigated the diurnal cycle of $PM_{2.5}$ in China with the observations obtained at 226 sites of China during the period of January of 2013 to December of 2015 and found the surface $PM_{2.5}$ ~~concentration~~concentrations reached the maximum in the morning over the YRD region.

Diurnal variation of surface PM ~~concentration~~concentrations can be controlled by many factors including emissions, chemical reactions, and meteorology (e.g., Wang et al., 2006; Huang et al., 2010; Wang et al., 2010; Menut et al., 2012; Qi et al., 2012; Quan et al., 2013; Tiwari et al., 2013; Li et al., 2014; Pal et al., 2014; Sun et al., 2015; Zhang and Cao, 2015; ~~RR Rodelas~~Roig et al., 2019; Xu et al., 2019). Wang et al. (2010) found that simulations with

hourly emission inventory can reproduce the diurnal variation patterns and magnitude of AOD better than simulations with daily emission inventory. Xu et al. (2019) compared the diurnal cycles of aerosol species between 2014 and 2016 observed by Aerodyne high--resolution aerosol mass spectrometer in Beijing and found that the increase of secondary inorganic nitrate, sulfate, and ammonium throughout the day in 2016 were mainly caused by the enhanced photochemical production. With the dataset of PBL height derived from the space-borne and ground-based lidar, Su et al. (2018) investigated the relationship between PBL height and surface PM concentrations across China and found nonlinearly negative responses of PM to PBL height evolution over polluted regions, especially when the PBL height is shallow and PM concentration is high.

Since very few studies evaluated the modeling performance of diurnal cycle of surface PM ~~concentration~~concentrations over East China and investigated the mechanisms underneath, this study investigates the WRF-Chem (Weather Research and Forecasting model coupled with Chemistry) simulation of diurnal variation of $PM_{2.5}$ over East China. WRF-Chem (Grell et al., ~~2005~~2005; Skamarock et al., 2008; Powers et al., 2017) is an online-coupled meteorology and chemistry model that simulates meteorological fields and air pollutant concentrations simultaneously. It has been widely used for studying the temporal and spatial variation of aerosols (e.g., Jiang et al., 2012; Zhou et al., 2014; Bei et al., 2016; Wang et al., 2016; Zhang et al., 2016; Zhong et al., 2016; Li P et al., 2017; Zhao et al., 2017; Zhou et al., 2017; Liu S et al., 2018; Ni et al., 2018) and their meteorological and climatic impacts over East China (e.g., Gong et al., 2007; Ding et al., 2013; Wu et al., 2013; Gao et al., 2014; Chen et al., 2014; Zhao et al., 2014; Zhang B et al., 2015; Zhang L et al., 2015; Huang et al., 2016; Liu et al., 2016; Petäjä et al., 2016; Zhao B et al., 2017). Most of the previous modeling studies with WRF-Chem over China investigated the influencing factors on spatial distribution and monthly or seasonal variation of PM. None of them focused on the performance of simulating diurnal variation of PM with WRF-Chem.

The study will examine the observed characteristics of diurnal variation of surface $PM_{2.5}$ ~~concentration~~concentrations over the YRD region of East China in four seasons of 2018. The WRF-Chem simulations are conducted for one month of each season over East China as shown in Fig 1a, and the simulated diurnal cycle of surface $PM_{2.5}$ ~~concentration~~concentrations will be evaluated through comparing with hourly observations of surface $PM_{2.5}$ ~~concentration~~concentrations released by the Ministry of Environmental Protection (MEP) of China for 190 stations over the YRD region of East China in 2018. The

model is also used to investigate the mechanisms driving the diurnal cycle of surface $PM_{2.5}$. This study will focus on the impacts from meteorology and anthropogenic emissions on the diurnal variation of surface $PM_{2.5}$ ~~concentration.~~concentrations. For meteorology, we will focus on the PBL mixing process that has been found largely controlling the diurnal variation of surface pollutant concentrations (Liu M et al., 2018). For emissions, based on the findings of Wang et al. (2010) and Yang et al. (2019), the diurnal variation and injection height of emission will be investigated. The rest of the paper is organized as follows. The detailed introduction of WRF-Chem model and numerical experiments, anthropogenic emissions, and observations will be presented in Section 2. The examination of simulated diurnal variation of surface $PM_{2.5}$ concentrations and the impacts of PBL mixing and emission will be discussed in Section 3. The ~~conclusions~~summary and discussion can be found in Section 4 and 5, respectively.

2. Methodology

2.1 Models and experiments

2.1.1 WRF-Chem

In this study, the version of WRF-Chem updated by University of Science and Technology of China (USTC version of WRF-Chem) is used. This USTC version of WRF-Chem includes some additional capabilities such as the diagnosis of radiative forcing of aerosol species, land surface coupled biogenic VOC (Volatile Organic Compounds) emission, aerosol-snow interaction compared with the ~~publically~~publicly released version (Zhao et al., 2013a,b, 2014, 2016; Hu et al., 2019). Particularly, in order to understand the modeling mechanisms driving the diurnal variations of surface $PM_{2.5}$ ~~concentration~~concentrations over East China, this study updates the USTC version of WRF-Chem to include the diagnosis of contribution to surface $PM_{2.5}$ ~~concentration~~concentrations from individual process including transport, emission, dry and wet deposition, PBL mixing, and chemical production/loss through estimating the difference of surface $PM_{2.5}$ ~~concentration~~ concentrations before and after individual process during the simulation. More specifically, the contribution of each process is estimated in the following formula:

$$CT_{P,S,T} = C_{P,S,T} - C_{P,S,T0}$$

where $C_{P,S,T0}$ and $C_{P,S,T}$ represent the concentration of species *S* before (model time *T0*) and after (model time *T*), respectively, the process *P*. Therefore, $CT_{P,S,T}$ represents the

contribution of the process *P* to the change of concentration of species *S* during the time period (*T-T0*). For example, if *C0* and *C* represent the surface concentrations of $PM_{2.5}$ before (*T0*) and after (*T*), respectively, the PBL mixing, the contribution (*CT*) of PBL mixing to the change of surface concentrations of $PM_{2.5}$ during the time period (*T-T0*) can be estimated as (C-C0). The overall contribution during a specific time period (e.g., one day) can be obtained through integrating $\boldsymbol{CT}_{P,S,T}$ for this time period.

The Model for Simulating Aerosol Interactions and Chemistry (MOSAIC, Zaveri and Peter,1999; Zaveri et al.,2008) and the CBM-Z (carbon bond mechanism) photochemical mechanism (Zaveri and Peters, 1999) are used. The MOSAIC aerosol scheme includes physical and chemical processes of nucleation, condensation, coagulation, aqueous phase chemistry, and water uptake by aerosols. All major aerosol components including sulfate, nitrate, ammonium, black carbon~~,~~ (BC), organic matter~~,~~ (OM), sea salt, mineral dust, and other inorganics (OIN) are simulated in the model. OIN represents the unidentified aerosol species other than OM, BC, sulfate, ammonium, and nitrate in emissions if any, which are composed mostly of minerals in emissions in this study. Aerosol size distributions are represented by eight discrete size bins through the bin approach (Fast et al., 2006). Dry deposition of aerosol mass and number is simulated following the approach of Binkowski and Shankar (1995), which includes both particle diffusion and gravitational effects. Wet removal of aerosols by grid resolved stratiform clouds/precipitation includes in-cloud removal (rainout) and below-cloud removal (washout) by impaction and interception, following Easter et al. (2004) and Chapman et al. (~~2009~~2008). In this study, cloud-ice-borne aerosols are not explicitly treated in the model but the removal of aerosols by the droplet freezing process is considered. Convective transport and wet removal of aerosols by cumulus clouds follow Zhao et al. (2013a). Aerosol radiative feedback is coupled with the Rapid Radiative Transfer Model (RRTMG) (Mlawer et al., 1997; ~~Lacono~~Iacono et al., 2000) for both SW and LW radiation as implemented by Zhao et al. (2011). The optical properties and direct radiative forcing of individual aerosol specie~~s~~ in the atmosphere are diagnosed following the methodology described in Zhao et al. (2013b). A detailed description of the computation of aerosol optical properties in WRF-Chem can be found in Fast et al. (2006) and Barnard et al. (2010). Aerosol-cloud interactions were included in the model by Gustafson et al. (2007) for calculating the activation and re-suspension between dry aerosols and cloud droplets.

2.1.2 Numerical experiments

In this study, WRF-Chem is conducted with two nested domains (one-way nesting) in one month of each season of 2018 (i.e., January, April, July, October of 2018). The outer quasi-global domain with 360×145 grid cells (180°W~180°E,67.5°S~77.5°N) at the 1°×1° horizontal resolution is used to provide the chemical boundary to the inner domain with 112×105 grid cells (109.0°E~124.9°E, 24.0°N~38.9°N) at the horizontal resolution of 15 km over East China covering the entire YRD region as shown in Figure 1a. More details about the quasi-global WRF-Chem simulation can be found in Zhao et al. (2013a) and Hu Z et al. (2016). To better resolve the PBL structure and mixing and examine the modeling sensitivity to vertical configuration within PBL, two experiments (CTL1 and CTL2, Table 1) are configured with 40 vertical layers but have different distributions (as shown Fig. 1b). One configuration (L1) has roughly 20 layers below 2 km above the ground, and the other has about 10 layers below 2 km (Fig. 1b). In both CTL1 and CTL2, MYNN2 PBL scheme (Nakanishi and Niino, 2006) is used. To demonstrate the modeling sensitivity to PBL parameterizations, the experiment CTL3 is conducted as the way similar to CTL2 but with the YSU PBL scheme (Hong et al., 2006). Since this study focuses on understanding the PBL mixing impact, the calculation of PBL mixing coefficient within the MYNN2 and YSU PBL schemes is briefly described here. In the local closure PBL scheme MYNN, the PBL mixing coefficient is calculated following Mellor et al. (1982):

$$K_{h,m} = lqS_{h,m}$$

where l is the mixing-length scale, S_h and S_m are stability functions, q is related to the turbulent kinetic energy (TKE) in the following formula:

$$\mathrm{q} = (2 * TKE)^{1/2}$$

In the non-local closure PBL scheme YSU, the momentum mixing coefficient K_m is formulated following Hong et al. (2006):

$$K_m = kw_s z(1 - \frac{z}{h})^p$$

where p is the profile shape exponent taken to be 2, k is the von-karman constant, z is the height from the surface and h is PBL height. For the eddy mixing coefficient for temperature and moisture K_h can be estimated from K_m with the relationship of the *Prandtl* number as in Noh et al. (2003):

$$\mathrm{Pr} = K_m/K_h$$

$$\mathrm{Pr} = 1 + (\mathrm{Pr}_0\text{-}1)\exp\left[\frac{\text{-}3(z\text{-}\varepsilon h)^2}{h^2}\right]$$

Two additional sensitivity experiments (EXP1 and EXP2, Table 1) are also conducted corresponding to the experiments CTL1 and CTL2, respectively, except that the PBL mixing coefficient is modified (see details in Section 3.2.2).

All these WRF-Chem experiments use the Morrison two-moment cloud microphysics (Morrison et al., 2009), Kain-Fritsch convective scheme (Kain et al., 2004), CLM land surface scheme, and RRTMG longwave and shortwave radiation schemes. The meteorological initial and lateral boundary conditions are derived from the NCEP Final reanalysis data with 1°×1° ~~degree~~ resolution and 6-hour temporal resolution. The modeled u component and v component wind and atmospheric temperature are nudged towards the reanalysis data only to the layers above the PBL with nudging coefficients of 3×10^{-4} s^{-1} with a nudging timescale of 6-hour (Stauffer and Seaman, 1990; Seaman et al., 1995).

2.1.3 Emissions

Anthropogenic emissions for the outer quasi-global simulation are obtained from the Hemispheric Transport of Air Pollution version-2 (HTAPv2) at 0.1°×0.1° horizontal resolution and a monthly temporal resolution for year 2010 (Janssens-Maenhout et al., 2015), except that emissions over China within the domains are from the Multi-resolution Emission Inventory for China (MEIC) at 0.1°×0.1° horizontal resolution for 2015 (Li M et al., ~~2017~~2017a,b), which is also used for the inner domain simulation over East China. Figure 1a shows the spatial distributions of emissions of primary $PM_{2.5}$, NO_x, and SO_2 over East China. The default anthropogenic emission inventories assume no diurnal variation of emissions and that all emissions are near the surface (e.g., the first model layer). Since diurnal variation of emissions and injection height of power plant emissions may have impacts on diurnal variation of surface pollutants, the experiments discussed above apply the diurnal profiles of anthropogenic emissions from five individual ~~sector~~sectors (i.e., agriculture, industry, transport, energy, and residential) following Olivier et al. (2003) and Wang et al. (2005) as shown in Fig. 1c and vertical distributions of anthropogenic power plant emissions following Wang et al. (2010) as shown in Table 2. Wang et al. (2010) derived the vertical profiles for East Asia based on the dataset of the U.S. and found that the profiles are comparable to those estimated in China and Japan (Woo et al., 2003; Wang et al., 2010). As shown in Fig. 1c, emissions from all sectors show peak values during the daytime, and the diurnal variations from agriculture, residential, and transportation are much stronger than those from industry and power plant. The emissions from power plant are distributed from the bottom to a height

of ~900 m with more than 90% below 500 m. Both diurnal and vertical variation profiles of anthropogenic emissions are prescribed without temporal variability. Two sensitivity experiments, EXP1_E1 and EXP1_E2, are conducted as the way similar to EXP1 except that EXP1_E1 assumes no diurnal variation of anthropogenic emissions and EXP1_E2 assumes all power plant emissions are placed near the surface (i.e., the first model layer). Comparing EXP1 with EXP1_E1 and EXP1_E2 can examine the impact of diurnal variation and injection height of anthropogenic emissions on diurnal cycle of surface $PM_{2.5}$, respectively. All these experiments are summarized in Table 1. Biomass burning emissions are obtained from the Fire Inventory from NCAR (FINN) with hourly temporal resolution and 1 km horizontal resolution (Wiedinmyer et al., 2011~~), and are vertically distributed following~~). The biomass burning emissions follow the diurnal variation provided by WRAP (2005) and the injection heights suggested by Dentener et al. (2006) from the Aerosol Comparison between Observations and Models (AeroCom) project. Sea-salt emission follows Zhao et al. (2013a), which includes correction of particles with radius less than 0.2 μm (Gong, 2003) and dependence of sea-salt emission on sea surface temperature (Jaeglé et al., 2011). The vertical dust fluxes are calculated with the GOCART dust emission scheme (Ginoux et al., 2001), and the emitted dust particles are distributed into the MOSAIC aerosol size bins following a theoretical expression based on the physics of scale-invariant fragmentation of brittle materials derived by Kok (2011). More details about the dust emission scheme coupled with MOSAIC aerosol scheme in WRF-Chem can be found in Zhao et al. (2010, 2013a).

2.2 Observations

The ground observations of hourly surface $PM_{2.5}$ mass ~~concentration~~concentrations in January, April, July, and October of 2018 are obtained from the website of the Ministry of Environmental Protection of China (MEP of China). Since this study focuses on the YRD region of East China, 190 stations over East China are selected for analysis. The locations of these 190 stations are shown in Fig. 1a within the black box (116.0°E~122.5°E,29.0°N~33.0°N). Besides regional average analysis, four cities (Fig. 1a) as the Center (Shanghai, 121.45°E and 31.21°N) and sub-Center (Nanjing, 118.78°E and 32.06°N; Hefei, 117.25°E and 31.85°N; Hangzhou, 120.08°E and 30.21°N) of the YRD city cluster are also selected for further analysis at urban areas.

3. Results

3.1 Modeling diurnal cycle of surface $PM_{2.5}$ concentration

In order to investigate the diurnal cycle of surface $PM_{2.5}$ ~~concentration~~concentrations, this study defines an index to better show the diurnal variation. The diurnal index (DI) is defined as the value of each hour divided by the minimum value within 24-hour on monthly average. The peak DI within 24-hour represents the amplitude of diurnal variation. Figure 2 shows the diurnal index of surface $PM_{2.5}$ ~~concentration~~concentrations within 24-hour averaged over the YRD region of East China (as shown as the black box in Fig. 1a) for January, April, July, October of 2018 from the WRF-Chem experiments and observations. The experiment CTL1 uses the MYNN PBL scheme and finer boundary layer configuration (L1 in Fig. 1b). The simulation results and the observations are sampled 3-hourly~~ and sampled~~ at the observational sites as shown in Fig. 1a. On regional average, the observed variation of DI is the weakest in winter with the peak value around 1.2 among the four seasons. The observed DI reaches the maximum of 1.5 in autumn. In spring and autumn, the observed diurnal variation of DI ~~is~~are similar, showing ~~two peaks in~~ the ~~morning and~~peak during the night~~, respectively~~, and reaching the minimum in the afternoon, which is consistent with previous findings with observations over East China (e.g., Zhang and Cao., 2015; Liu et al.,2016; Guo et al.,2017). In summer, different from other seasons, the observed diurnal variation of DI shows the single peak around 1.4 near the noon time. The CTL1 experiment can generally reproduce ~~two peaks in spring and autumn~~the peak during the night, however, the CTL1 simulation overestimates the observed peak DI in the two seasons, particularly in autumn. The experiment generally captures the seasonality of DI of surface $PM_{2.5}$ ~~concentration~~concentrations that is higher DI in spring and autumn and the weakest DI in winter, except that in summer the experiment significantly overestimates the DI during the night and produces opposite diurnal pattern with the minimum DI near the noon time. The spatial distributions of DI over East China are also generally consistent between observations and simulations and show similar seasonality (Figure S1 in the supporting material). The area with higher surface $PM_{2.5}$ ~~concentration~~concentrations generally has higher DI (Figure S2 in the supporting material), particularly from the simulation.

Therefore, the DI ~~distribution~~distributions at the four cities as the Center (Shanghai) and sub-Center (Nanjing, Hefei, Hangzhou) of the YRD city cluster in East China (as shown in Fig. 1a) are further analyzed. Figure 3 shows the diurnal index of surface $PM_{2.5}$ ~~concentration~~concentrations within 24-hour averaged over the four cities for January, April, July, October of 2018 from the WRF-Chem experiments and observations. The observed diurnal variation of DI in these four cities are consistent with that on regional average of East

China. The diurnal variation of DI ~~is~~are more evident in the two inland cities (Hefei and Nanjing) than the two coastal cities (Hangzhou and Shanghai). Consistent with the results based on regional average, the CTL1 experiment can generally capture the diurnal variation of DI of surface $PM_{2.5}$ in the four cities, but overestimates the DI in the night, particularly in spring and autumn. In summer, again, the CTL1 significantly overestimates the DI during the night and produces the opposite diurnal pattern compared to observations. In general, the CTL1 produces even higher DI during the night in the four cities than regional average, which results in larger diurnal amplitudes in the four cities than regional average. The CTL1 can generally simulate stronger diurnal variation in the two inland cities than in the two coastal cities.

The analysis above for both regional average and city average indicates that the CTL1 simulation has high positive biases of DI during the night. In order to understand the modeling biases and the mechanisms driving the simulated diurnal variations of surface $PM_{2.5}$ ~~concentration~~concentrations over East China, the contribution to diurnal variation of surface $PM_{2.5}$ ~~concentration~~concentrations from individual process including transport, emission, dry and wet deposition, mixing, and chemical production/loss is estimated. The contribution is calculated as the difference of surface $PM_{2.5}$ ~~concentration~~concentrations before and after individual process during the simulation. Figure 4 shows the contribution of individual process to the variation of surface $PM_{2.5}$ ~~concentration~~concentrations every 3-hour in Hefei from the WRF-Chem experiments averaged for January, April, July, and October of 2018. The 3-hourly tendency (the difference between the current time and the time 3-hour earlier) of surface $PM_{2.5}$ ~~concentration~~concentrations is also shown. The contributions and tendencies are divided by monthly mean surface $PM_{2.5}$ ~~concentration~~concentrations for each month. The results for the other three cities (Nanjing, Hangzhou, Shanghai) are similar to that of Hefei and are shown in the supporting material (Figure S3a-c). Process contribution analysis is verified by comparing the variations of surface $PM_{2.5}$ ~~concentration~~concentrations with the sum of the ~~contribution~~contributions from each individual process. As shown in Figure S4, the sum contributions of all processes are consistent with the variations in surface $PM_{2.5}$ ~~concentration~~concentrations following the principle of mass balance.

In Fig. 4, positive value denotes relative increase of surface $PM_{2.5}$ ~~concentration~~concentrations and negative value denotes relative decrease. From the CTL1 experiment, the contributions from emission and chemistry are positive through the day, while the contributions from transport, PBL mixing, wet and dry deposition are negative through the day. The CTL1 simulates the largest variation of tendency in summer and the

smallest variation in winter. The ~~tendency is~~tendencies are negative from the morning to the afternoon, resulting the simulated minimum surface $PM_{2.5}$ ~~concentration~~concentrations in the afternoon in all seasons, which is consistent with the result shown in Fig. 3. It is evident that emission, PBL mixing, and transport are the three main processes controlling the diurnal variation of surface $PM_{2.5}$ ~~concentration~~concentrations, and emission and PBL mixing are the dominant two. Emission increases the surface $PM_{2.5}$ ~~concentration~~concentrations and reaches the maximum near the noon time, while PBL mixing reduces the surface $PM_{2.5}$ ~~concentration~~concentrations and also reaches the maximum reduction near the noon time. The combined effect of emission and PBL mixing is reflected as the overall tendency. Therefore, PBL mixing is the determinant process leading to the simulated minimum DI near the noon time and higher DI during the night. To further demonstrate the contribution of each $PM_{2.5}$ composition to the diurnal variation of surface $PM_{2.5}$ ~~concentration~~concentrations, Figure 5 shows the diurnal variation of surface concentration of each $PM_{2.5}$ composition in Hefei from the WRF-Chem experiments averaged for January, April, July, and October of 2018. The diurnal variations of surface concentrations of OM, BC, and OIN are larger than other components of $PM_{2.5}$, showing evident higher ~~concentration~~concentrations during the night and minimum near the noon time in all seasons except winter. The sum of OM and OIN contribute to more than half of surface $PM_{2.5}$ ~~concentration.~~concentrations. Therefore, it suggests that the PBL mixing of the primary $PM_{2.5}$ determines the simulated diurnal variation of surface $PM_{2.5}$ ~~concentration.~~concentrations. The results for the other three cities (Nanjing, Hangzhou, Shanghai) are similar to that of Hefei and are shown in the supporting material (Figure S5a-c).

In order to understand the possible reasons for this modeling biases, some basic meteorological fields are evaluated with available observations. Since the modeled winds at the layers above the PBL are nudged towards the reanalysis data, the large-scale circulation can be well simulated. The winds at 850 hPa for each season are compared with the NCEP Final reanalysis dataset (FNL) and ERA5 reanalysis dataset (https://rda.ucar.edu/datasets/ds630.0/, last access: 28 December 2019) (Fig. S6 in the supporting material). The simulated wind circulation is highly correlated with the two reanalysis datasets with the spatial correlation coefficients of 0.9-0.97 over East China. The simulated temperature at 2m is also evaluated with the available observations by the China Meteorological Administration (CMA) at the stations of East China (Fig. S7 and Fig. S8 in the supporting material). The model captures the diurnal variation of near-surface temperature very well over East China. For near surface winds, although the model generally

overestimates the observed values by less than 10%, the simulated diurnal variation is generally consistent with the observations over East China (Fig. S9 and Fig. S10 in the supporting material). As the evaluation shows, the basic meteorological fields are generally simulated reasonably. The characteristics associated with the PBL mixing are further investigated below.

3.2 Sensitivity to PBL mixing

3.2.1 Sensitivity to the PBL configuration

As discussed above, the PBL mixing is very important for modeling diurnal variation of surface $PM_{2.5}$ ~~concentration~~concentrations, and it may be affected by PBL parameterizations and vertical layer ~~configuration~~configurations within the PBL. Therefore, two experiments, CTL2 and CTL3, are conducted to examine the sensitivity of simulated diurnal variation of surface $PM_{2.5}$ ~~concentration~~concentrations to different PBL configurations. The CTL2 uses the MYNN PBL scheme as the CTL1 but is configured with different vertical layer distribution (L2) as shown in Fig. 1b, in which less vertical layers are put within the PBL as described in Section 2.2. The CTL3 uses the YSU PBL scheme and is configured with the L2 vertical layer distribution as the CTL2. As shown in Fig. 2, on regional average, the CTL2 and CTL3 generally simulate similar diurnal and seasonal patterns as that by the CTL1 with the minimum DI near the noon time and the peak DI during the night. The CTL2 simulates lower DI than the CTL1 during the night in all seasons. This indicates that the model with finer vertical resolution within the PBL, which is supposed to better resolve the PBL structure, produces higher positive biases of DI. The CTL3 simulates similar diurnal variation of DI as the CTL2 but overestimate the DI during the night to some extent, particularly in summer, which indicates the model with the YSU PBL scheme produces higher positive biases of DI during the night compared to the one with the MYNN PBL scheme. In the four cities as shown in Fig. 3, the CTL2 and CTL3 also simulate similar diurnal and seasonal patterns as that by the CTL1. It is also interesting to note that the difference of DI between CTL2 and CTL1 ~~are~~is larger than that between CTL3 and CTL2, which indicate that the modeling sensitivity of DI to the vertical layer ~~configuration~~configurations within the PBL is even greater than that to the PBL ~~scheme~~schemes. Overall, all these three WRF-Chem experiments produce similar positive biases of DI during the night compared to the observations in all seasons over the YRD region of East China, particularly in cities. This is consistent with previous findings about the simulated positive biases of diurnal variation of surface $PM_{2.5}$ ~~concentration over East China (e.g., Liu M et al., 2018). The~~concentrations over East China

(e.g., Liu M et al., 2018). Liu M et al. (2018) found that the air quality model (WRF-CMAQ v5.0.1) also overestimated the surface concentrations of $PM_{2.5}$ during the nighttime in October-December, 2013. They speculated that the overestimation is due to the weak PBL mixing in the nighttime, and claimed that the newer version of CMAQ v5.1 driven by WRF v3.7 revised the PBL mixing scheme (ACM2) and might reduce the nighttime biases. To verify this, two experiments are conducted using the ACM2 PBL scheme with WRF-Chem v3.5 and WRF-Chem v4.0, respectively, over East China for October of 2018. The results showed that the PBL mixing of ACM2 scheme is enhanced in v4.0 compared to v3.5 especially during the night, and the simulated nighttime surface $PM_{2.5}$ concentrations are reduced to some extent in v4.0 compared to v3.5 (not shown). However, the simulation still significantly overestimates the surface $PM_{2.5}$ concentrations during the night. Therefore, the changes of PBL schemes and vertical configurations within the PBL can affect the simulated DI but cannot improve the simulations to reproduce the observations.

In order to better understand the modeling sensitivity of DI to the PBL configuration, Fig. 4 and 5 also show~~s~~ the simulated results for the city of Hefei from the CTL2 and CTL3. Similar as CTL1, the results from CTL2 and CTL3 also show that emission, PBL mixing, and transport are the three main processes controlling the diurnal variation of surface $PM_{2.5}$ ~~concentration~~concentrations, and emission and PBL mixing are the dominant two (Fig. 4). Since the number of vertical layer within the PBL in CTL2 and CTL3 is much less than that in CTL1, the thickness of first model layer in CTL2 and CTL3 is about a factor 2 of that in CTL1. With the same emission flux, CTL2 and CTL3 simulate much smaller ~~contribution~~contributions from emission to the surface $PM_{2.5}$ ~~concentration~~concentrations than does CTL1. Correspondingly, the ~~contribution~~contributions from PBL mixing to the surface $PM_{2.5}$ ~~concentration~~concentrations in CTL2 and CTL3 ~~is~~are also lower than that in CTL1. The combined effect of emission and PBL mixing results in weaker diurnal variation of surface $PM_{2.5}$ ~~concentration~~concentrations in CTL2 and CTL3 than that in CTL1, as shown by the diurnal variation of overall tendency of surface $PM_{2.5}$ ~~concentration.~~concentrations. CTL3 with the YSU PBL scheme simulates stronger diurnal variation of surface $PM_{2.5}$ ~~concentration~~concentrations than does the CTL2 with the MYNN PBL scheme, primarily due to its larger diurnal variation of PBL mixing. With less contribution from emission to the surface $PM_{2.5}$ ~~concentration~~concentrations, CTL2 and CTL3 simulate less primary $PM_{2.5}$ (OIN, OM, BC) than does CTL1 (Fig. 5), particularly during the night when the PBL mixing is weak. This leads to the weaker diurnal variation of total surface $PM_{2.5}$ ~~concentration~~concentrations in CTL2 and CTL3 as discussed above. The higher DI during the

night in CTL3 than CTL2 can also be explained by the higher primary $PM_{2.5}$ during the night due to weaker PBL mixing.

3.2.2 Sensitivity to the PBL mixing coefficient

The results discussed above suggest that, the WRF-Chem simulated diurnal variation of surface $PM_{2.5}$ ~~concentration~~concentrations over East China is largely controlled by the PBL mixing process, and is sensitive to the PBL scheme and vertical layer configuration within the PBL. However, the increase of number of vertical ~~layer~~layers within the PBL and use of different PBL schemes cannot reduce the modeling biases in diurnal variation of surface $PM_{2.5}$ ~~concentration.~~concentrations. Many previous studies investigated the PBL mixing of pollutants through establishing the relationship between surface pollutant concentration and PBL height. However, it is noteworthy that in most atmospheric models, the mixing of pollutants within the PBL is treated either as full mixing within the PBL ~~height~~heights (i.e., uniformly distributed within the PBL ~~height~~heights) or as calculated based on the mixing coefficient diagnosed from the PBL scheme. The former method represents the strongest PBL mixing and the surface ~~concentration~~concentrations can be largely influenced by the PBL ~~height. However, the~~heights. The latter one means that the pollutant mixing does not depend explicitly on PBL ~~height.~~ heights, although the PBL heights still reflects the boundary mixing strength.

In WRF-Chem, the PBL mixing of pollutants is treated with the second approach. In order to further examine the simulated PBL mixing process in this study, Figure 6 shows the diurnal variation of PBL heights and PBL mixing coefficients below PBL ~~height~~heights in Hefei in January, April, July, and October of 2018 from the WRF-Chem experiments CTL1, CTL2, and CTL3. The black line represents the PBL ~~height~~heights while the contour shading represents the PBL mixing coefficients within the PBL ~~height~~heights. First of all, the PBL heights simulated from the three experiments all show evident diurnal variation with the maximum in the daytime and the minimum during the night. The simulated PBL heights from CTL1 and CTL2 with the same PBL scheme (MYNN) show very similar diurnal pattern, indicating the vertical layer configuration has small impact on modeling PBL ~~height~~heights. Both experiments simulate the largest diurnal variation of PBL ~~height~~heights in summer with a changing factor of ~10 from ~2 km in the afternoon to ~200 m in the early morning, and the smallest diurnal variation of PBL heights in winter with a changing factor of 2 from ~700 m in the afternoon to ~350 m in the early morning. The CTL3 simulation with the YSU PBL scheme shows similar diurnal variation of PBL heights as those from the CTL1 and CTL2

simulations. The CTL3 simulates similar PBL heights during the daytime but lower values during the night, particularly in October. The simulated PBL heights are evaluated with the long-term averaged PBL heights, primarily for 8 am and 8 pm local time, derived from the air sounding observations available at the four stations of East China as reported in Guo et al. (2016) (Fig. S11 in the supporting material). In general, throughout the four seasons, the CTL3 with the YSU scheme simulates reasonable PBL heights in the early morning and night, while the CTL1 and CTL2 with the MYNN scheme overestimate the PBL heights compared to the derived values. The comparison between simulations and observations (Fig. 2 and 3) suggests the positive modeling biases of DI during the night may be partly due~~height in winter with a changing factor of 2 from ~700 m in the afternoon to ~350 m in the early morning. It should be noted that the PBL mixing coefficients within the PBL~~ to the underestimation of the PBL mixing during the night, which cannot be explained by the modeling biases of PBL heights during the night.

It should be noted that the PBL mixing coefficients within the PBL in all the three experiments also exhibit evident diurnal variation with a changing factor of ~1000 and ~50 in summer and winter, respectively, which is much larger than that of the PBL height in all seasons. ~~The CTL3 simulation with the YSU PBL scheme also show that the diurnal variation of PBL mixing coefficient is much larger than that of PBL height.~~ More WRF experiments with different PBL schemes are conducted and all show similar results that the diurnal variation of PBL mixing coefficients is much stronger than that of PBL heights (not shown). ~~he difference between CTL2 and CTL3 is consistent with the analysis about the simulated diurnal variation of surface $PM_{2.5}$ concentration, further demonstrating that the WRF-Chem simulated diurnal variation of surface $PM_{2.5}$ concentration is determined by the PBL mixing coefficient instead of PBL height. For example, in autumn the PBL height during the night is lower in CTL3 than in CTL2, while the DI during the night is lower in CTL3 than in CLT2 (Fig. 3) due to the higher PBL mixing coefficient during the night in CTL3 than in CTL2. More WRF experiments with different PBL schemes are conducted and all show similar results that the diurnal variation of PBL mixing coefficient is much stronger than that of PBL height (not shown).~~

With relatively large values of PBL mixing coefficient during the daytime, the emitted pollutants can be mixed up roughly reaching the layer of PBL ~~height~~heights. Therefore, the PBL height is very critical for determining the surface pollutant mixing strength during the daytime. However, weak PBL mixing coefficient during the night results in that the emitted $PM_{2.5}$ and its precursors will stay near the surface (i.e., within the first layer of model) during

the night and cannot be mixed up reaching the PBL height (Fig. ~~S6~~S12 in the supporting material). This leads to the large difference of DI between CTL1 and CTL2 with different ~~thickness~~thicknesses of first model layer during the night although they simulate similar PBL ~~height~~heights. Another example in autumn, the PBL heights during the night are lower in CTL3 than in CTL1, while the DI during the night are higher in CTL1 than in CTL3 (Fig. 3) due to the weak PBL mixing coefficients during the night that cannot mix the pollutants up to the PBL height. This further demonstrates that the WRF-Chem simulated diurnal variation of surface PM2.5 concentration is not explicitly controlled by the PBL height instead by the PBL mixing coefficient. In fact, in WRF-Chem, there is an existing empirical parameterization~~. The comparison between simulations and observations (Fig. 2 and 3) suggests the positive modeling biases of DI during the night may be partly due~~ to ~~the underestimation of~~ enhance the PBL mixing ~~during~~of pollutants in urban area based on the strength of anthropogenic emissions. However, it is only applied to gas pollutants if the MOSAIC aerosol scheme is selected as this study. It also tends to enhance the mixing up to half number of model vertical layers, which is beyond the ~~night. To~~PBL in most cases during the night. In this study, in order to examine the sensitivity of simulated DI to the PBL mixing coefficient, the sensitivity experiments, EXP1 and EXP2, are conducted corresponding to CTL1 and CTL2, respectively, through setting the lower limit of PBL mixing coefficient from 0.1 m^2/s (default in the publically released version of WRF-Chem) to 5 m^2/s within the PBL~~.~~, which is applied to both gas and aerosol pollutants.

Figure 7 shows the simulated PBL height and mixing coefficients from the two sensitivity experiments, EXP1 and EXP2, in January, April, July, and October of 2018 in Hefei. It shows that the PBL mixing coefficient increases during the night within the PBL compared to the results shown in Fig. 6, while the values during the daytime remain almost the same. The difference of simulated surface $PM_{2.5}$ between CTL1 and EXP1 is relatively small during the daytime, but significant during the night, which is due to that EXP1 can mix up the surface $PM_{2.5}$ to the PBL ~~height~~heights during the night (Fig. ~~S6~~S12). It is noteworthy that the lower limit parameter of 5 m^2/s is entirely empirical. It is selected to represent the moderate mixing strength between the full PBL mixing and no PBL mixing. A few other values such as 1 m^2/s and 10 m^2/s are also tested. The results do not change the conclusion found in this study and therefore are not shown.

The change of PBL mixing coefficient during the night can significantly affect the diurnal variation of PBL mixing. Figure 8 shows the contribution of individual process to the variation of surface $PM_{2.5}$ ~~concentration~~concentrations every 3-hour in Hefei simulated by

EXP1 and EXP2 averaged for January, April, July, and October of 2018. The 3-hourly tendency of surface $PM_{2.5}$ ~~concentration~~concentrations is also shown. Same as Fig. 4, the contributions and tendencies are divided by monthly mean surface $PM_{2.5}$ ~~concentration~~concentrations for each month. The results for the other three cities (Nanjing, Hangzhou, Shanghai) are similar to that of Hefei and are shown in the supporting material (Figure ~~S7a~~S13a-c). Compared to the results from CTL1 and CTL2 shown in Fig. 4, it is evident that the diurnal variation of tendency of surface $PM_{2.5}$ ~~concentration~~concentrations is significantly reduced in all seasons. This is mainly resulted from the significantly ~~reduced~~increased diurnal variation of PBL mixing contribution. Specifically, the PBL mixing contribution during the night is increased. Figure 9 shows the diurnal variation of surface concentration of each $PM_{2.5}$ composition in Hefei simulated by the EXP1 and EXP2 averaged for January, April, July, and October of 2018. The diurnal variations of surface concentrations of OM, BC, and OIN are significantly reduced primarily due to their reduced ~~concentration~~concentrations during the night in EXP1 and EXP2, compared to CTL1 and CTL2 (Fig. 5). The results for the other three cities (Nanjing, Hangzhou, Shanghai) are similar to that of Hefei and are shown in the supporting material (Figure ~~S8a~~S14a-c).

The change of PBL mixing and diurnal variation of primary $PM_{2.5}$ near the surface turn out different DI. Figure 10 shows the diurnal variation of DI of surface $PM_{2.5}$ averaged over the YRD region of East China for January, April, July, and October of 2018 from the observations and the experiments CTL1, CTL2, EXP1, and EXP2. In general, the simulated DI are reduced significantly during the night in EXP1 and EXP2 much more consistent with the observations compared to the ones in CTL1 and CTL2. In spring, the EXP1 and EXP2 slightly underestimate DI during night. Figure 11 shows the diurnal variation of DI averaged over the four cities for January, April, July, October of 2018 from the observations and the experiments CTL1, CTL2, EXP1, and EXP2. As discussed above the diurnal variation of DI is much stronger in cities with relatively more emissions. The simulated DI is also more sensitive to the change of PBL mixing coefficient in these four cities compared to that on regional average. The EXP1 and EXP2 produce much more consistent DI with the observations in the four cities than do CTL1 and CTL2 in all seasons. It is also noteworthy that the difference between EXP1 and EXP2 and that between CTL1 and CTL2 is reduced both on city average and regional average, which indicates that the enhanced PBL exchange coefficient during the night help reduce the modeling sensitivity to the vertical layer ~~configuration.~~configurations. The analysis above suggests that the simulated PBL mixing during the night in the publically-released WRF-Chem may be too weak.

Comparing the simulated surface concentrations of $PM_{2.5}$ components between CTL1 (Fig. 5) and EXP1 (Fig. 9), it can be found that the daily average surface $PM_{2.5}$ mass ~~concentration~~concentrations should also be reduced when the diurnal variation is reduced due to the reduction of nighttime surface $PM_{2.5}$ ~~concentration.~~concentrations. The model overestimates largely the monthly mean surface $PM_{2.5}$ at the stations of East China in the seasons other than winter from the control experiments. These modeling biases are significantly reduced at most stations of East China (Fig. S15 in the supporting material) in the sensitivity experiments. Figure 12 shows the comparison of monthly mean surface $PM_{2.5}$ ~~concentration~~concentrations between the observations and the simulations from CTL1 and EXP1 at each observation site over the YRD region of East China for January, April, July, and October of 2018. In all seasons, the CTL1 significantly overestimates the observed surface $PM_{2.5}$ ~~concentration~~concentrations with the normalized mean biases (NMB) of 22% (winter) - 109% (summer) on regional average. The EXP1 reduces the NMB to 7% (winter) - 38% (summer) on regional average. In CTL1, the NMB of simulation exceeds 50% at 20%, 35%, 65%, and 60% of observational sites over the YRD region of East China in January, April, July, and October, respectively, which reduces to 0%, 10%, 35%, and 20% of all sites in EXP1. In addition, the EXP1 also increases the spatial correlation between observations and simulated results in all seasons (Fig. 12), although with the improvement of modeling diurnal variation the EXP1 still cannot fully capture the observed spatial variability of surface $PM_{2.5}$ ~~concentration~~concentrations among the observational sites. This may be related to the biases in spatial distributions of emission and model processes contributed to the spatial variability of surface $PM_{2.5}$ ~~concentration~~concentrations, which deserves further investigation in future.

3.3 Impacts from emission distributions

3.3.1 Impacts from emission diurnal variability

Besides the meteorology such as PBL mixing as discussed above, the diurnal variation of emissions may also play an important role in determining the DI of surface $PM_{2.5}$ ~~concentration.~~concentrations. One sensitivity experiment, EXP1_E1, without diurnal variation of anthropogenic emissions (Fig. ~~1b~~1c) is conducted. Figure 13 shows the spatial distribution of the difference in maximum DI between EXP1 and EXP1_E1 over East China. As removing diurnal variation of emissions will lead to more emissions during the night and thus increase the DI during the night over polluted area, which generally results in larger maximum DI. Therefore, EXP1 has lower maximum DI than EXP1_E1 over most regions of East China in

seasons other than winter. EXP1 could have slightly larger maximum DI in winter when the diurnal variation of DI is relatively small (Fig. 2 and 3) and over the relatively clean region (Fig. 1a) in summer. Figure 14 shows the diurnal index of surface $PM_{2.5}$ ~~concentration~~concentrations within 24-hour averaged over the four cities for January, April, July, and October of 2018 from observations and the EXP1 and EXP1_E1 experiments. In general, EXP1 shows lower DI than EXP1_E1 during the night, and therefore has smaller diurnal variation of DI in four cities. The largest difference between EXP1 and EXP1_E1 in four cities exists in summer and the smallest is in winter. Comparing to the impacts from PBL mixing as shown in Fig. 11, the reduction of diurnal variation of DI by adding diurnal variation of anthropogenic emissions is much smaller.

Fig. 13 shows that EXP1 with diurnal variation of emissions could simulate slightly larger diurnal variation of DI over the relatively clean region than EXP1_E1 in winter and summer. The higher DI in EXP1 than EXP1_E1 is primarily in the afternoon and evening (Fig. ~~S9~~S16 in the supporting material). One grid over south Anhui is selected for analysis of contributions from different processes in the model to the diurnal variation of surface $PM_{2.5}$ ~~concentration~~concentrations from the experiments EXP1 and EXP1_E1 (Fig. 15). Different from the process contributions over the relatively polluted region (Fig. 8), the contribution from direct local emission to the surface $PM_{2.5}$ ~~concentration~~concentrations is relatively small over the clean region. Instead, the contributions from chemistry, dry deposition, PBL mixing, and transport dominate the diurnal variation of surface $PM_{2.5}$ ~~concentration.~~concentrations. The PBL mixing could increase the surface $PM_{2.5}$ ~~concentration~~concentrations during the daytime because of mixing down the pollutants transported from polluted regions above the surface. The diurnal change of surface $PM_{2.5}$ ~~concentration~~concentrations between EXP1 and EXP1_E1 is very similar with slightly difference that results in their slight difference in DI in the afternoon and night.

3.3.2 Impacts from emission injection height

Previous studies suggested that the injection height of emissions from power plants may also affect the diurnal cycle of surface pollutant ~~concentration~~concentrations, particularly for SO_2 (e.g., Wang et al.,2010; Lin et al.,2012; Qi et al.,2012; Xu et al.,2014). Therefore, one sensitivity experiment, EXP1_E2, is conducted with setting the anthropogenic emissions placed only in the first layer of model. Figure 16 shows the spatial distribution of the difference in maximum DI between EXP1 and EXP1_E2 over East China. Over most areas of East China, EXP1 simulates lower maximum DI than EXP1_E2, and the difference is

primarily in spring and summer. The impact of injection height is negligible in winter. The distribution of impacts correlates highly with the distribution of power plant locations. The reduction of DI of surface SO_2 ~~concentration~~concentrations in EXP1 compared to EXP1_E2 is mainly due to more emissions are placed above the PBL during the night (Fig. ~~S10~~S17 in the supporting material). As shown in Table 2, most of power plant emissions are placed below 500 m in EXP1. The larger impact in summer than in winter is mainly due to the higher PBL ~~height~~heights during the night in winter (Fig. 7). Therefore, emissions are still placed within the PBL even with the injection height, which results in the small difference of DI of surface SO_2 ~~concentration~~concentrations between EXP1 and EXP1_E2. For surface $PM_{2.5}$ ~~concentration~~concentrations, the impact of emission injection height is even smaller and only distinguishable in summer (Fig. ~~S11~~S18 in the supporting material). Overall, impact from the injection height of emission on the diurnal variation of surface $PM_{2.5}$ ~~concentration~~concentrations is much smaller than that from PBL mixing.

4. Summary ~~and discussion~~

In this study, the observed characteristics of diurnal variation of surface $PM_{2.5}$ ~~concentration~~concentrations over the YRD region of East China in four seasons of 2018 is examined based on the hourly surface observations at 190 stations of the region. On regional average, the observed diurnal variation is the weakest in winter and the strongest in autumn. In spring and autumn, the observed patterns of diurnal variation are similar, showing the minimum surface $PM_{2.5}$ concentration in the afternoon, consistent with previous studies (e.g., Zhang and Cao et al.,2015; Liu et al.,2016; Guo et al.,2017). In summer, different from other seasons, the observed diurnal variation shows the maximum surface $PM_{2.5}$ concentration near the noon time.

The WRF-Chem experiments ~~are conducted over East China and the simulated diurnal variations of surface $PM_{2.5}$ concentration are compared with the observations. The model~~ generally ~~captures~~capture the observed seasonality of diurnal variation of surface $PM_{2.5}$ ~~concentration~~concentrations, except that in summer the model significantly overestimates the diurnal peak during the night and produces opposite diurnal pattern with the minimum concentration near the noon time. The model can generally reproduce the patterns with the minimum noontime concentration in spring and autumn, but overestimates the observed nighttime peaks, particularly in autumn. ~~The modeling biases and the mechanisms driving the diurnal variation of surface $PM_{2.5}$ concentration in four seasons are further investigated.~~

Emission and PBL mixing are found to be the two dominant processes controlling the diurnal variation of surface $PM_{2.5}$ ~~concentration~~concentrations over the polluted areas, and the PBL mixing leads to the simulated diurnal pattern of surface $PM_{2.5}$ ~~concentration.~~concentrations. More specifically, the simulations suggest that the PBL mixing of the primary $PM_{2.5}$ determines the modelled diurnal variation of surface $PM_{2.5}$ ~~concentration.~~concentrations. Although the observation of $PM_{2.5}$ components is not available to evaluate the diurnal variation of primary $PM_{2.5}$, the simulated diurnal variation of surface mixing ratio of CO that is normally used to represent the primary pollutant ~~supports the findings (Fig. S12 in the supporting material).~~is compared with the observations (Fig. S19 in the supporting material). The results from experiments with enhanced nighttime PBL mixing are more consistent with the observations compared to the control experiments, which supports the findings about $PM_{2.5}$.

The modeling results are found sensitive to the PBL schemes and the vertical configuration (i.e., the number of model layers within PBL) of simulations. However, none of the PBL schemes in WRF-Chem can reduce the modeling biases in diurnal variation of surface $PM_{2.5}$ ~~concentration.~~concentrations. Contrary to the intuition, more model layers within PBL worsen the model performance, which is mainly due to that more layers within PBL makes the first model layer thinner and enlarges the contribution from emission if PBL mixing is not efficient. The analysis indicates that ~~the PBL~~ although PBL height is an important factor to reflect the PBL mixing strength, the PBL mixing process is more explicitly controlled by the PBL mixing coefficient instead of the ~~PBL~~ height ~~controls the PBL mixing~~ in WRF-Chem, particularly during the night. Increasing the lower limit of PBL mixing coefficient within the PBL can significantly reduce the modeling biases in diurnal variation of surface $PM_{2.5}$ ~~concentration~~concentrations, primarily during the night. In addition, it can also reduce the modeling sensitivity to the model vertical configuration. The model performance of daily mean surface $PM_{2.5}$ ~~concentration~~concentrations is also largely improved when the biases of diurnal variation are reduced. The diurnal variation of anthropogenic emissions and injection height of power plant emissions can affect the diurnal cycle of surface $PM_{2.5}$ ~~concentration~~concentrations to some extent, but the impact is much smaller than that of PBL mixing.

5. Discussion

This study highlights the importance of modeling PBL mixing coefficient within PBL in models like WRF-Chem that simulates the PBL mixing process based on the mixing coefficient instead of PBL height. Some studies found that other models also overestimated the diurnal variation of observed surface $PM_{2.5}$ ~~concentration~~concentrations over East China (e.g., Cai et al.,2011; Liu M et al.,2018). Our finding suggests that those models may also have the problems in modeling PBL mixing during the night. Many of previous modeling and observation studies focus on investigating the variation of PBL height and its interaction with aerosol concentration (e.g., Sawyer et al., 2015; Ding et al, ~~2016~~2013; Li Z et al, 2017; Song et al.,2018; Su et al., 2018). However, this study reveals that the PBL mixing flux is ~~more~~also critical ~~than~~in addition to the PBL height in terms of understanding the mixing of pollutants within PBL, particularly during the night, which can ~~not only~~ significantly affect not only the diurnal variation but also the daily mean of surface pollutant ~~concentration~~concentrations. The increase of PBL mixing during the night reduces the modeling biases, which may suggest that the simulated PBL mixing during the night in WRF-Chem is too weak. One possible reason may be due to urban heat island effect that is not accounted in this study, because the observation sites are mostly at urban or sub-urban areas. The test simulations with the current version of WRF-Chem using Noah land surface model with urban effect can increase the nighttime PBL mixing coefficient from 0.1 m^2/s to 1-10 m^2/s during some cases at urban areas, but the results are sensitive to the urban schemes (not shown), which deserves investigation in future. The model horizontal resolution may also affect the modeling results of PBL mixing and urbanization. However, one sensitivity experiment at 4 km horizontal resolution shows that the PBL mixing at the stations does not change significantly (not shown). The modeling at higher resolution particularly down to large-eddy scale deserves further investigation. Another suggestion is that the PBL mixing of pollutants may not be able to follow directly the mixing coefficient diagnosed by PBL parameterization for meteorology, which deserves further investigation. The improvement of modeling PBL ~~height~~heights is not enough for understanding the PBL mixing of pollutants. ~~This suggests that the understanding of~~In order to better understand PBL structure and detailed mixing process ~~are needed. Besides~~, besides the observation or retrieval of PBL height, observations of PBL characteristics are needed.

Although the sensitivity adjustment of PBL mixing coefficient during the night can largely reduce the modeling biases in diurnal variation of surface $PM_{2.5}$ ~~concentration~~concentrations, one evident deficiency is that the model produces opposite

diurnal pattern compared with observations in summer. It needs to be noted that the WRF-Chem simulations conducted in this study do not consider the SOA production that still has large uncertainties in mechanisms. One sensitivity experiment with the SOA production shows that the model can better represent the observed diurnal pattern of surface $PM_{2.5}$ ~~concentration~~concentrations in summer showing the maximum concentration in the daytime (Fig. ~~S13~~S20 in the supporting material). This indicates that the SOA production may be important for modeling the diurnal variation of surface $PM_{2.5}$ ~~concentration~~concentrations in summer over East China, which suggests more detailed analysis of impact of SOA production on diurnal cycle of surface $PM_{2.5}$ ~~concentration~~concentrations is needed with observations. It is also noteworthy that the impact of SOA production on diurnal variation of surface $PM_{2.5}$ ~~concentration~~concentrations is only significant in summer, likely due to the strong photochemistry activity in summer. Another uncertainty of the results in this study may be related to emissions. Although the diurnal variation and injection height of emission do not contribute significantly to the night time positive biases of surface $PM_{2.5}$ ~~concentration~~concentrations, the emission uncertainties of primary PM may influence the diurnal cycle of surface $PM_{2.5}$. For example, overestimation of primary PM emission can increase the diurnal variation. Therefore, this study suggests that the long-term measurements of $PM_{2.5}$ components at more stations and the in-situ measurements of vertical profiles of $PM_{2.5}$ concentrations within PBL during the night are needed to further investigate the characteristics of diurnal variation of $PM_{2.5}$, which can improve our understanding of the impacts of multiple processes, such as chemical production, emissions, and meteorology, on the formation and evolution of air pollution.

Data availability

The release version of WRF-Chem can be download from http://www2.mmm.ucar.edu/wrf/users/download/get_source.html. The updated USTC version of WRF-Chem can be downloaded from http://aemol.ustc.edu.cn/product/list/ or contact chunzhao@ustc.edu.cn. Also, the code modifications will be incorporated the release version of WRF-Chem in future.

Author contributions

Qiuyan Du and Chun Zhao designed the experiments, conducted and analyzed the simulations. All authors contributed to the discussion and final version of the paper.

Acknowledgements

This research was supported by the Fundamental Research Funds for the Central Universities, and the National Natural Science Foundation of China (grant 41775146). The study used the computing resources from the High-Performance Computing Center of University of Science and Technology of China (USTC). Part of the observation data is from the Qingyue Open Environmental Data Center (https://data.epmap.org).

Reference

Ackerman, T. P.: A Model of the Effect of Aerosols on Urban Climates with Particular Applications to the Los Angeles Basin, J. Atmos. Sci., 34, 531–547, doi:10.1175/1520-0469(1977)034<0531:AMOTEO>2.0.CO;2, 1977.

Arola, A., Eck, T. F., Huttunen, J., Lehtinen, K. E. J., Lindfors, A. V., Myhre, G., Smirnov, A., Tripathi, S. N., and Yu, H.: Influence of observed diurnal cycles of aerosol optical depth on aerosol direct radiative effect, Atmos. Chem. Phys., 13, 7895-7901, 2013.

Bacmeister, J. T., Wehner, M. F., Neale, R. B., Gettelman, A., Hannay, C., Lauritzen, P. H., Caron, J. M., and Truesdale, J. E.: Exploratory High-Resolution Climate Simulations using the Community Atmosphere Model (CAM), J. Climate, 27, 3073–3099, doi:10.1175/JCLI-D-13-00387.1, 2014.

Barnard, J. C., Fast, J. D., Paredes-Miranda, G., Arnott, W. P., and Laskin, A.: Technical Note: Evaluation of the WRF-Chem "Aerosol Chemical to Aerosol Optical Properties" Module using data from the MILAGRO campaign, Atmos. Chem. Phys., 10, 7325–7340, doi:10.5194/acp-10-7325-2010, 2010.

Bei, N., Li, G., Huang, R., Cao, J., Meng, N., Feng, T., Liu, S., Zhang, T., Zhang, Q., and Molina, L. T.: Typical synoptic situations and their impacts on the wintertime air pollution in the Guanzhong basin, China, Atmos. Chem. Phys., 16, e7387, 2016.

Binkowski, F. S. and Shankar, U.: The Regional Particulate Matter Model: 1. Model Description and Preliminary Results, J. Geophys. Res., 100, 26191–26209, 1995.

Cai, H. and Xie, S.: Traffic-related air pollution modeling during the 2008 Beijing Olympic Games: the effects of an odd-even day traffic restriction scheme, The Science of the total environment, 409, 1935–1948, doi:10.1016/j.scitotenv.2011.01.025, 2011.

Chapman, E. G., Gustafson, W. I., Easter, R. C., Barnard, J. C., Ghan, S. J., Pekour, M. S., and Fast, J. D.: Coupling aerosol-cloud-radiative processes in the WRF-Chem model: investigating the radiative impact of elevated point sources, Atmos. Chem. Phys., 9, 945-964, 2008.

Chen, D., Cui, H., Zhao, Y., Yin, L., Lu, Y., and Wang, Q.: A two-year study of carbonaceous aerosols in ambient $PM_{2.5}$ at a regional background site for western Yangtze River Delta, China, Atmospheric Research, 183, 351–361, doi:10.1016/j.atmosres.2016.09.004, 2017.

Chen, S., Zhao, C., Qian, Y., Leung, L. R., Huang, J., Huang, Z., Bi, J., Zhang, W., Shi, J., Yang, L., Li, D., and Li, J.: Regional modeling of dust mass balance and radiative forcing over East Asia using WRF-Chem, Aeolian Research, 15, 15–30, doi:10.1016/j.aeolia.2014.02.001, 2014.

Chen, T., He, J., Lu, X., She, J., and Guan, Z.: Spatial and Temporal Variations of $PM_{2.5}$ and Its Relation to Meteorological Factors in the Urban Area of Nanjing, China, International journal of environmental research and public health, 13, doi:10.3390/ijerph13090921, 2016.

Chen, W., Tang, H., and Zhao, H.: Diurnal, weekly and monthly spatial variations of air pollutants and air quality of Beijing, Atmospheric Environment, 119, 21–34, doi:10.1016/j.atmosenv.2015.08.040, 2015.

Cheng, Y., Zheng, G., Wei, C., Mu, Q., Zheng, B., Wang, Z., Gao, M., Zhang, Q., He, K., Carmichael, G., Pöschl, U., and Su, H.: Reactive nitrogen chemistry in aerosol water as a source of sulfate during haze events in China, Science advances, 2, e1601530, doi:10.1126/sciadv.1601530, 2016.

Davidson C I, Phalen R F, Solomon P A.: Airborne particulate matter and human health: A review, 39(8), 737–749, 2005.

Dentener, F., Kinne, S., Bond, T., Boucher, O., Cofala, J., Generoso, S., Ginoux, P., Gong, S., Hoelzemann, J. J., Ito, A., Marelli, L., Penner, J. E., Putaud, J.-P., Textor, C., Schulz, M., van der Werf, G. R., and Wilson, J.: Emissions of primary aerosol and precursor gases in the years 2000 and 1750, prescribed data-sets for AeroCom, Atmos. Chem. Phys., 6, 4321-4344, 2006.

Dickerson, R. R., Kondragunta, S., Stenchikov, G., Civerolo, K. L., Doddridge, B. G., and Holben, B. N.: The impact of aerosols on solar ultraviolet radiation and photochemical smog, Science (New York, N.Y.), 278, 827–830, doi:10.1126/science.278.5339.827, 1997.

Ding, A. J., Fu, C. B., Yang, X. Q., Sun, J. N., Petäjä, T., Kerminen, V. M., Wang, T., Xie, Y., Herrmann, E., Zheng, L. F., Nie, W., Liu, Q., Wei, X. L., Kulmala, M.: Intense atmospheric pollution modifies weather: a case of mixed biomass burning with fossil fuel combustion pollution in eastern China, Atmospheric Chemistry and Physics, 13, 10545–10554, 2013.

Du, Q., Faber, V., & Gunzburger, M.: Centroidal Voronoi tessellations: Applications and algorithms, SIAM review, 41, 637–676, 1999.

Easter, R. C., Ghan, S. J., Zhang, Y., Saylor, R. D., Chapman, E. G., Laulainen, N. S., Abdul-Razzak, H., Leung, L. R., Bian, X., and Zaveri, R. A.: MIRAGE: Model Description and Evaluation of Aerosols and Trace Gases, J. Geophys. Res., 109, D20210, doi:10.1029/2004JD004571, 2004.

Fast, J. D, Gustafson Jr., W. I., Easter, R. C., Zaveri, R. A., Barnard, J. C., Chapman, E. G., and Grell, G. A.: Evolution of ozone, particulates, and aerosol direct forcing in an urban area using a new fully-coupled meteorology, chemistry, and aerosol model, J. Geophys. Res., 111, D21305, doi:10.1029/2005JD006721, 2006.

Feng, J., Zhong, M., Xu, B., Du, Y., Wu, M., Wang, H., and Chen, C.: Concentrations, seasonal and diurnal variations of black carbon in $PM_{2.5}$ in Shanghai, China, Atmospheric Research, 147-148, 1–9, doi:10.1016/j.atmosres.2014.04.018, 2014.

Fu, Q., Zhuang, G., Wang, J., Xu, C., Huang, K., Li, J., Hou, B., Lu, T., and Streets, D. G.: Mechanism of formation of the heaviest pollution episode ever recorded in the Yangtze River Delta, China, Atmospheric Environment, 42, 2023–2036, doi:10.1016/j.atmosenv.2007.12.002, 2008.

Gakidou, E., Afshin, A., Abajobir, A. A., Abate, K. H., Abbafati, C., Abbas, K. M., ... & Abu-Raddad, L.: Global, regional, and national comparative risk assessment of 84 behavioural, environmental and occupational, and metabolic risks or clusters of risks, 1990–2016: a systematic analysis for the Global Burden of Disease Study 2016, The Lancet, 390, 1345-1422, 2017.

Gao, Y., Liu, X., Zhao, C., and Zhang, M.: Emission controls versus meteorological conditions in determining aerosol concentrations in Beijing during the 2008 Olympic Games, Atmos. Chem. Phys., 11, 12437–12451, doi:10.5194/acp-11-12437-2011, 2011.

Gao, Y., Zhao, C., Liu, X., Zhang, M., and Leung, L. R.: WRF-Chem simulations of aerosols and anthropogenic aerosol radiative forcing in East Asia, Atmospheric Environment, 92, 250–266, doi:10.1016/j.atmosenv.2014.04.038, 2014.

Geng, G., Zhang, Q., Martin, R. V., van Donkelaar, A., Huo, H., Che, H., Lin, J., and He, K.: Estimating long-term $PM_{2.5}$ concentrations in China using satellite-based aerosol optical depth and a chemical transport model, Remote Sensing of Environment, 166, 262–270, doi:10.1016/j.rse.2015.05.016, 2015.

Ginoux, P., Chin, M., Tegen, I., Prospero, J. M., Holben, B., Dubovik, O., and Lin, S.: Sources and distributions of dust aerosols simulated with the GOCART model, J. Geophys. Res., 106, 20225–20273, 2001.

Gong, D.Y., Ho, C.-H., Chen, D., Qian, Y., Choi, Y.-S., and Kim, J.: Weekly cycle of aerosol-meteorology interaction over China, J. Geophys. Res., 112, L03819, doi:10.1029/2007JD008888, 2007.

Gong, S. L.: A parameterization of sea-salt aerosol source function for sub- and super-micron particles, Global Biogeochem. Cycles, 17, n/a-n/a, doi:10.1029/2003GB002079, 2003.

Grell, G. A., Peckham, S. E., Schmitz, R., and McKeen, S. A., Frost, G., Skamarock, W. C., and Eder, B.: Fully coupled "online" chemistry within the WRF model, Atmos. Environ., 39, 6957–6976, 2005.

Gu, Z., Feng, J., Han, W., Li, L., Wu, M., Fu, J., and Sheng, G.: Diurnal variations of polycyclic aromatic hydrocarbons associated with $PM_{2.5}$ in Shanghai, China, Journal of environmental sciences (China), 22, 389–396, 2010.

Guo J, Miao Y, Zhang Y, et al.: The climatology of planetary boundary layer height in China derived from radiosonde and reanalysis data, Atmospheric Chemistry and Physics, 16(20): 13309, 2016.

Guo, H., Cheng, T., Gu, X., Wang, Y., Chen, H., Bao, F., Shi, S., Xu, B., Wang, W., Zuo, X., Zhang, X., and Meng, C.: Assessment of $PM_{2.5}$ concentrations and exposure throughout China using ground observations, The Science of the total environment, 601-602, 1024–1030, doi:10.1016/j.scitotenv.2017.05.263, 2017.

Guo, J., Xia, F., Zhang, Y., Liu, H., Li, J., Lou, M., He, J., Yan, Y., Wang, F., Min, M., and Zhai, P.: Impact of diurnal variability and meteorological factors on the $PM_{2.5}$ - AOD relationship: Implications for $PM_{2.5}$ remote sensing, Environmental pollution (Barking, Essex 1987), 221, 94–104, doi:10.1016/j.envpol.2016.11.043, 2017.

Gustafson, W. I., Chapman, E. G., Ghan, S. J., Easter, R. C., and Fast, J. D.: Impact on modeled cloud characteristics due to simplified treatment of uniform cloud condensation nuclei during NEAQS 2004, Geophys. Res. Lett., 34, L19809, doi:10.1029/2007GL030021, 2007.

Ho, H. C., Wong, M. S., Yang, L., Shi, W., Yang, J., Bilal, M., and Chan, T.-C.: Spatiotemporal influence of temperature, air quality, and urban environment on cause-specific mortality during hazy days, Environment international, 112, 10–22, doi:10.1016/j.envint.2017.12.001, 2018.

Hong, S.-Y., Noh, Y., and Dudhia, J.: A New Vertical Diffusion Package with an Explicit Treatment of Entrainment Processes, Mon. Wea. Rev., 134, 2318–2341, doi:10.1175/MWR3199.1, 2006.

Hu, J., Chen, J., Ying, Q., and Zhang, H.: One-Year Simulation of Ozone and Particulate Matter in China Using WRF/CMAQ Modeling System, Atmos. Chem. Phys., 16, 10333, 2016.

Hu, J., Wang, Y., Ying, Q., and Zhang, H.: Spatial and temporal variability of $PM_{2.5}$ and PM_{10} over the North China Plain and the Yangtze River Delta, China, Atmospheric Environment, 95, 598–609, doi:10.1016/j.atmosenv.2014.07.019, 2014.

Hu, ~~J.,~~ Z., Huang, J., Zhao, C., Bi, J., Jin, Q., Qian, Y., Leung, L. R., Feng, T., Chen, S., and Ma, J.: Modeling the contributions of Northern Hemisphere dust sources to dust outflow from East Asia, Atmospheric Environment, 202, 234–243, doi:10.1016/j.atmosenv.2019.01.022, 2019.

Hu, ~~Chen, J., Ying, Q., and Zhang, H.: One-Year Simulation of Ozone and Particulate Matter in China Using WRF/CMAQ Modeling System, Atmos. Chem. Phys., 16, 10333, 2016.~~

~~Hu,~~ Z., Zhao, C., Huang, J., Leung, L. R., Qian, Y., Yu, H., Huang, L., and Kalashnikova, O. V.: Trans-pacific transport and evolution of aerosols: Evaluation of quasi global WRF-Chem simulation with multiple observations, Geosci. Model Dev. Discuss., 1–65, doi:10.5194/gmd-2015-248, 2016.

~~Hu, Z., Huang, J., Zhao, C., Bi, J., Jin, Q., Qian, Y., Leung, L. R., Feng, T., Chen, S., and Ma, J.: Modeling the contributions of Northern Hemisphere dust sources to dust outflow from East Asia, Atmospheric Environment, 202, 234–243, doi:10.1016/j.atmosenv.2019.01.022, 2019.~~

Huang, G., Cheng, T., Zhang, R., Tao, J., Leng, C., Zhang, Y., Zha, S., Zhang, D., Li, X., and Xu, C.: Optical properties and chemical composition of $PM_{2.5}$ in Shanghai in the spring of 2012, Particuology, 13, 52–59, doi:10.1016/j.partic.2013.10.005, 2014.

Huang, X., Ding, A., Liu, L., Liu, Q., Ding, K., Nie, W., Xu, Z., Chi, X., Wang, M., Sun, J., Guo, W., and Fu, C.: Effects of aerosol-radiation interaction on precipitation during biomass-burning season in East China, Atmos. Chem. Phys., 16, 2016.

Huang, X.F., He, L.Y., Hu, M., Canagaratna, M. R., Sun, Y., Zhang, Q., Zhu, T., Xue, L., Zeng, L.-W., Liu, X.-G., Zhang, Y.-H., Jayne, J. T., Ng, N. L., and Worsnop, D. R.: Highly time-resolved chemical characterization of atmospheric submicron particles during 2008 Beijing Olympic Games using an Aerodyne High-Resolution Aerosol Mass Spectrometer, Atmos. Chem. Phys., 10, 8933-8945, 2010.

Iacono, M. J., Mlawer, E. J., Clough, S. A., & Morcrette, J. J.: Impact of an improved longwave radiation model, RRTM, on the energy budget and thermodynamic

properties of the NCAR community climate model, CCM3, Journal of Geophysical Research: Atmospheres, 105, 14873-14890, 2000.

Jacobson, M. Z.: Studying the effects of aerosols on vertical photolysis rate coefficient and temperature profiles over an urban airshed, J. Geophys. Res., 103, 10593–10604, doi:10.1029/98JD00287, 1998.

Jaeglé, L., Quinn, P. K., Bates, T. S., Alexander, B., & Lin, J. T.: Global distribution of sea salt aerosols: new constraints from in situ and remote sensing observations, Atmospheric Chemistry and Physics, 11, 3137-3157, 2011.

Janssens-Maenhout, G., Crippa, M., Guizzardi, D., Dentener, F., Muntean, M., Pouliot, G., Keating, T., Zhang, Q., Kurokawa, J., Wankmüller, R., van der Denier Gon, H., Klimont, Z., Frost, G., Darras, S., and Koffi, B.: HTAP_v2: a mosaic of regional and global emission gridmaps for 2008 and 2010 to study hemispheric transport of air pollution, Atmos. Chem. Phys. Discuss., 15, 12867–12909, doi:10.5194/acpd-15-12867-2015, 2015.

Jia, M., Zhao, T., Cheng, X., Gong, S., Zhang, X., Tang, L., Liu, D., Wu, X., Wang, L., and Chen, Y.: Inverse Relations of $PM_{2.5}$ and O_3 in Air Compound Pollution between Cold and Hot Seasons over an Urban Area of East China, Atmosphere, 8, 59, doi:10.3390/atmos8030059, 2017.

Jiang, F., Liu, Q., Huang, X., Wang, T., Zhuang, B., and Xie, M.: Regional modeling of secondary organic aerosol over China using WRF/Chem, Journal of Aerosol Science, 43, 57–73, doi:10.1016/j.jaerosci.2011.09.003, 2012.

Kain, J. S.: The Kain–Fritsch convective parameterization: An update, J. Appl. Meteorol., 43, 170–181, 2004.

Kassianov, E., Barnard, J., Pekour, M., Berg, L. K., Michalsky, J., Lantz, K., and Hodges, G.: Do diurnal aerosol changes affect daily average radiative forcing?, Geophys. Res. Lett., 40, 3265–3269, doi:10.1002/grl.50567, 2013.

Kok, J. F.: A scaling theory for the size distribution of emitted dust aerosols suggests climate models underestimate the size of the global dust cycle, Proceedings of the National Academy of Sciences of the United States of America, 108, 1016–1021, doi:10.1073/pnas.1014798108, 2011.

Kuang, Y., Zhao, C. S., Tao, J. C., and Ma, N.: Diurnal variations of aerosol optical properties in the North China Plain and their influences on the estimates of direct aerosol radiative effect, Atmos. Chem. Phys., 15, 5761–5772, doi:10.5194/acp-15-5761-2015, 2015.

Li, G., Wang, Y., Lee, K. H., Diao, Y., & Zhang, R.: Impacts of aerosols on the development and precipitation of a mesoscale squall line, Journal of Geophysical Research: Atmospheres, 114, 2009.

Li, J., Wang, G., Aggarwal, S. G., Huang, Y., Ren, Y., Zhou, B., Singh, K., Gupta, P. K., Cao, J., and Zhang, R.: Comparison of abundances, compositions and sources of elements, inorganic ions and organic compounds in atmospheric aerosols from Xi'an and New Delhi, two megacities in China and India, The Science of the total environment, 476-477, 485–495, doi:10.1016/j.scitotenv.2014.01.011, 2014.

Li, J., Yang, W., Wang, Z., Chen, H., Hu, B., Li, J., Sun, Y., Fu, P., and Zhang, Y.: Modeling study of surface ozone source-receptor relationships in East Asia, Atmospheric Research, 167, 77–88, doi:10.1016/j.atmosres.2015.07.010, 2016.

Li, M., Liu, H., Geng, G., Hong, C., Liu, F., Song, Y., ... & Zhang, Q.: Anthropogenic emission inventories in China: a review, National Science Review, 4, 834-866, ~~2017~~2017a.

Li, M., Zhang, Q., Kurokawa, J.-i., Woo, J.-H., He, K., Lu, Z., Ohara, T., Song, Y., Streets, D. G., Carmichael, G. R., Cheng, Y., Hong, C., Huo, H., Jiang, X., Kang, S., Liu, F., Su, H., and Zheng, B.: MIX: a mosaic Asian anthropogenic emission inventory under the international collaboration framework of the MICS-Asia and HTAP, Atmos. Chem. Phys., 17, 935–963, doi:10.5194/acp-17-935-2017, ~~2017~~2017b.

Li, P., Wang, L., Guo, P., Yu, S., Mehmood, K., Wang, S., Liu, W., Seinfeld, J. H., Zhang, Y., Wong, D. C., Alapaty, K., Pleim, J., and Mathur, R.: High reduction of ozone and particulate matter during the 2016 G-20 summit in Hangzhou by forced emission controls of industry and traffic, Environ Chem Lett, 15, 709–715, doi:10.1007/s10311-017-0642-2, 2017.

Li, R., Li, Z., Gao, W., Ding, W., Xu, Q., & Song, X.: Diurnal, seasonal, and spatial variation of $PM_{2.5}$ in Beijing, Science Bulletin, 60, 387-395, 2015.

Li, T., Horton, R. M., Bader, D. A., Liu, F., Sun, Q., and Kinney, P. L.: Long-term projections of temperature-related mortality risks for ischemic stroke, hemorrhagic stroke, and acute ischemic heart disease under changing climate in Beijing, China, Environment international, 112, 1–9, doi:10.1016/j.envint.2017.12.006, 2018.

Li, X., Zhang, Q., Zhang, Y., Zheng, B., Wang, K., Chen, Y., Wallington, T. J., Han, W., Shen, W., Zhang, X., and He, K.: Source contributions of urban $PM_{2.5}$ in the Beijing–Tianjin–Hebei region: Changes between 2006 and 2013 and relative impacts

of emissions and meteorology, Atmospheric Environment, 123, 229–239, doi:10.1016/j.atmosenv.2015.10.048, 2015.

Li, Z., Guo, J., Ding, A., Liao, H., Liu, J., Sun, Y., ... & Zhu, B.: Aerosol and boundary-layer interactions and impact on air quality, National Science Review, 4, 810-833, 2017.

Liao, J., Wang, T., Wang, X., Xie, M., Jiang, Z., Huang, X., and Zhu, J.: Impacts of different urban canopy schemes in WRF/Chem on regional climate and air quality in Yangtze River Delta, China, Atmospheric Research, 145-146, 226–243, doi:10.1016/j.atmosres.2014.04.005, 2014.

Lin, M., Tao, J., Chan, C.-Y., Cao, J.-J., Zhang, Z.-S., Zhu, L.-H., and Zhang, R.-J.: Regression Analyses between Recent Air Quality and Visibility Changes in Megacities at Four Haze Regions in China, Aerosol Air Qual. Res., 12, 1049–1061, doi:10.4209/aaqr.2011.11.0220, 2012.

Lin, W., Xu, X., Ma, Z., Zhao, H., Liu, X., and Wang, Y.: Characteristics and recent trends of sulfur dioxide at urban, rural, and background sites in north China: effectiveness of control measures, Journal of environmental sciences (China), 24, 34–49, 2012.

Liu, J., Li, J., and Li, W.: Temporal Patterns in Fine Particulate Matter Time Series in Beijing: A Calendar View, Scientific reports, 6, 32221, doi:10.1038/srep32221, 2016.

Liu, M., Lin, J., Wang, Y., Sun, Y., Zheng, B., Shao, J., ... & Yan, Y.: Spatiotemporal variability of ~~NO 2~~NO_2 and $PM_{2.5}$ over Eastern China: observational and model analyses with a novel statistical method, Atmospheric Chemistry and Physics, 18, 12933-12952, 2018.

Liu, S., Hua, S., Wang, K., Qiu, P., Liu, H., Wu, B., Shao, P., Liu, X., Wu, Y., Xue, Y., Hao, Y., and Tian, H.: Spatial-temporal variation characteristics of air pollution in Henan of China: Localized emission inventory, WRF/Chem simulations and potential source contribution analysis, The Science of the total environment, 624, 396–406, doi:10.1016/j.scitotenv.2017.12.102, 2018.

Liu, T., Cai, Y., Feng, B., Cao, G., Lin, H., Xiao, J., Li, X., Liu, S., Pei, L., Fu, L., Yang, X., Zhang, B., and Ma, W.: Long-term mortality benefits of air quality improvement during the twelfth five-year-plan period in 31 provincial capital cities of China, Atmospheric Environment, 173, 53–61, doi:10.1016/j.atmosenv.2017.10.054, 2018.

Liu, X.-Y., Zhang, Y., Zhang, Q., and He, K.-B.: Application of online-coupled WRF/Chem-MADRID in East Asia: Model evaluation and climatic effects of

anthropogenic aerosols, Atmospheric Environment, 124, 321–336, doi:10.1016/j.atmosenv.2015.03.052, 2016.

Ma, Q., Wu, Y., Tao, J., Xia, Y., Liu, X., Zhang, D., Han, Z., Zhang, X., and Zhang, R.: Variations of Chemical Composition and Source Apportionment of $PM_{2.5}$ during Winter Haze Episodes in Beijing, Aerosol Air Qual. Res., 17, 2791–2803, doi:10.4209/aaqr.2017.10.0366, 2017.

Ma, Y., Xu, X., Song, W., Geng, F., and Wang, L.: Seasonal and diurnal variations of particulate organosulfates in urban Shanghai, China, Atmospheric Environment, 85, 152–160, doi:10.1016/j.atmosenv.2013.12.017, 2014.

Mellor G L, Yamada T.: Development of a turbulence closure model for geophysical fluid problems, Reviews of Geophysics, 20(4): 851-875, 1982.

Menut, L., Goussebaile, A., Bessagnet, B., Khvorostiyanov, D., and Ung, A.: Impact of realistic hourly emissions profiles on air pollutants concentrations modelled with CHIMERE, Atmospheric Environment, 49, 233–244, doi:10.1016/j.atmosenv.2011.11.057, 2012.

Miao, Y., Guo, J., Liu, S., Zhao, C., Li, X., Zhang, G., Wei, W., and Ma, Y.: Impacts of synoptic condition and planetary boundary layer structure on the trans-boundary aerosol transport from Beijing-Tianjin-Hebei region to northeast China, Atmospheric Environment, 181, 1–11, doi:10.1016/j.atmosenv.2018.03.005, 2018.

Mlawer, E. J., S. J. Taubman, P. D. Brown, M. J. Iacono, and S. A. Clough.: Radiative transfer for inhomogeneous atmosphere: RRTM, a validated correlated-k model for the longwave, J. Geophys. Res., **102**, 16 663–16 682, 1997.

Morrison, H., Thompson, G., and Tatarskii, V.: Impact of Cloud Microphysics on the Development of Trailing Stratiform Precipitation in a Simulated Squall Line: Comparison of One- and TwoMoment Schemes, Mon. Weather Rev., 137, 991–1007, 2009.

Nakanishi, M. and Niino, H.: An Improved Mellor–Yamada Level-3 Model: Its Numerical Stability and Application to a Regional Prediction of Advection Fog, Boundary-Layer Meteorol, 119, 397–407, doi:10.1007/s10546-005-9030-8, 2006.

Ni, Z.-Z., Luo, K., Zhang, J.-X., Feng, R., Zheng, H.-X., Zhu, H.-R., Wang, J.-F., Fan, J.-R., Gao, X., and Cen, K.-F.: Assessment of winter air pollution episodes using long-range transport modeling in Hangzhou, China, during World Internet Conference,

2015, Environmental pollution (Barking, Essex 1987), 236, 550–561, doi:10.1016/j.envpol.2018.01.069, 2018.

Noh, Y., W.-G. Cheon, S.-Y. Hong, and S. Raasch.: Improvement of the K-profile model for the planetary boundary layer based on large eddy simulation data, Bound.-Layer Meteor., 107, 401–427, doi:10.1023/A:1022146015946, 2003.

Olivier, J., Peters, J., Granier, C., Petron, G., Muller, J. F., and Wallens, S.: Present and Future surface emissions of anthropogenic compounds, POET report #2, EU project EVK2-1999-00011, 2003.

Pal, S., Lee, T. R., Phelps, S., and Wekker, S. F. J. de: Impact of atmospheric boundary layer depth variability and wind reversal on the diurnal variability of aerosol concentration at a valley site, The Science of the total environment, 496, 424–434, doi:10.1016/j.scitotenv.2014.07.067, 2014.

Pathak, R. K., Wang, T., and Wu, W. S.: Nighttime enhancement of $PM_{2.5}$ nitrate in ammonia-poor atmospheric conditions in Beijing and Shanghai: Plausible contributions of heterogeneous hydrolysis of N_2O_5 and HNO_3 partitioning, Atmospheric Environment, 45, 1183–1191, doi:10.1016/j.atmosenv.2010.09.003, 2011.

Petäjä, T., Järvi, L., Kerminen, V.-M., Ding, A. J., Sun, J. N., Nie, W., Kujansuu, J., Virkkula, A., Yang, X.-Q., Fu, C. B., Zilitinkevich, S., and Kulmala, M.: Enhanced air pollution via aerosol-boundary layer feedback in China, Scientific reports, 6, 18998, doi:10.1038/srep18998, 2016.

Pope III C A, Dockery D W.: Health effects of fine particulate air pollution: lines that connect, Journal of the air & waste management association, 56, 709-742, 2006.

Powers, J. G., et al.: THE WEATHER RESEARCH AND FORECASTING MODEL Overview, System Efforts, and Future Directions, Bull. Amer. Meteorol. Soc., 98(8), 1717-1737, doi:10.1175/bams-d-15-00308.1, 2017.

Qi, H., Lin, W., Xu, X., Yu, X., and Ma, Q.: Significant downward trend of SO_2 observed from 2005 to 2010 at a background station in the Yangtze Delta region, China, Sci. China Chem., 55, 1451–1458, doi:10.1007/s11426-012-4524-y, 2012.

Quan, J., Gao, Y., Zhang, Q., Tie, X., Cao, J., Han, S., Meng, J., Chen, P., and Zhao, D.: Evolution of planetary boundary layer under different weather conditions, and its impact on aerosol concentrations, Particuology, 11, 34–40, doi:10.1016/j.partic.2012.04.005, 2013.

Roig Rodelas, R., Perdrix, E., Herbin, B., and Riffault, V.: Characterization and variability of inorganic aerosols and their gaseous precursors at a suburban site in northern France over one year (2015–2016), Atmospheric Environment, 200, 142–157, doi:10.1016/j.atmosenv.2018.11.041, 2019.

Sawyer V R. Interaction between aerosol and the planetary boundary layer depth at sites in the US and China[C]//AGU Fall Meeting Abstracts. 2015.

Seaman, N. L., Stauffer, D. R., and Lario-Gibbs, A. M.: A Multiscale Four-Dimensional Data Assimilation System Applied in the San Joaquin Valley during SARMAP. Part I: Modeling Design and Basic Performance Characteristics, J. Appl. Meteor., 34, 1739–1761, doi:10.1175/1520-0450(1995)034<1739:AMFDDA>2.0.CO;2, 1995.

Seaton, A., MacNee, W., Donaldson, K., and Godden, D.: Particulate air pollution and acute health effects, Lancet (London, England), 345, 176–178, doi:10.1016/s0140-6736(95)90173-6, 1995.

Shao, J., Chen, Q., Wang, Y., Lu, X., He, P., Sun, Y., Shah, V., Martin, R. V., Philip, S., Song, S., Zhao, Y., Xie, Z., Zhang, L., and Alexander, B.: Heterogeneous sulfate aerosol formation mechanisms during wintertime Chinese haze events: air quality model assessment using observations of sulfate oxygen isotopes in Beijing, Atmos. Chem. Phys., 19, 6107–6123, doi:10.5194/acp-19-6107-2019, 2019.

Skamarock W C, Klemp J B, Dudhia J, et al. A description of the Advanced Research WRF version 3. NCAR Technical note-475+ STR[J]. 2008.

Song, J., Xia, X., Che, H., Wang, J., Zhang, X., and Li, X.: Daytime variation of aerosol optical depth in North China and its impact on aerosol direct radiative effects, Atmospheric Environment, 182, 31–40, doi:10.1016/j.atmosenv.2018.03.024, 2018.

Stauffer, D. R. and Seaman, N. L.: Use of four-dimensional data assimilation in a limited-area mesoscale model, Part I: Experiments with synoptic-scale data, Mon. Weather Rev., 118, 1250–1277, 1990.

Su, T., Li, Z., and Kahn, R.: Relationships between the planetary boundary layer height and surface pollutants derived from lidar observations over China, Atmos. Chem. Phys., 18, 15921-15935, 2018.

Sun, Y. L., Wang, Z. F., Du, W., Zhang, Q., Wang, Q. Q., Fu, P. Q., Pan, X. L., Li, J., Jayne, J., and Worsnop, D. R.: Long-term real-time measurements of aerosol particle composition in Beijing, China: seasonal variations, meteorological effects, and source analysis, Atmos. Chem. Phys., 15, 10149-10165, 2015.

Tao, M., Chen, L., Li, R., Wang, L., Wang, J., Wang, Z., Tang, G., and Tao, J.: Spatial oscillation of the particle pollution in eastern China during winter: Implications for regional air quality and climate, Atmospheric Environment, 144, 100–110, doi:10.1016/j.atmosenv.2016.08.049, 2016.

Tao, W., Liu, J., Ban-Weiss, G. A., Hauglustaine, D. A., Zhang, L., Zhang, Q., Cheng, Y., Yu, Y., and Tao, S.: Effects of urban land expansion on the regional meteorology and air quality of Eastern China, Atmos. Chem. Phys., 15, 8597-8614, 2015.

Tiwari, S., Srivastava, A. K., Bisht, D. S., Parmita, P., Srivastava, M. K., and Attri, S. D.: Diurnal and seasonal variations of black carbon and $PM_{2.5}$ over New Delhi, India: Influence of meteorology, Atmospheric Research, 125-126, 50–62, doi:10.1016/j.atmosres.2013.01.011, 2013.

Verma, V., Ning, Z., Cho, A. K., Schauer, J. J., Shafer, M. M., and Sioutas, C.: Redox activity of urban quasi-ultrafine particles from primary and secondary sources, Atmospheric Environment, 43, 6360–6368, doi:10.1016/j.atmosenv.2009.09.019, 2009.

Wang, G., Zhang, R., Gomez, M. E., Yang, L., Levy Zamora, M., Hu, M., Lin, Y., Peng, J., Guo, S., Meng, J., Li, J., Cheng, C., Hu, T., Ren, Y., Wang, Y., Gao, J., Cao, J., An, Z., Zhou, W., Li, G., Wang, J., Tian, P., Marrero-Ortiz, W., Secrest, J., Du, Z., Zheng, J., Shang, D., Zeng, L., Shao, M., Wang, W., Huang, Y., Wang, Y., Zhu, Y., Li, Y., Hu, J., Pan, B., Cai, L., Cheng, Y., Ji, Y., Zhang, F., Rosenfeld, D., Liss, P. S., Duce, R. A., Kolb, C. E., and Molina, M. J.: Persistent sulfate formation from London Fog to Chinese haze, Proceedings of the National Academy of Sciences of the United States of America, 113, 13630–13635, doi:10.1073/pnas.1616540113, 2016.

Wang, J., Christopher, S. A., Nair, U. S., Reid, J. S., Prins, E. M., Szykman, J., & Hand, J. L.: Mesoscale modeling of Central American smoke transport to the United States: 1."Top-down" assessment of emission strength and diurnal variation impacts, Journal of Geophysical Research: Atmospheres, 111, 2006.

Wang, T., Jiang, F., Deng, J., Shen, Y., Fu, Q., Wang, Q., Fu, Y., Xu, J., and Zhang, D.: Urban air quality and regional haze weather forecast for Yangtze River Delta region, Atmospheric Environment, 58, 70–83, doi:10.1016/j.atmosenv.2012.01.014, 2012.

Wang, X., Liang, X.-Z., Jiang, W., Tao, Z., Wang, J. X.L., Liu, H., Han, Z., Liu, S., Zhang, Y., and Grell, G. A.: WRF-Chem simulation of East Asian air quality: Sensitivity to temporal and vertical emissions distributions, Atmospheric Environment, 44, 660–669, doi:10.1016/j.atmosenv.2009.11.011, 2010.

Wang, X.P., Mauzerall, D. L., Hu, Y., Russell, A. G., Larson, E. D., Woo, J.-H., Streets, D. G., and Guenther, A.: A high-resolution emission inventory for eastern China in 2000 and three scenarios for 2020, Atmospheric Environment, 39, 5917–5933, doi:10.1016/j.atmosenv.2005.06.051, 2005.

Wang, Y.G., Ying, Q., Hu, J., and Zhang, H.: Spatial and temporal variations of six criteria air pollutants in 31 provincial capital cities in China during 2013–2014, Environment international, 73, 413–422, doi:10.1016/j.envint.2014.08.016, 2014.

Wang, Y.J., Li, L., Chen, C., Huang, C., Huang, H., Feng, J., Wang, S., Wang, H., Zhang, G., Zhou, M., Cheng, P., Wu, M., Sheng, G., Fu, J., Hu, Y., Russell, A. G., and Wumaer, A.: Source apportionment of fine particulate matter during autumn haze episodes in Shanghai, China, J. Geophys. Res. Atmos., 119, 1903–1914, doi:10.1002/2013JD019630, 2014.

Wang, Y.X., Zhang, Q., Jiang, J., Zhou, W., Wang, B., He, K., Duan, F., Zhang, Q., Philip, S., and Xie, Y.: Enhanced sulfate formation during China's severe winter haze episode in January 2013 missing from current models, J. Geophys. Res. Atmos., 119, 10,425-10,440, doi:10.1002/2013JD021426, 2014.

Wang, Z., Liu, D., Wang, Y., and Shi, G.: Diurnal aerosol variations do affect daily averaged radiative forcing under heavy aerosol loading observed in Hefei, China, Atmos. Meas. Tech., 8, 2901–2907, doi:10.5194/amt-8-2901-2015, 2015.

Wang, Z.F., Li, J., Wang, Z., Yang, W., Tang, X., Ge, B., Yan, P., Zhu, L., Chen, X., Chen, H., Wand, W., Li, J., Liu, B., Wang, X., Zhao, Y., Lu, N., and Su, D.: Modeling study of regional severe hazes over mid-eastern China in January 2013 and its implications on pollution prevention and control, Sci. China Earth Sci., 57, 3–13, doi:10.1007/s11430-013-4793-0, 2014.

Wiedinmyer, C., Akagi, S. K., Yokelson, R. J., Emmons, L. K., Al-Saadi, J. A., Orlando, J. J., and Soja, A. J.: The Fire INventory from NCAR (FINN) – a high resolution global model to estimate the emissions from open burning, Geosci. Model Dev. Discuss., 3, 2439–2476, doi:10.5194/gmdd-3-2439-2010, 2010.

Woo J H, Baek J M, Kim J W, et al.: Development of a multi-resolution emission inventory and its impact on sulfur distribution for Northeast Asia, Water, air, and soil pollution, 148(1-4): 259-278, 2003.

WRAP (Western Regional Air Partnership): 2002 Fire Emission Inventory for the WRAP Region- Phase II, Project No. 178-6, available at:

http://www.wrapair.org/forums/fejf/tasks/FEJFtask7PhaseII.html (last access: 02 January 2020), 22 July 2005.

Wu, L., Su, H., and Jiang, J. H.: Regional simulation of aerosol impacts on precipitation during the East Asian summer monsoon, J. Geophys. Res. Atmos., 118, 6454–6467, doi:10.1002/jgrd.50527, 2013.

Xie, Y., Zhao, B., Zhang, L., and Luo, R.: Spatiotemporal variations of $PM_{2.5}$ and PM_{10} concentrations between 31 Chinese cities and their relationships with SO_2, NO_2, CO and O_3, Particuology, 20, 141–149, doi:10.1016/j.partic.2015.01.003, 2015.

Xu, W. Y., Zhao, C. S., Ran, L., Lin, W. L., Yan, P., & Xu, X. B.: SO_2 noontime-peak phenomenon in the North China Plain, Atmospheric Chemistry and Physics, 14, 7757-7768, 2014.

Xu, W., Sun, Y., Wang, Q., Zhao, J., Wang, J., Ge, X., Xie, C., Zhou, W., Du, W., Li, J., Fu, P., Wang, Z., Worsnop, D. R., and Coe, H.: Changes in Aerosol Chemistry From 2014 to 2016 in Winter in Beijing: Insights From High-Resolution Aerosol Mass Spectrometry, J. Geophys. Res. Atmos., 124, 1132–1147, doi:10.1029/2018JD029245, 2019.

Yang Y, Liao H, Lou S.: Increase in winter haze over eastern China in recent decades: Roles of variations in meteorological parameters and anthropogenic emissions, Journal of Geophysical Research: Atmospheres, 121,050-13,065, 2016.

Yang, Y., Smith, S. J., Wang, H., Lou, S., and Rasch, P. J.: Impact of Anthropogenic Emission Injection Height Uncertainty on Global Sulfur Dioxide and Aerosol Distribution, J. Geophys. Res. Atmos., 124, 4812–4826, doi:10.1029/2018JD030001, 2019.

Ying, Z., Tie, X., and Li, G.: Sensitivity of ozone concentrations to diurnal variations of surface emissions in Mexico City: A WRF/Chem modeling study, Atmospheric Environment, 43, 851–859, doi:10.1016/j.atmosenv.2008.10.044, 2009.

Zaveri, R. A. and Peters, L. K.: A new lumped structure photochemical mechanism for large-scale applications, J. Geophys. Res., 104, 30387–30415, doi:10.1029/1999JD900876, 1999.

Zaveri, R. A., Easter, R. C., Fast, J. D., & Peters, L. K.: Model for simulating aerosol interactions and chemistry (MOSAIC), Journal of Geophysical Research: Atmospheres, 113, 2008.

Zhang, B., Wang, Y., and Hao, J.: Simulating aerosol–radiation–cloud feedbacks on meteorology and air quality over eastern China under severe haze conditionsin winter, Atmos. Chem. Phys., 15, 2387–2404, doi:10.5194/acp-15-2387-2015, 2015.

Zhang, H., Wang, Y., Hu, J., Ying, Q., and Hu, X.-M.: Relationships between meteorological parameters and criteria air pollutants in three megacities in China, Environmental research, 140, 242–254, doi:10.1016/j.envres.2015.04.004, 2015.

Zhang, L., Liao, H., and Li, J.: Impacts of Asian summer monsoon on seasonal and interannual variations of aerosols over eastern China, J. Geophys. Res., 115, D10307, doi:10.1029/2009JD012299, 2010.

Zhang, L., Wang, T., Lv, M., and Zhang, Q.: On the severe haze in Beijing during January 2013: Unraveling the effects of meteorological anomalies with WRF-Chem, Atmospheric Environment, 104, 11–21, doi:10.1016/j.atmosenv.2015.01.001, 2015.

Zhang, R., Li, G., Fan, J., Wu, D. L., and Molina, M. J.: Intensification of Pacific storm track linked to Asian pollution, Proceedings of the National Academy of Sciences of the United States of America, 104, 5295–5299, doi:10.1073/pnas.0700618104, 2007.

Zhang, Y., Zhang, X., Wang, L., Zhang, Q., Duan, F., and He, K.: Application of WRF/Chem over East Asia: Part I. Model evaluation and intercomparison with MM5/CMAQ, Atmospheric Environment, 124, 285–300, doi:10.1016/j.atmosenv.2015.07.022, 2016.

Zhang, Y.-L. and Cao, F.: Fine particulate matter ($PM_{2.5}$) in China at a city level, Scientific reports, 5, 14884, doi:10.1038/srep14884, 2015.

~~Zhao,~~ Zhao C, Liu X, Leung L R.: Impact of the Desert dust on the summer monsoon system over Southwestern North America, Atmospheric Chemistry and Physics, 12, 3717-3731, 2012.

Zhao, B., Liou, K.-N., Gu, Y., Li, Q., Jiang, J. H., Su, H., He, C., Tseng, H.-L. R., Wang, S., Liu, R., Qi, L., Lee, W.-L., and Hao, J.: Enhanced $PM_{2.5}$ pollution in China due to aerosol-cloud interactions, Scientific reports, 7, 4453, doi:10.1038/s41598-017-04096-8, 2017.

Zhao, C., ~~Liu, X., Leung, L. R., Johnson, B., McFarlane, S. A., Gustafson, W. I., Fast, J. D., and Easter, R.: The spatial distribution of mineral dust and its shortwave radiative forcing over North Africa: modeling sensitivities to dust emissions and aerosol size treatments, Atmospheric Chemistry and Physics, 10, 8821-8838, 2010.~~

Zhao, C., Liu, X., Leung, L. R., and Hagos, S.: Radiative impact of mineral dust on monsoon precipitation variability over West Africa, Atmospheric Chemistry and Physics, 11, 1879-1893, 2011.

Zhao C, Liu X, Leung L R.: Impact of the Desert dust on the summer monsoon system over Southwestern North America, Atmospheric Chemistry and Physics, 12, 3717-3731, 2012.

Zhao, C., Chen, S., Leung, L. R., Qian, Y., Kok, J., Zaveri, R., and Huang, J.: Uncertainty in modeling dust mass balance and radiative forcing from size parameterization, Atmospheric Chemistry and Physics, 13, 10733-10753, 2013a.

Zhao, C., Ruby Leung, L., Easter, R., Hand, J., and Avise, J.: Characterization of speciated aerosol direct radiative forcing over California, J. Geophys. Res. Atmos., 118, 2372–2388, doi:10.1029/2012JD018364, 2013b.

Zhao, C., Hu, Z., Qian, Y., Leung, L. R., Huang, J., Huang, M., Jin, J., Flanner, M., Zhang, R., Wang, H., Yan, H., Lu, Z., and Streets, D. G.: Simulating black carbon and dust and their radiative forcing in seasonal snow: a case study over North China with field campaign measurements, Atmospheric Chemistry and Physics, 14, 11475-11491, 2014.

Zhao, C., Huang, M., Fast, J. D., Berg, L. K., Qian, Y., Guenther, A., ... & Pfister, G.: Sensitivity of biogenic volatile organic compounds to land surface parameterizations and vegetation distributions in California, Geosci. Model Dev, 9, 1959-1976, 2016.

Zhao, C., Liu, X., Leung, L. R., and Hagos, S.: Radiative impact of mineral dust on monsoon precipitation variability over West Africa, Atmospheric Chemistry and Physics, 11, 1879-1893, 2011.

Zhao, C., Liu, X., Leung, L. R., Johnson, B., McFarlane, S. A., Gustafson, W. I., Fast, J. D., and Easter, R.: The spatial distribution of mineral dust and its shortwave radiative forcing over North Africa: modeling sensitivities to dust emissions and aerosol size treatments, Atmospheric Chemistry and Physics, 10, 8821-8838, 2010.

Zhao, C., Ruby Leung, L., Easter, R., Hand, J., and Avise, J.: Characterization of speciated aerosol direct radiative forcing over California, J. Geophys. Res. Atmos., 118, 2372–2388, doi:10.1029/2012JD018364, 2013b.

Zhao, S., Yu, Y., Yin, D., He, J., Liu, N., Qu, J., and Xiao, J.: Annual and diurnal variations of gaseous and particulate pollutants in 31 provincial capital cities based on in situ air quality monitoring data from China National Environmental Monitoring

Center, Environment international, 86, 92–106, doi:10.1016/j.envint.2015.11.003, 2016.

Zhong M, Saikawa E, Liu Y, et al. Air quality modeling with WRF-Chem v3. 5 in East Asia: sensitivity to emissions and evaluation of simulated air quality[J]. Geoscientific Model Development, 2016, 9(3).

Zhou, G., Xu, J., Xie, Y., Chang, L., Gao, W., Gu, Y., and Zhou, J.: Numerical air quality forecasting over eastern China: An operational application of WRF-Chem, Atmospheric Environment, 153, 94–108, doi:10.1016/j.atmosenv.2017.01.020, 2017.

Zhou, G., Yang, F., Geng, F., Xu, J., Yang, X., Tie, X.: Measuring and modeling aerosol: relationship with haze events in Shanghai, China, Aerosol and air quality research, 14, 783-792, 2014.

Table 1 Numerical experiments conducted in this study.

Name	PBL scheme	Vertical structure	PBL mixing coefficient (m^2/s)	Emission diurnal cycle	Emission injection height
CTL1	MYNN	layer1	Minimum=0.1	Yes	Yes
CTL2	MYNN	layer2	Minimum=0.1	Yes	Yes
CTL3	YSU	layer2	Minimum=0.1	Yes	Yes
EXP1	MYNN	layer1	Minimum = 5.0	Yes	Yes
EXP2	MYNN	layer2	Minimum = 5.0	Yes	Yes
EXP1_E1	MYNN	layer1	Minimum = 5.0	No	Yes
EXP1_E2	MYNN	layer1	Minimum = 5.0	Yes	No

Table 2 Vertical distributions of power plant emissions: percentage of each species allocated to the height of the vertical layers in the WRF-Chem model.

Species	Height of Emission Layers (m)				
	0-76	**76-153**	**153-308**	**308-547**	**547-871**
SO_2	5%	30%	35%	25%	5%
NO_x	5%	40%	25%	25%	5%
CO	5%	70%	20%	5%	0%
NH_3	5%	75%	15%	5%	0%
NMVOC	5%	85%	10%	0%	0%
$PM_{2.5}$	5%	45%	25%	20%	5%
PM_{10}	5%	55%	20%	15%	5%
OC	5%	70%	15%	10%	0%
BC	5%	65%	20%	10%	0%

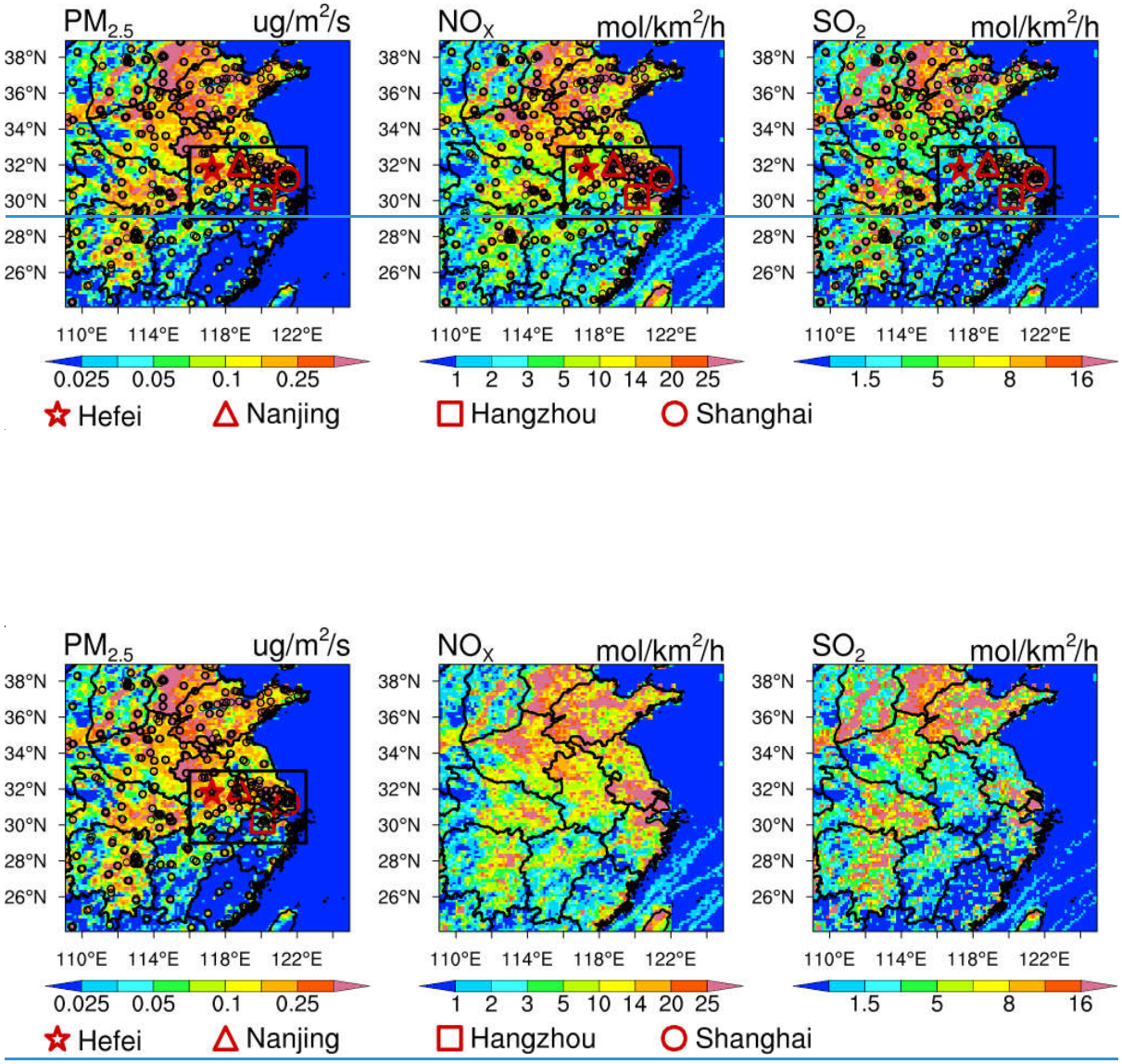

Figure 1a. ~~MEIC China emission~~Emissions of SO_2, NO_2, $PM_{2.5}$ from the MEIC China inventory over the simulation domain (109.0° E~124.9° E, 24.0° N~38.9° N) with black boxes showing the analyzed domain (116.0° E~122.5° E, 29.0° N~33.0° N), overlaid with observational sites and four cities as the Center (Shanghai, 121.45°E and 31.21°N) and sub-Center (Nanjing, 118.78°E and 32.06°N; Hefei, 117.25°E and 31.85°N; Hangzhou, 120.08°E and 30.21°N) of the YRD city cluster.

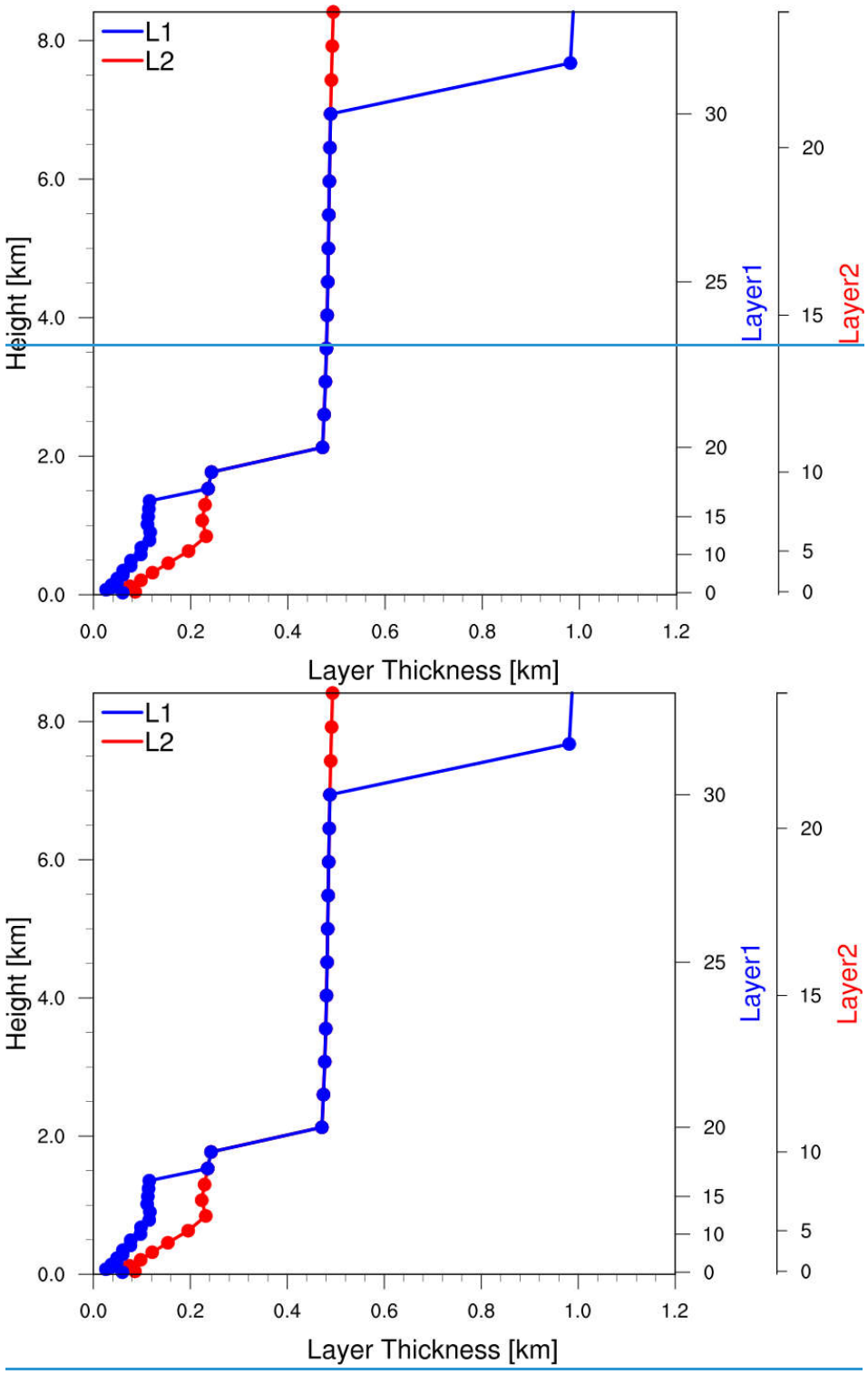

Figure 1b. Vertical profiles of the layer thickness from L1 and L2 layer configuration.

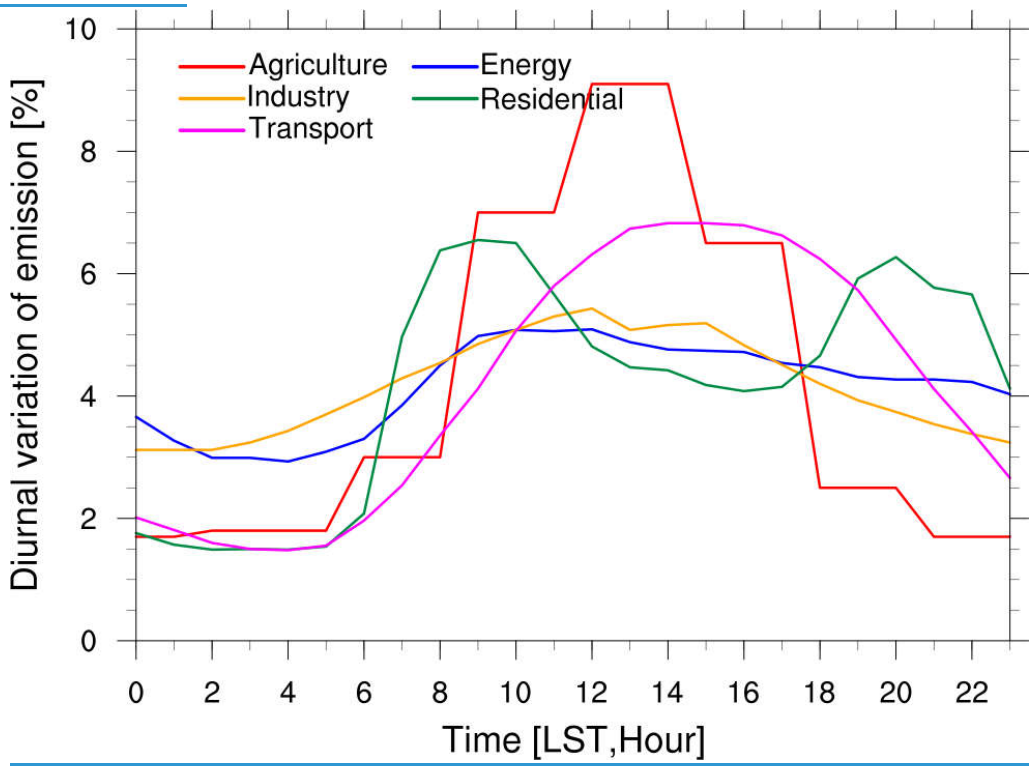

Figure 1c. Diurnal profiles of emissions from five individual sectors (agriculture, industry, transport, energy, and residential).

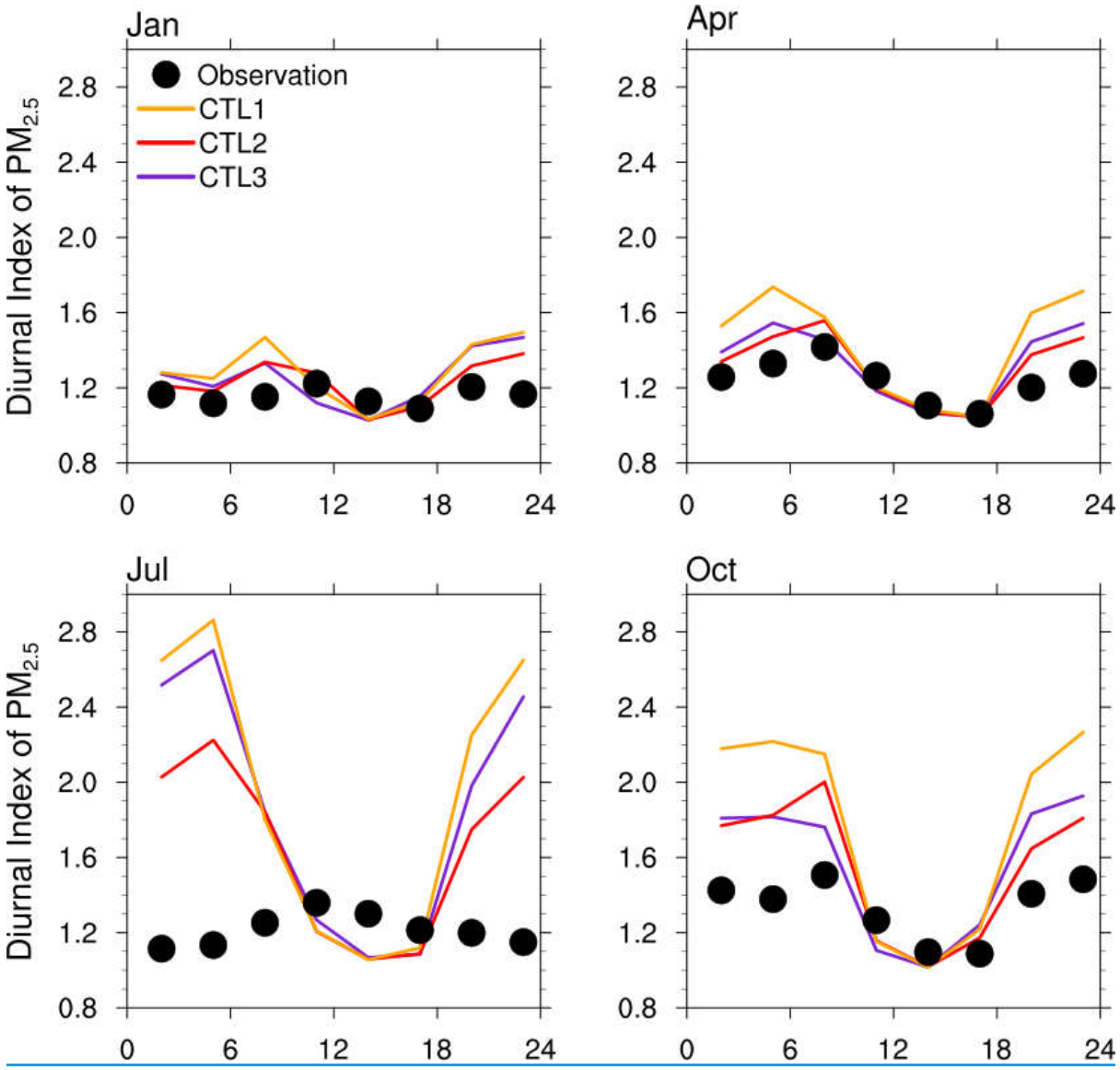

Figure 2. Diurnal index of surface $PM_{2.5}$ ~~concentration~~concentrations within 24-hour averaged over the YRD region of East China (within the black box of Fig. 1a) for January, April, July, and October of 2018 from the experiments CTL1, CTL2, CTL3, and observations. ~~The~~Both the simulated results and observations are ~~from 3-hourly output and~~ sampled at the ~~observational sites~~model output frequency, i.e., 3-hourly.

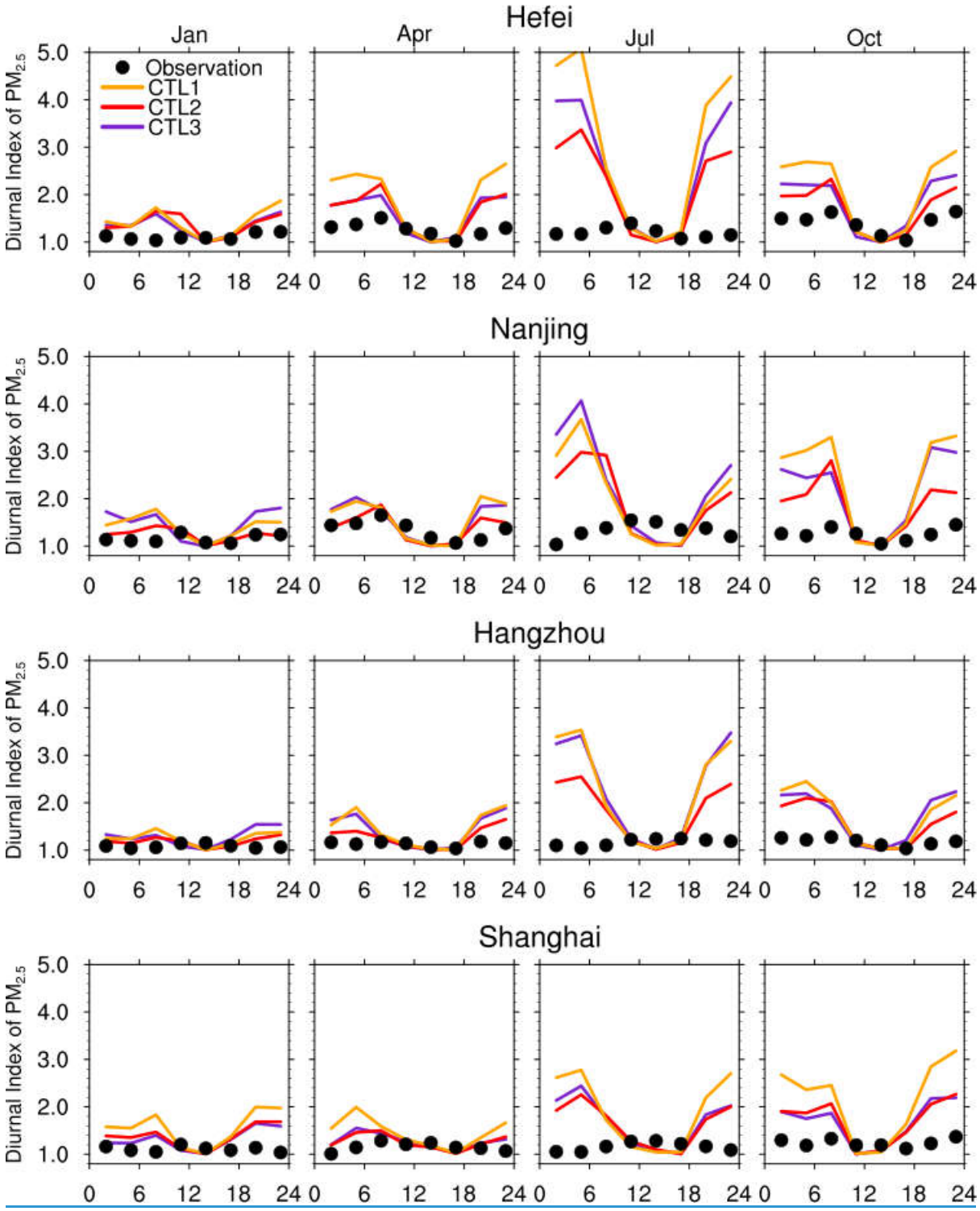

Figure 3. Diurnal index of surface $PM_{2.5}$ ~~concentration~~concentrations within 24-hour averaged over four cities (Hefei, Nanjing, Hangzhou, Shanghai) for January, April, July, and October of 2018 from the experiments CTL1, CTL2, CTL3, and observations.

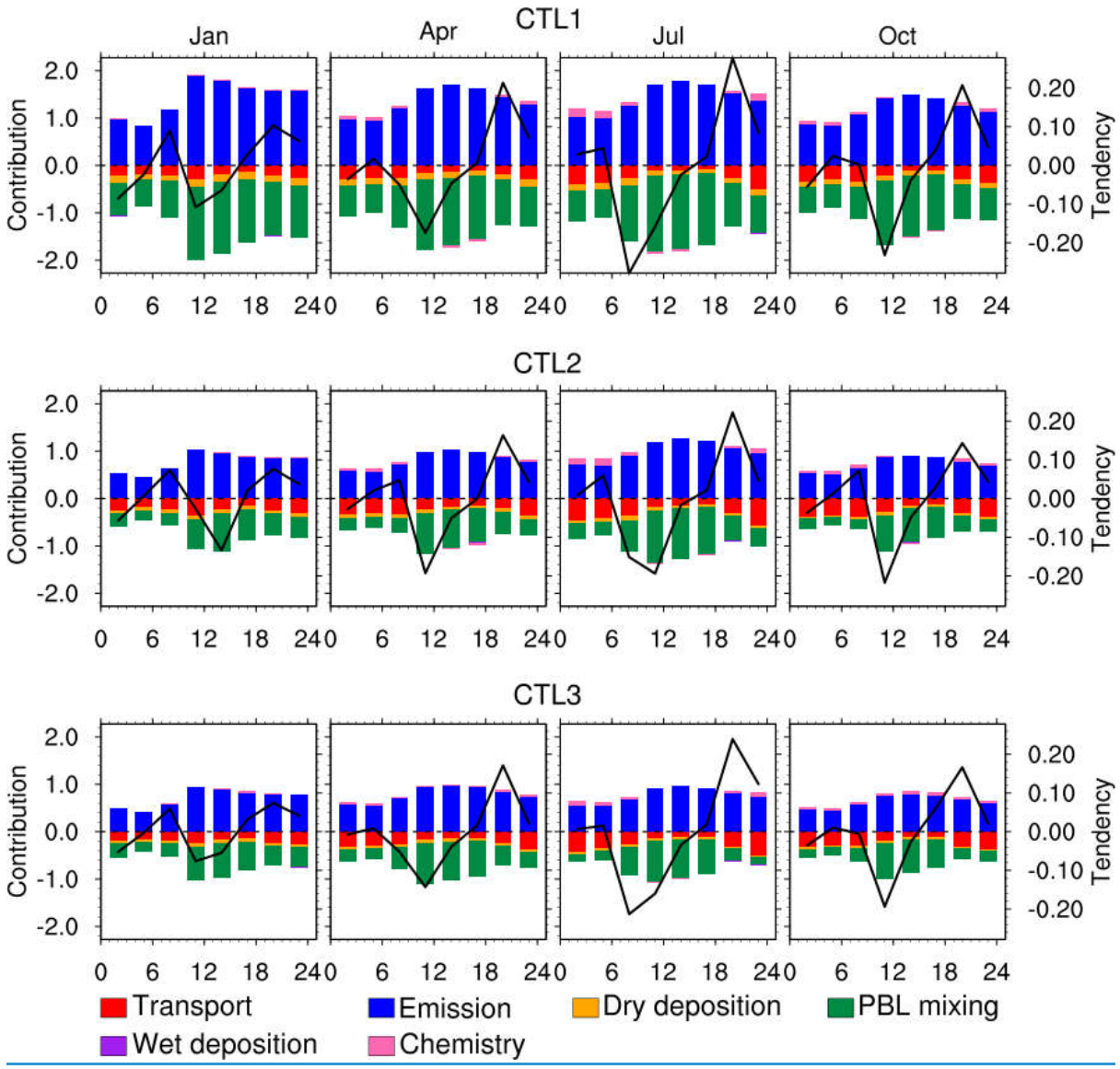

Figure 4. ~~Contribution~~Relative contribution (normalized by monthly mean surface $PM_{2.5}$ concentrations for each month) to surface $PM_{2.5}$ ~~concentration~~concentrations every 3-hour from individual process (transport, emission, dry and wet deposition, PBL mixing, chemical production/loss) averaged over Hefei for January, April, July, and October of 2018 from the experiments CTL1, CTL2, and CTL3. The 3-hourly relative tendency of surface $PM_{2.5}$ ~~concentration~~concentrations is also shown as the black line.

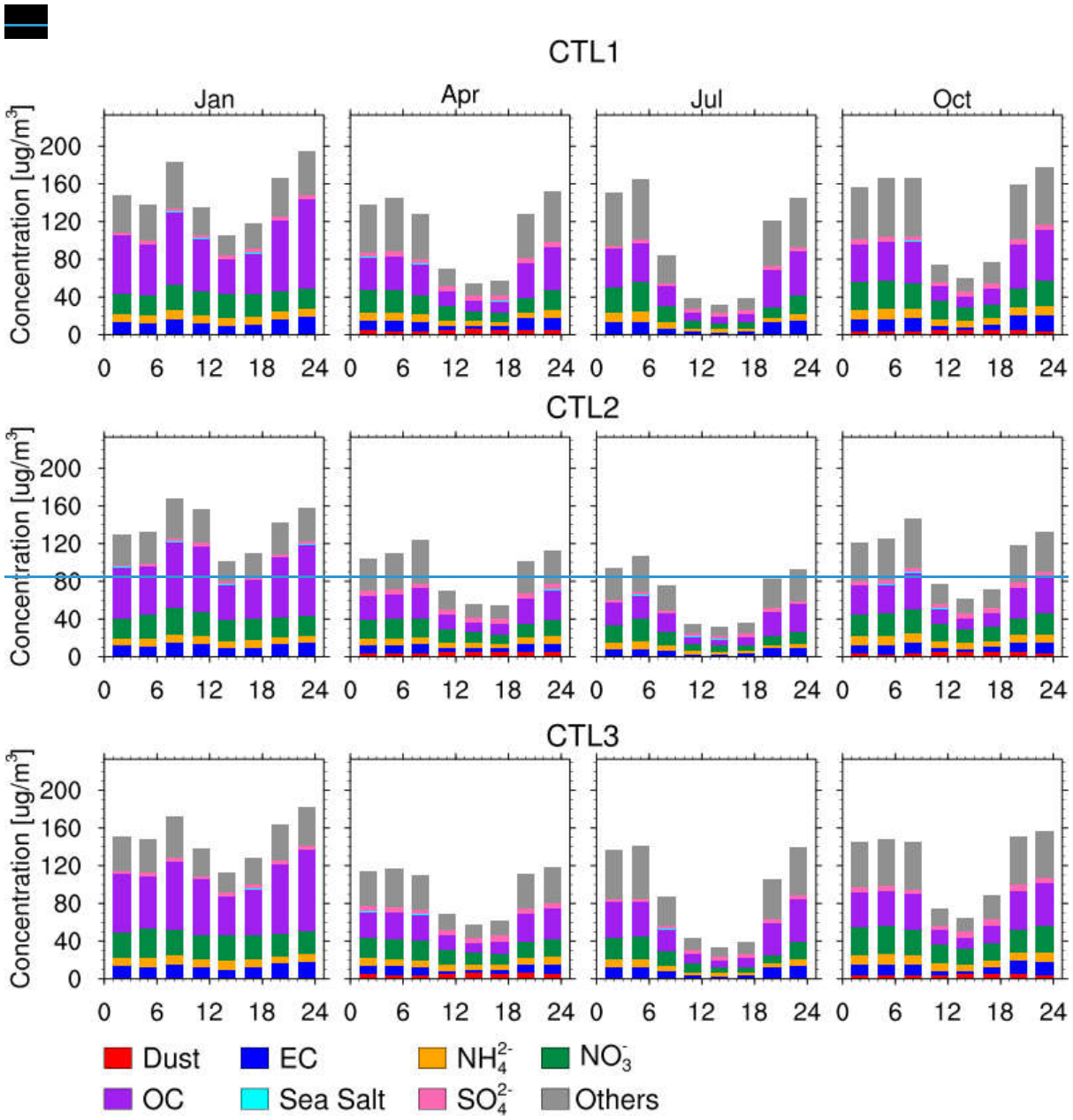
CTL1
Jan
Apr
Jul
Oct
Concentration [ug/m3]
0
40
80
120
160
200
0 6 12 18 24
CTL2
CTL3
Dust
EC
NH4 2-
NO3-
OC
Sea Salt
SO4 2-
Others

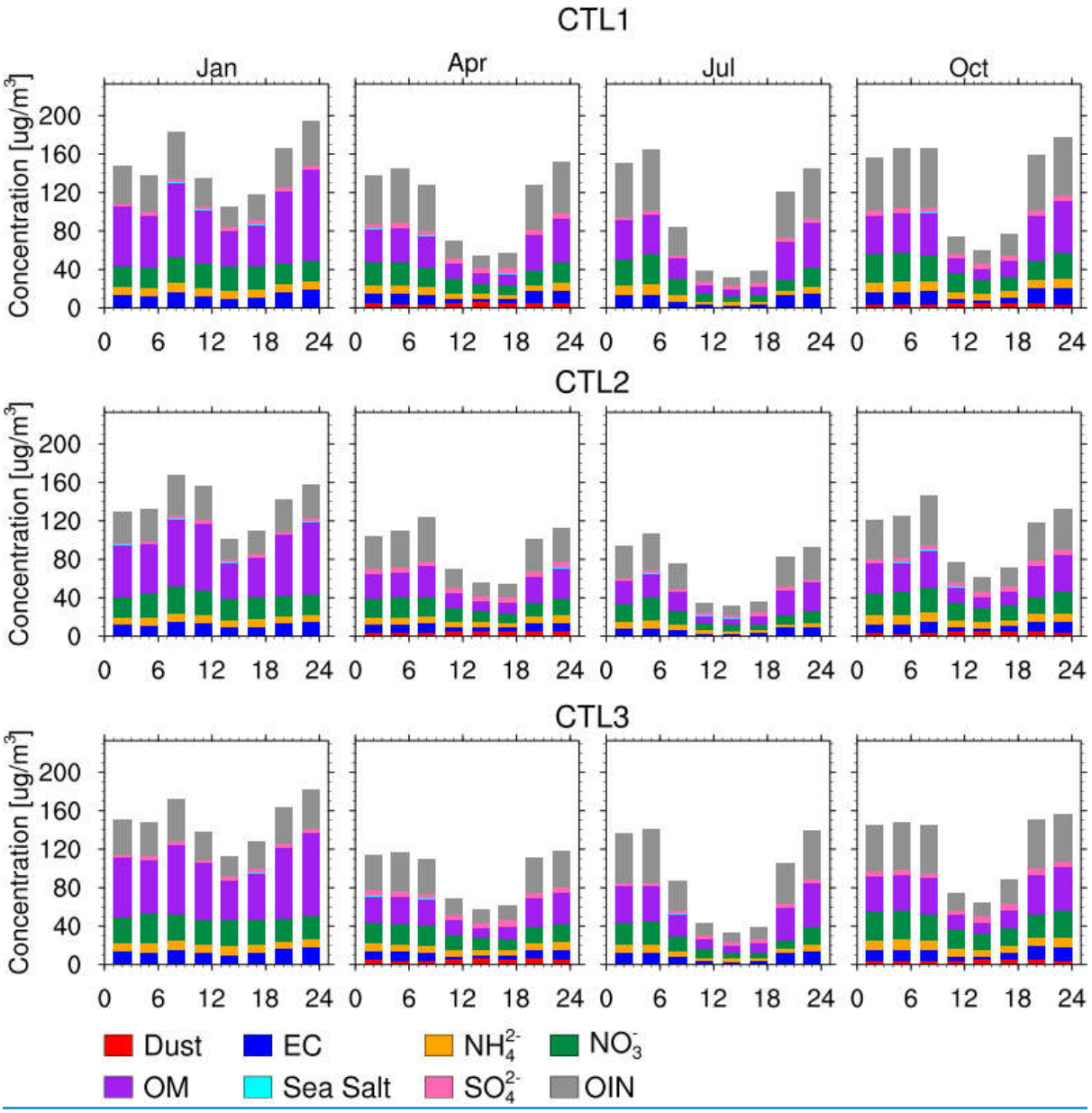

Figure 5. Diurnal variation of surface ~~concentration~~concentrations of each $PM_{2.5}$ composition (Dust, ~~OC~~OM, EC, Sea Salt, NH_4^{2-}, SO_4^{2-}, NO_3^-, and other inorganics) averaged over Hefei for January, April, July, and October of 2018 from the experiments CTL1, CTL2, and CTL3.

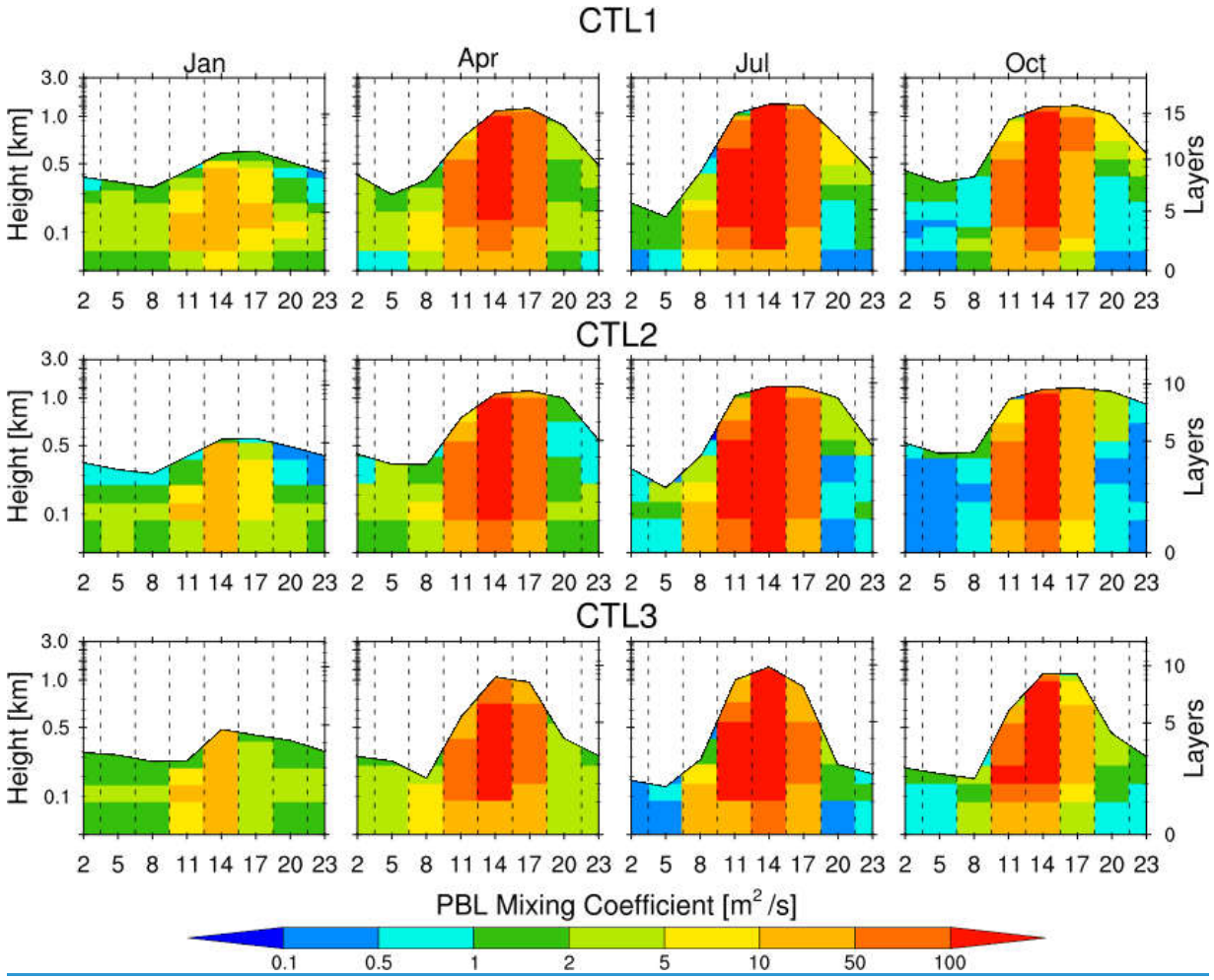

Figure 6. Diurnal variation of PBLH and PBL mixing coefficient below PBLH averaged over Hefei for January, April, July, and October of 2018 from the experiments CTL1, CTL2, and CTL3.

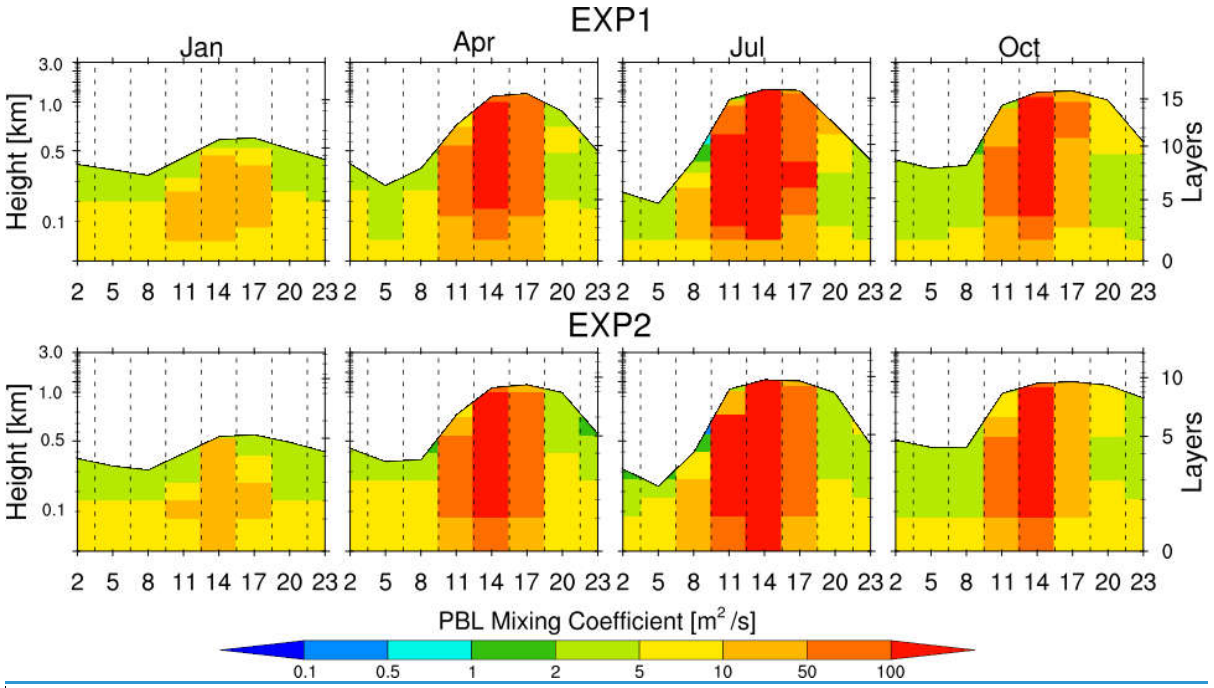

Figure 7. Diurnal variation of PBLH and PBL mixing coefficient below PBLH averaged over Hefei for January, April, July, and October of 2018 from the experiments EXP1 and EXP2.

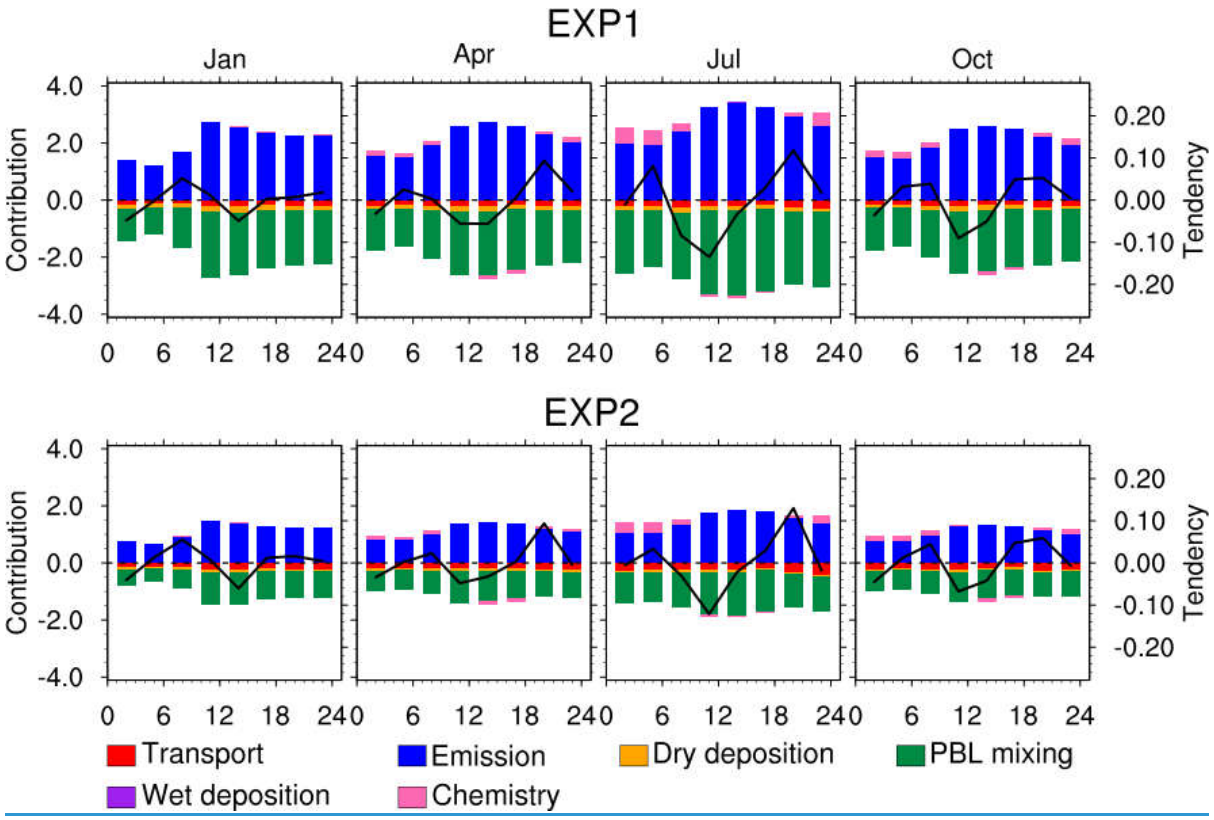

Figure 8. ~~Contribution~~Relative contribution (normalized by monthly mean surface $PM_{2.5}$ concentrations for each month) to surface $PM_{2.5}$ ~~concentration~~concentrations every 3-hour from individual ~~processes~~process (transport, emission, dry and wet deposition, PBL mixing, ~~and~~ chemical production/loss) averaged over Hefei for January, April, July, and October of 2018 from the experiments EXP1 and EXP2. The 3-hourly relative tendency of surface $PM_{2.5}$ concentrations is also shown as the black line.

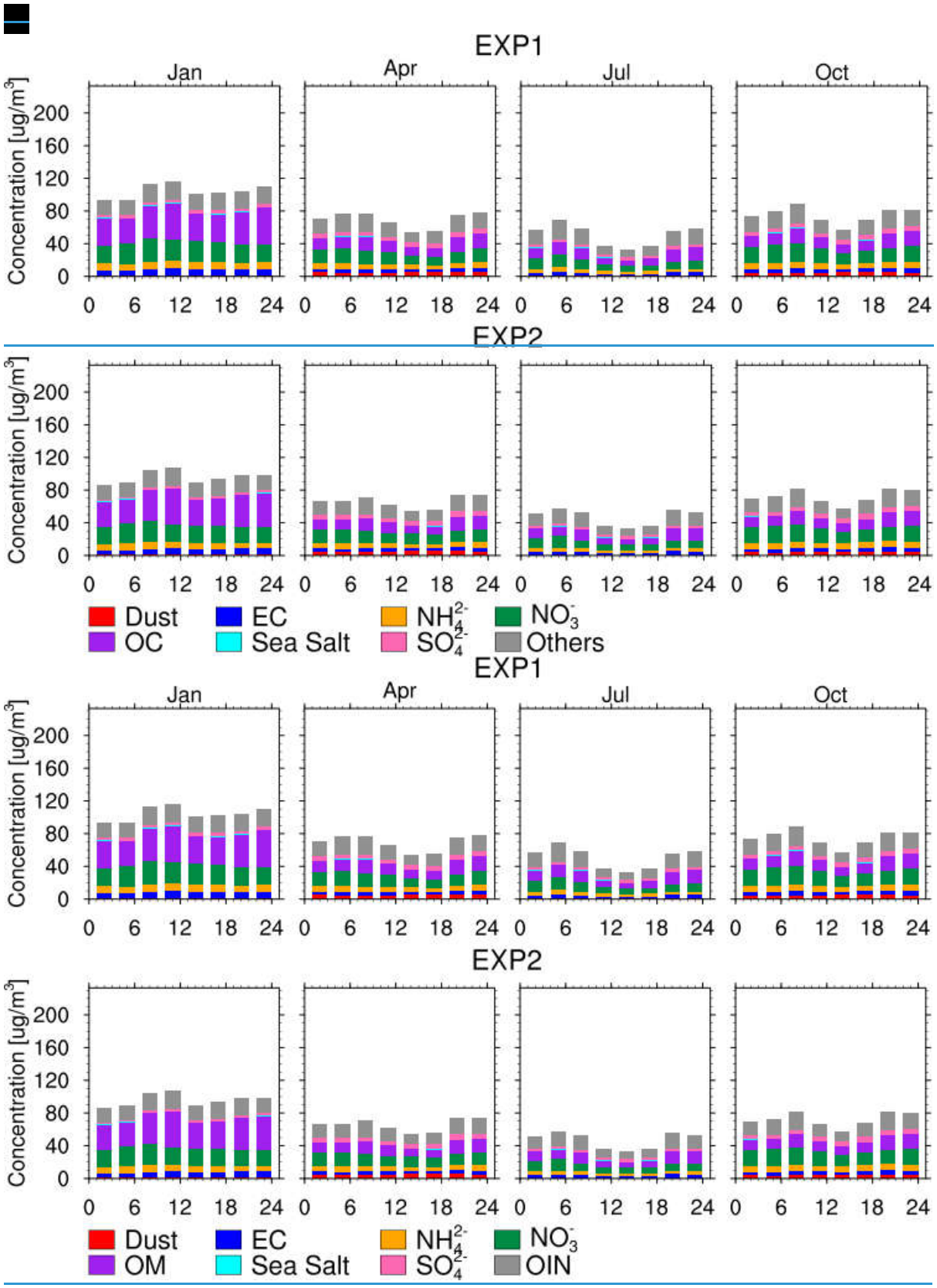

Figure 9. Diurnal cycle of surface $PM_{2.5}$ ~~compositions concentration~~composition concentrations (Dust, ~~OC~~OM, EC, Sea Salt, NH_4^{2-}, SO_4^{2-}, NO_3^-, and other inorganics)

averaged over Hefei for January, April, July, and October of 2018 from the experiments EXP1 and EXP2.

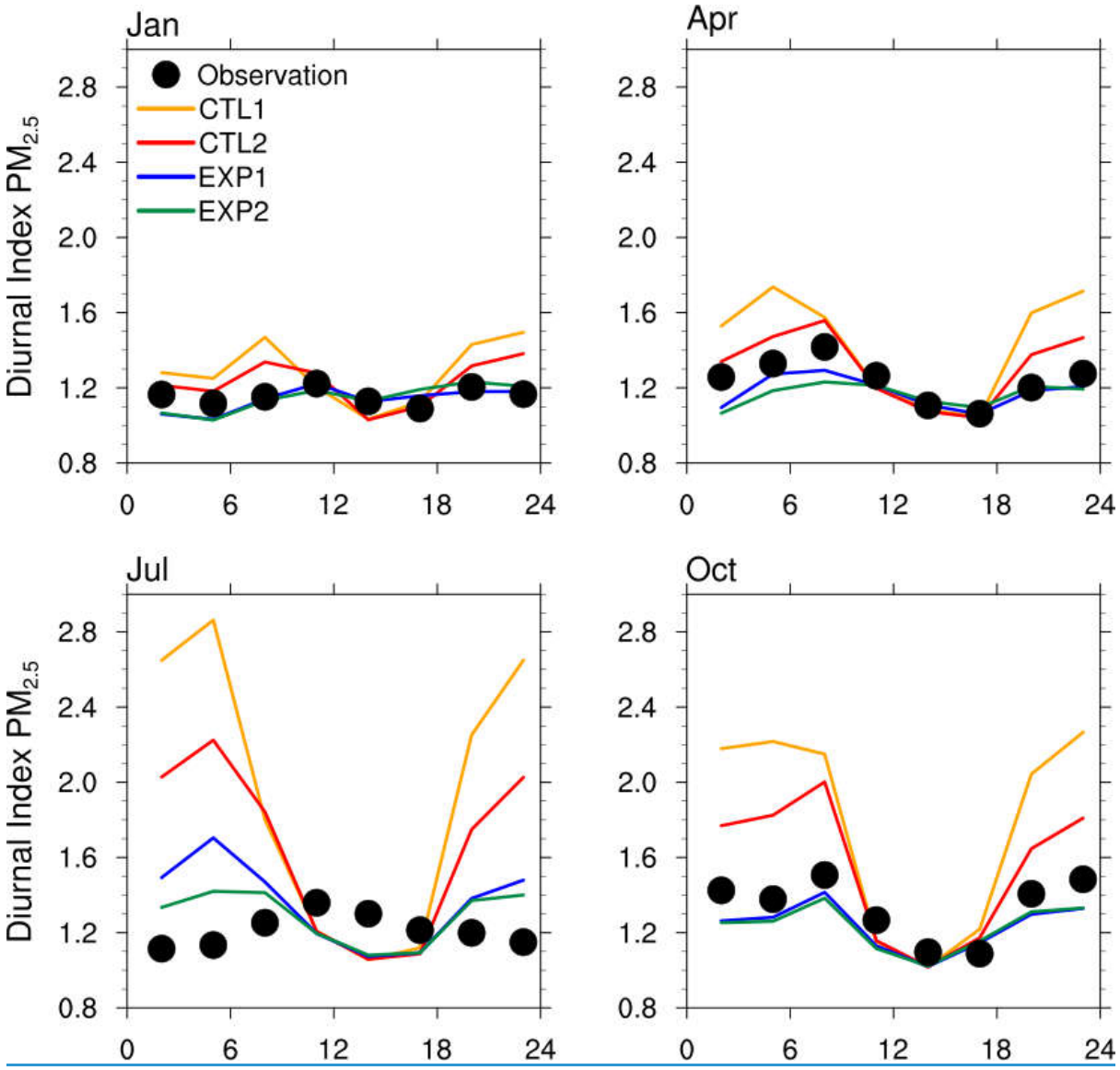

Figure 10. Diurnal index of surface $PM_{2.5}$ ~~concentration~~concentrations within 24-hour averaged over the YRD region of East China (within black box of Fig. 1a) for January, April, July, and October of 2018 from the experiments CTL1, CTL2, EXP1, EXP2, and observations. ~~The~~Both the simulated results and observations are ~~from 3-hourly output and~~ sampled at the ~~observational sites~~model output frequency, i.e., 3-hourly.

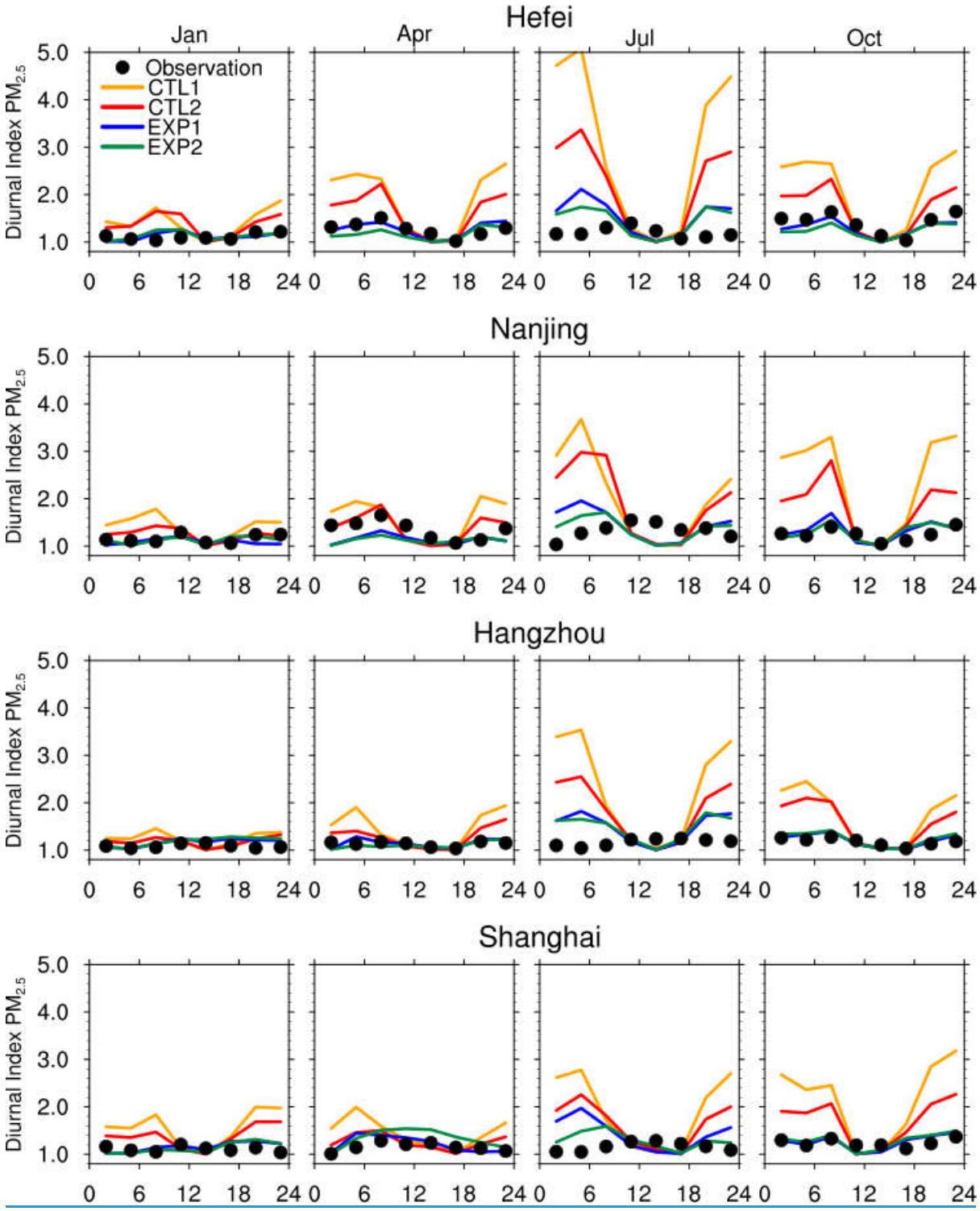

Figure 11. Diurnal index of surface $PM_{2.5}$ ~~concentration~~concentrations within 24-hour averaged over four cities (Hefei, Nanjing, Hangzhou, Shanghai) for January, April, July, and October of 2018 from the experiments CTL1, CTL2, EXP1, EXP2, and observations.

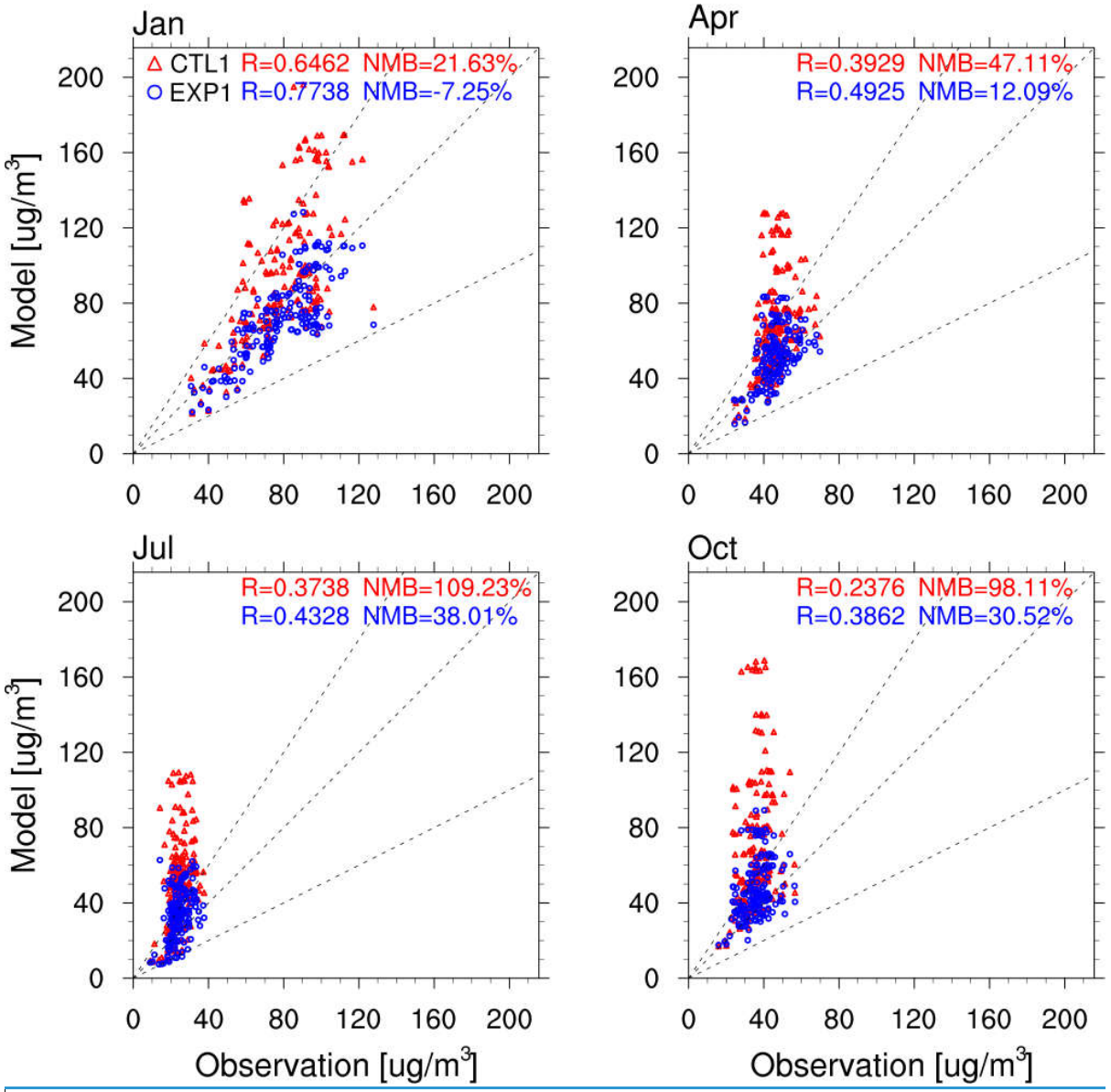

Figure 12. Comparison of monthly mean surface $PM_{2.5}$ ~~concentration~~concentrations between the observations and the simulations from the experiments CTL1 and EXP1 at each observation site over the YRD region of East China (as shown in Fig. 1a within the black box) for January, April, July, and October of 2018. The dashed lines represent -50%, 0, 50% of the NMB of simulation.

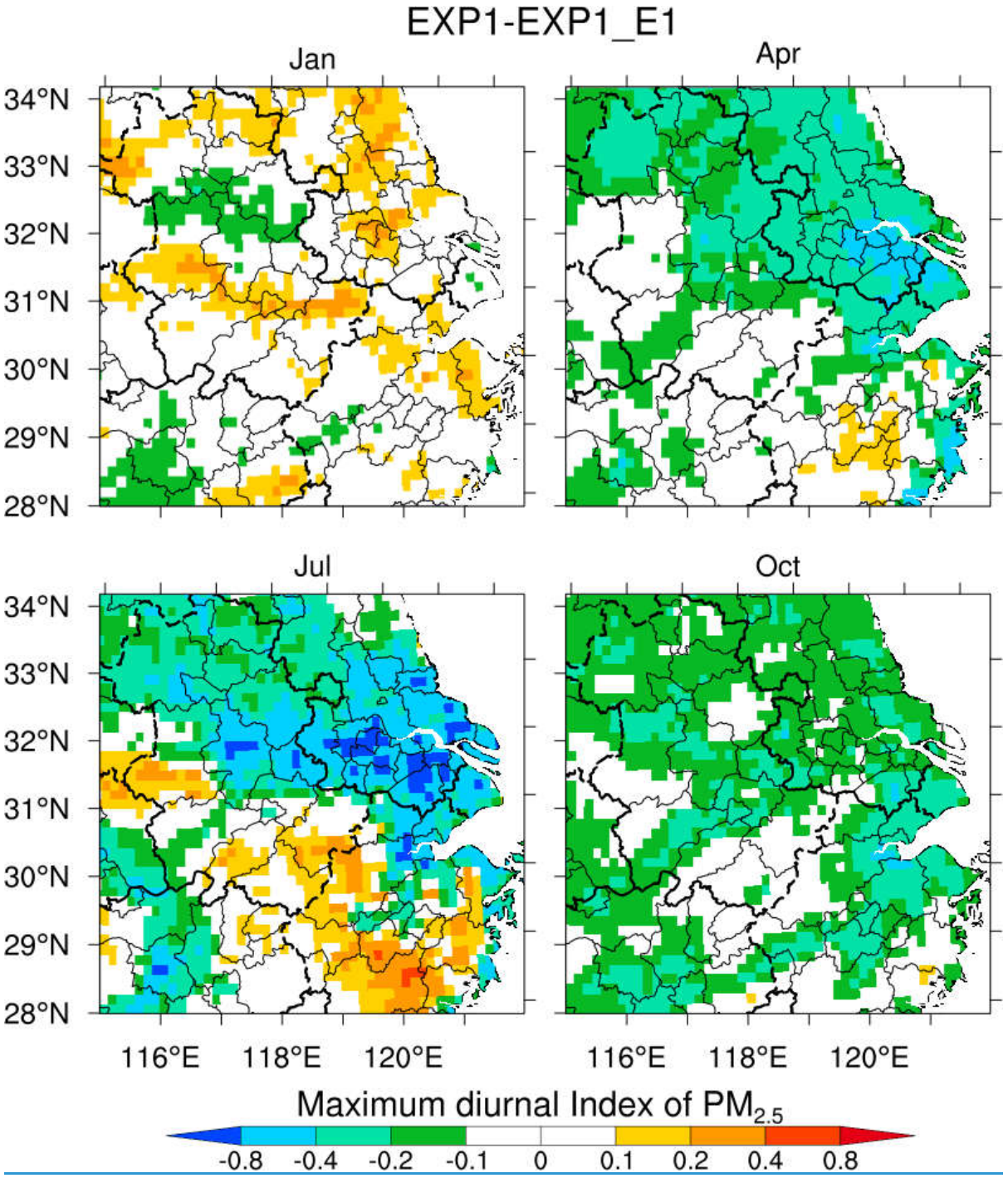

Figure 13. Spatial distribution of the difference in daily maximum diurnal index of surface $PM_{2.5}$ concentrations between the experiments EXP1 and EXP1_E1 over East China in January, April, July, and October of 2018.

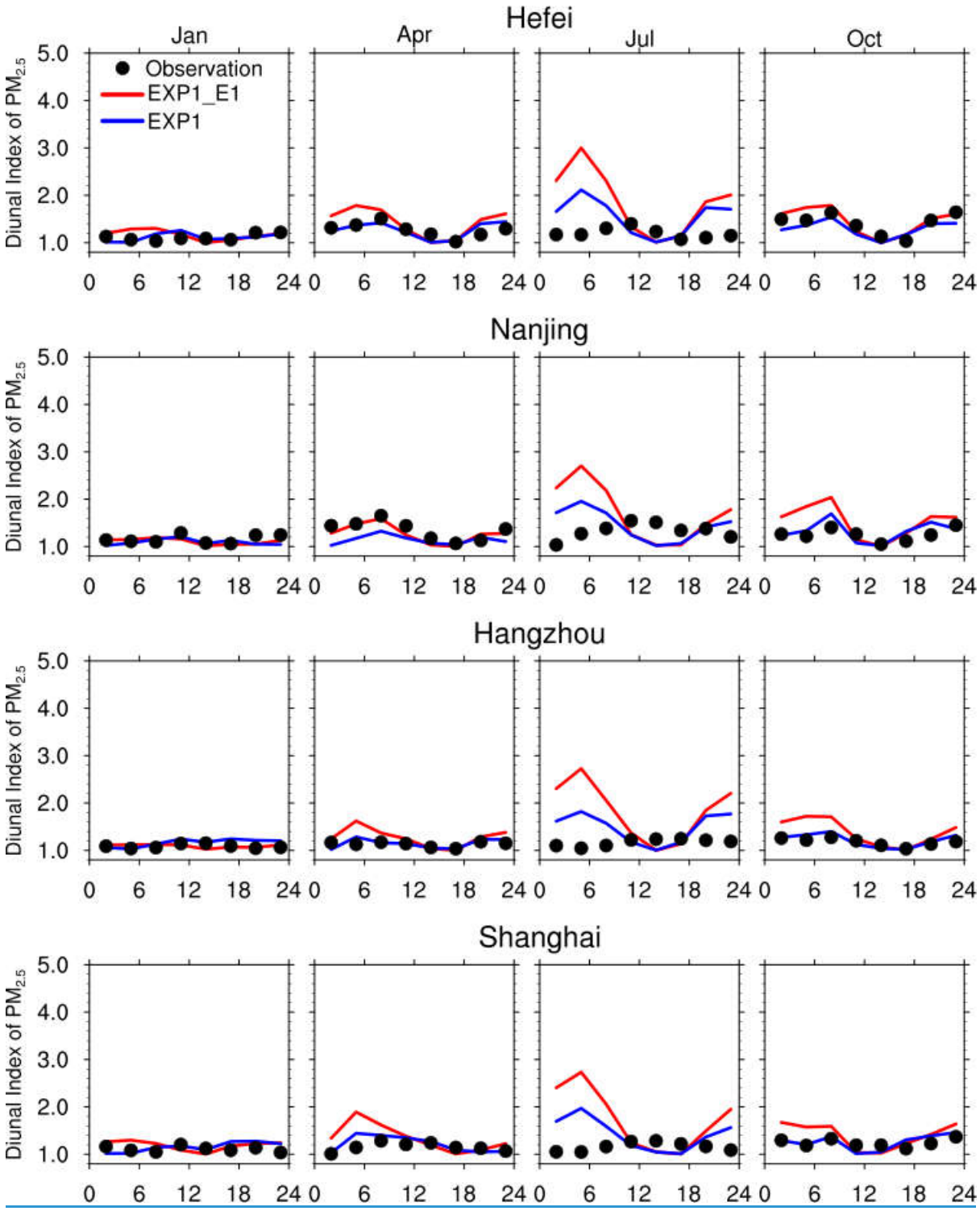

Figure 14. Diurnal index of surface $PM_{2.5}$ ~~concentration~~concentrations within 24-hour averaged over four cities (Hefei, Nanjing, Hangzhou, Shanghai) for January, April, July, and October of 2018 from the experiments EXP1_E1, EXP1, and observations.

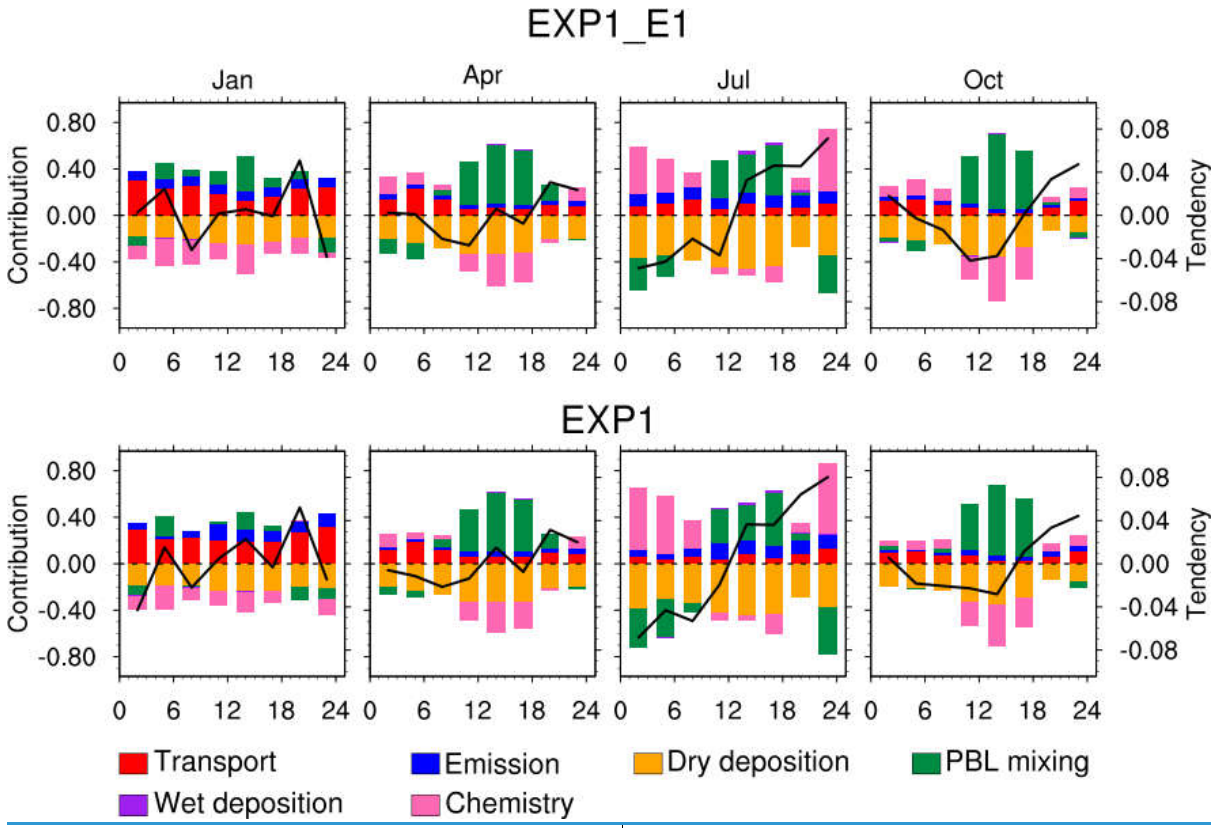

Figure 15. ~~Contribution to diurnal variation of~~Relative contribution (normalized by monthly mean surface $PM_{2.5}$ ~~concentration~~concentrations for each month) to surface $PM_{2.5}$ concentrations every 3-hour from individual ~~processes~~process (transport, emission, dry and wet deposition, PBL mixing, ~~and~~ chemical production/loss) averaged over South Anhui for January, April, July, and October of 2018 from the experiments EXP1_E1 and EXP1. The 3-hourly relative tendency of surface $PM_{2.5}$ concentrations is also shown as the black line.

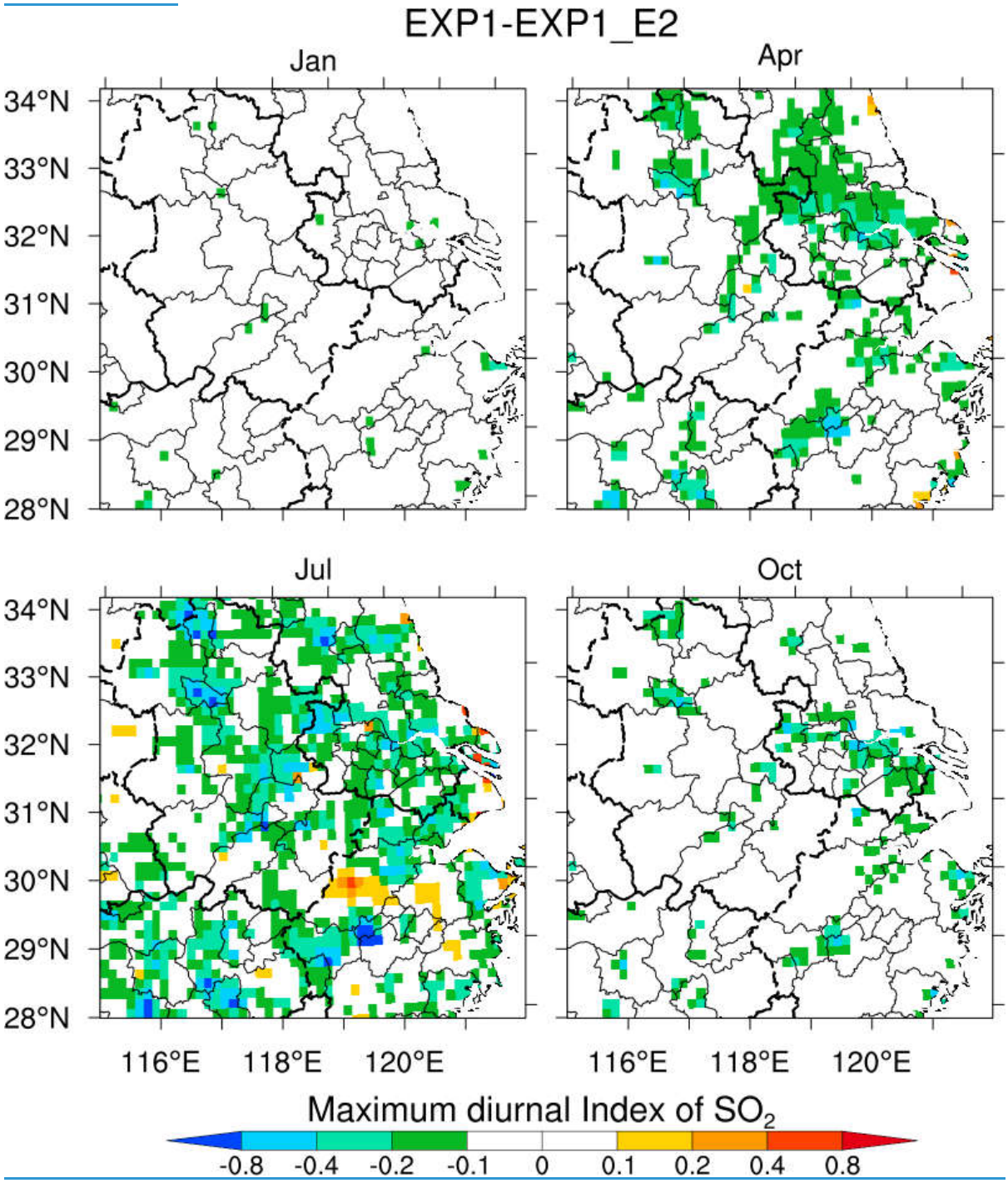

Figure 16. Spatial distribution of the difference in daily maximum diurnal index of surface SO_2 concentrations between the experiments EXP1_E2 and EXP1 over East China in January, April, July, and October of 2018.